Characterisation of Block Copolymers by On-line HPLC-NMR

Vom Fachbereich Chemie
der Technischen Universität Darmstadt
zur
Erlangung des akademischen Grades eines

Doctor rerum naturalium
(Dr. rer. nat.)

genehmigte
Dissertation

vorgelegt von

Pritish Sinha (M.Sc.)
Aus Kalkutta, Indien

Berichterstatter:	Prof. Dr. H. Pasch
Mitberichterstatter:	PD. Dr. R. Meusinger
Tag der Einreichung:	14.05.2009
Tag der mündlichen Prüfung:	29.06.2009

Darmstadt 2009
D 17

Acknowledgement

I wish to extend my deepest appreciation to my research adviser, Prof. Dr. Harald Pasch who believed in my abilities as a graduate student and gave me the opportunity to work in his research group. I am also thankful to him for providing me a challenging research topic and for the liberty I had for performing the research work.

I would like to thank Dr. Wolf Hiller who introduced me to the field of nuclear magnetic resonance spectroscopy as well as the coupling of HPLC-NMR. His constant guidance and encouragement has proved invaluable in my research activities. I also appreciate him for his moral support, compliments and optimistic discussions.

I would like to express my gratitude to all my former and present colleagues of DKI who morally supported me during my stay in the institute as well as for a pleasant working atmosphere. Moreover, I would like to appreciate all my friends who made my stay in Germany a pleasant one.

Finally I thank my parents and sister for their encouragement, support and patience during the course of my study as well as the PhD work.

Diese Arbeit wurde unter der Leitung von Herrn Prof. Dr. Harald Pasch am Deutschen Kunststoff-Institut in der Zeit vom Februar 2006 bis zum April 2009 durchgeführt.

Publications:

1. W. Hiller, P. Sinha, H. Pasch:
   "On-line HPLC-NMR of PS-b-PMMA and Blends of PS and PMMA: LCCC-NMR at Critical Conditions of PS"
   Macromol. Chem. Phys., **2007**, 208, 1965

2. W. Hiller, P. Sinha, H. Pasch:
   "On-line HPLC-NMR of PS-b-PMMA and Blends of PS and PMMA: LCCC-NMR at Critical Conditions of PMMA"
   Macromol. Chem. Phys., **2009**, 210, 605

Oral presentation:

1. "Characterisation of poly [(styrene)-co-(methyl methacrylate)] block copolymers by on-line hyphenation of liquid chromatography at critical conditions and nuclear magnetic resonance spectroscopy"
   3rd International Symposium on the Separation and Characterisation of Natural and Synthetic Macromolecules, 31.01-2.02.07, Amsterdam, Netherlands

2. "Block copolymer analysis by coupled HPLC-NMR"
   15th DKI Colloquium, 30.03.07, Darmstadt, Germany

3. "Analysis of block copolymers by HPLC-NMR"
   19th DKI Colloquium, 27.03.09, Darmstadt, Germany

Posters:

1. "Characterisation of poly (styrene-block-methyl methacrylate) copolymers with on-line hyphenation of HPLC-NMR"
   13th International Symposium on Separation Science, 26-29.06.07, High Tatra, Slovakia

2. "Separation and characterisation of PS-b-PI copolymers by different

chromatographic techniques”
21st International Symposium on Polymer Analysis and Characterisation, 08-11.06.08, Delaware, United States of America

3. “2D-LC Separation of fatty alcohol ethoxylates simultaneously by endgroup and chain length with on-line ^{1}H-NMR”
   10th Annual UNESCO/IUPAC Conference on Macromolecules & Materials, 08-11.09.08, Mpumalanga, South Africa

4. “Characterisation of poly (styrene-block-isoprene) copolymers by on-line hyphenation of HPLC and ^{1}H-NMR“
   International Symposium ‘Microstructural Control in Free-Radical Polymerisation’ 05-08.10.08, Clausthal, Germany

5. “Characterisation of blends of PS and PI by HPLC-NMR"
   4th International Symposium on the Separation and Characterisation of Natural and Synthetic Macromolecules, 28-30.01.07, Amsterdam, Netherlands

CONTENT

1. Summary in German

Blockcopolymere sind Makromoleküle, die aus zwei oder mehr chemisch verschiedenen Polymer-Segmenten bestehen, die miteinander kovalent verbunden sind. Sie stellen eine vielseitige Klasse von Materialen für verschiedene Anwendungen dar, denn sie verbinden die unterschiedlichen Eigenschaften von bekannten Polymersegmenten in vorteilhafter Weise und führen so zu neuen Eigenschaftsprofilen. Die Fähigkeit dieser Polymere Grenzflächeneigenschaften zu verändern und so zur Verbesserung der Mischbarkeit von Polymerblends beizutragen, macht diese Art von segmentierten Polymeren attraktiv für die Anwendung als thermoplastische Elastomere, als Materialien für die Informationsspeicherung und für photonische Materialien.

Ziel der vorliegenden Arbeit war es, chromatographische Methoden für Blockcopolymere zu entwickeln. Mit diesen Methoden sollten die Polymere selektiv nach der chemischen Heterogenität getrennt werden. Die quantitative Bestimmung der Zusammensetzungsverteilung und der Taktizität der einzelnen Blöcke sollte durch on-line gekoppelte HPLC-^{1}H-NMR erfolgen.

Im ersten Abschnitt der Arbeit sollten analytische Methoden zur Charakterisierung von PS-*b*-PMMA-Blockcopolymeren entwickelt werden. Diese Blockcopolymere wurden durch anionische Polymerisation hergestellt. Damit war zu erwarten, dass die Proben zusätzlich Anteile an Homopolymeren enthalten. Durch die Kopplung der Chromatographie am kritischen Punkt der Adsorption (LC-CC) mit der ^{1}H-NMR konnten nun die unterschiedlichen molekularen Parameter wie Molmassenverteilung und chemische Zusammensetzungsverteilung quantitativ bestimmt werden. Mittels LC-CC gelang es zum einen, die Blocklängen der einzelnen Blöcke zu bestimmen. Zum anderen konnte durch NMR-Detektion die Taktizität der PMMA-Blöcke in den Blockcopolymeren ermittelt werden.

Der zweite Teil der Arbeit beschäftigte sich mit der Entwicklung von analytischen Methoden zur Charakterisierung von Gemischen aus 1,4-PI und 3,4-PI. Chromatographische Methoden wurden für die Trennung dieser Mischungen entwickelt. Dabei zeigte sich, dass diese Homopolymere nicht einheitlich in ihrer Taktizität waren. Sie wiesen jeweils neben der Haupttaktizität verschiedene Mikrostrukturen der Monomereinheiten (z.B. 1,2-PI, 3,4-PI und 1,4-PI) auf. Durch

gekoppelte HPLC-NMR wurde es möglich, die Taktizitätsverteilung als Funktion der Molmasse darzustellen.

Im dritten Teil der Arbeit wurden PS-*b*-PI-Blockcopolymere untersucht. Diese Blockcopolymere wurden durch zwei Methoden hergestellt, (1) durch sequentielle lebende anionische Polymerisation und (2) durch Kupplung von lebenden Precursor-Blöcken. Auch bei diesen Proben zeigte sich, dass sie neben den eigentlichen Blockcopolymeren Homopolymerfraktionen enthalten. Der Anteil diese Homopolymere sowie die Zusammensetzung und Molmasse der Blockcopolymere konnte wiederum quantitativ durch HPLC-NMR ermittelt werden. Die Stereochemie der PI-Blöcke ergab sich aus der ^{1}H-NMR-Analyse von chromatographisch getrennten Fraktionen.

Im letzten Teil der Arbeit wurden PI-*b*-PMMA-Blockcopolymere charakterisiert. Diese Blockcopolymere wurden ebenfalls durch anionische Polymerisation hergestellt. Zur Analyse dieser Copolymere wurden HPLC-Verfahren entwickelt, bei denen mobile Phasen aus einem Lösungsmittel verwendet wurden. Demgegenüber wurden bei den vorherigen Untersuchungen jeweils mit binären mobilen Phasen gearbeitet. Der Vorteil dieses neuen Verfahrens liegt nun darin, dass sich der kritische Punkt der Adsorption durch Variation der Temperatur einstellen lässt. Gleichzeitig wird die Lösungsmittelunterdrückung bei der NMR wesentlich vereinfacht. Auch hier gelang es, neben der Molmasse und der chemischen Zusammensetzung die Mikrostruktur der beiden Blöcke als Funktion der Molmasse quantitativ darzustellen.

2. Introduction and Motivation

Block copolymers are macromolecules consisting of two or more chemically different polymer segments of a single type of monomer unit, covalently bound together. They represent a versatile class of functional materials for a multitude of applications because they combine the properties of incompatible but well known polymers. Among other properties, the ability of these polymers to modify interfacial properties and to enhance the compatibility of polymer blends makes this polymer type attractive for applications ranging from thermoplastic elastomers, information storage, drug delivery and photonic materials. With the development of living anionic polymerisation[1] the synthesis of block copolymers, especially those with complex architectures, has recently received increased attention due to interests in both academia and industry.

Diblock copolymers of polystyrene (PS) and poly (methyl methacrylate) (PMMA) [PS-*b*-PMMA] have been extensively used to make templates for fabrication of nanostructured materials.[2] Block copolymers of polyisoprene (PI) and PMMA [PI-*b*-PMMA] have been used as emulsifiers for the fabrication of polyester nanoparticles.[3] Copolymers of PI-*b*-PMMA are interesting because they can be used for rubber production, as effective compatibilisers for natural rubber/acrylic polymer blends[4], and as potential materials for medical applications[5].

Diblock copolymers of PS and PI [PS-*b*-PI] are thermoplastic elastomers. Chemical modification of these polymers, for example sulphonation, can give access to functional materials. These block copolymers can be used as templates for nanolithographic processes[6].

Block copolymers are complex materials. The physical properties of block copolymers are determined by their molecular characteristics, such as molar mass, chemical composition and chain architecture. In order to establish a detailed relationship between the molecular characteristics and macroscopic properties of a block copolymer, it is essential to perform a comprehensive analysis to determine their chemical composition distribution (CCD) and molar mass distribution (MMD). Generally, block copolymers are synthesised by sequential monomer addition, in which several factors should be controlled effectively, including the initiation efficiency of the macroinitiator (MI), the desired total molar mass and the molar mass distribution of each block. Standard characterisation methods such as nuclear

magnetic resonance spectroscopy (NMR) and Fourier transform infrared spectroscopy (FTIR), cannot differentiate the block copolymer from homopolymer blends. In other words, they cannot determine the existence of unreacted macroinitiator and/or the newly generated homopolymers in the final block copolymer product[7].

Since the 1950's, high performance liquid chromatography (HPLC) has emerged as a powerful technique to analyse various molecular distributions in synthetic (co)polymers. Size exclusion chromatography (SEC) is the most prevalent example of the use of HPLC for polymer characterisation separating macromolecules with regard to their hydrodynamic volume in solution. Because of the simple relationship between hydrodynamic volume and the molar mass for linear homopolymers, SEC has become the established method to determine the molar mass and MMD of synthetic polymers[8]. However; two intrinsic reasons hinder SEC from being an effective tool in fully characterising block copolymers. The first reason is the low resolution of SEC, which in most cases cannot fully separate the block copolymer from its precursor macroinitiator. The second reason is that the hydrodynamic volume of a copolymer is influenced by both molar mass and chemical composition. Specifically, SEC cannot provide information on the MMD of each individual block in the block copolymer. Therefore, new HPLC methods, such as liquid adsorption chromatography (LAC)[9-11,14] and liquid chromatography at critical conditions (LC-CC)[26,44] were developed, which consider the contribution of the enthalpic interactions between the analyte and the stationary phase in the column as a factor for polymer separation. Since chromatographic methods do not provide information about the microstructure of the monomer units in the block copolymers it is necessary to couple these selective separation techniques on-line with spectroscopic techniques such as NMR. The on-line coupling of HPLC and ^{1}H-NMR is a powerful and time saving tool for the analysis of complex mixtures. To our knowledge, there are no applications of LC-CC-NMR for the characterisation of block copolymers yet.

The main focus of this research work is to develop chromatographic methods for the characterisation of block copolymers. The developed separation methods are then directly coupled on-line with ^{1}H-NMR for fast and complete characterisation of these copolymers.

In the first experimental chapter PS-*b*-PMMA copolymers will be investigated. These block copolymers are synthesised by living anionic polymerisation. When block copolymers are synthesised by this method in addition to the copolymer there is also a possibility for the formation of homopolymer fractions. To get an exhaustive description of the MMD and CCD of the block copolymers as well as the homopolymers formed during synthesis, chromatographic techniques shall be developed and coupled with NMR to comprehensively characterise the samples. By using chromatography at critical conditions the copolymers shall be separated from the corresponding homopolymers. The sizes of the individual blocks shall be calculated. By using NMR as detector the tacticity of the PMMA block in the block copolymers shall be analysed selectively.

In the second experimental chapter blends of homopolymers of 1,4-PI and 3,4-PI will be investigated. Chromatographic techniques shall be developed for separation of these blends. The homopolymers of 1,4-PI and 3,4-PI are not homogeneous and each of them contains different isomeric structures of monomeric units such as 1,4-PI, 3,4-PI and 1,2-PI. The chemical composition of the blends and the microstructure of the homopolymers shall be determined by NMR.

PS-*b*-PI copolymers will be investigated in the third experimental chapter. These copolymers are synthesised by two different approaches: sequential living anionic polymerisation and coupling of living precursor blocks. When the copolymers are synthesised by these methods homopolymers are also formed. Samples shall then be analysed by developing chromatographic methods. The block lengths of the individual blocks, the chemical composition of the block copolymers and the microstructure of the PI blocks shall be analysed.

The fourth experimental chapter is dedicated to the analysis of PI-*b*-PMMA copolymers. These block copolymers are synthesised by living anionic polymerisation. New chromatographic methods shall be developed for the analysis of these samples. By coupling chromatographic techniques with NMR the block lengths of the individual blocks as well as the chemical composition of the copolymers shall be calculated. By using NMR as detector the microstructure of the individual blocks shall be identified and calculated.

3. Basic Theoretical Principles

3.1 High Performance Liquid Chromatography (HPLC)

HPLC is a common method for the analysis of polymers. By using this method complex polymer samples can be separated into different components. Depending on the chromatographic method used polymer samples can be separated according to molecular size, different types and numbers of functional groups, different types of monomers present in the polymer molecule and different architectures of the polymer molecules.

In a chromatographic experiment the complex polymer sample is dissolved in the mobile phase. This diluted polymer sample is then injected into the chromatographic column. The separation in any chromatographic process is related to the selective distribution of the analyte between a mobile and a stationary phase of a given chromatographic system[12]. The separation process in liquid chromatography can be described by:

$$\Delta G = \Delta H - T\Delta S = -RT \ln K_d \quad \text{.....(1)}$$

$$\ln K_d = \frac{-\Delta G}{RT} = \frac{-\Delta H + T\Delta S}{RT} \quad \text{.....(2)}$$

where R is the universal gas constant, T is the absolute temperature, ΔH and ΔS are the changes in interaction enthalpy and conformational entropy, respectively.

K_d is the distribution coefficient which is the ratio of the concentrations of the analyte in the stationary and in the mobile phase. There is still a debate concerning the exact definition of the volume of the stationary phase for polymer molecules[13]. K_d is related thermodynamically to the free energy difference ΔG of the molecules in the two phases[14]. This difference in free energy comprises of enthalpic (ΔH) and entropic (ΔS) contributions[15]. Experimentally K_d is determined from the following equation:

$$K_d = \frac{V_R - V_i}{V_P} \quad \text{.....(3)}$$

where V_R is the retention volume of the analyte, V_p the pore volume of the stationary phase and V_i the interstitial volume of the column.

Depending on the choice of the mobile and the stationary phase as well as temperature there are three different modes of liquid chromatography i.e. size exclusion chromatography (SEC), liquid adsorption chromatography (LAC) and liquid chromatography at critical conditions (LC-CC).

3.2 Size Exclusion Chromatography (SEC)

In size exclusion chromatography the change in conformational entropy of the macromolecules when interacting with the stationary phase is the dominant factor for the distribution coefficient. For a given pore size, macromolecules of different sizes may or may not enter these pores. Large macromolecules cannot penetrate the complete pore volume. Entering the pores from the free mobile phase causes a loss of entropy. Certain conformations of the macromolecules do not fit into the pores[16]. In addition, for a given fixed polymer conformation, the centre of gravity cannot access certain regions of the pore volume, due to steric exclusion of parts of the molecule from the pore wall[17]. In ideal SEC, separation is accomplished exclusively due to the hydrodynamic size of the macromolecules since no enthalpic interaction exists *(i.e.* $\Delta H = 0$) between the stationary phase and the polymer molecules[18]. The distribution coefficient is given by:

$$K_{SEC} = \exp\frac{(\Delta S)}{R} \qquad (4)$$

Since $\Delta S<0$ the distribution coefficient in SEC ranges from 0-1. The smaller the macromolecules the more pore volume they can penetrate and the longer they are retained in the stationary phase. Large macromolecules will be eluted earlier followed by macromolecules of smaller sizes. By using a suitable calibration the molar mass distribution, the molar mass averages and polydispersity of a polymer sample can be determined.

3.3 Liquid Adsorption Chromatography (LAC)

Liquid adsorption chromatography is classically employed for the separation of small molecules. However, it is increasingly used for the separation of polymers regarding chemical composition distribution. In polymer adsorption chromatography, the separation mechanism is driven by adsorptive interactions between the macromolecules and different functional groups attached to the stationary phase. In ideal LAC conformational changes are assumed to be zero *($\Delta S=0$)* because the pores of the stationary phase are sufficiently large to accommodate all macromolecules. The enthalpic contribution (ΔH) is due to the attractive interactions of the molecules with the stationary phase. The distribution coefficient in adsorptive mode is given by:

$$K_{LAC} = \exp\frac{(-\Delta H)}{RT} \quad \text{.....(5)}$$

Since ΔH is negative the values of the distribution coefficient are $K_{LAC} > 1$. In order to achieve enthalpic interactions between the dissolved polymer molecules and the stationary phase a thermodynamically poor solvent is used as the mobile phase. By using a thermodynamically good solvent such interactions can be suppressed. Such good solvents are used in the case of SEC.

The retention volume V_R is given by:

$$V_R = V_O + K_{LAC}(V_P + V_{stat}) \quad \text{.....(6)}$$

where V_p is the pore volume of the stationary phase, V_O is the void volume of the column and V_{stat} is the volume of the stationary phase. The separation in LAC is achieved by the interactions between the polymer and the stationary phase. At weak interactions with the stationary phase, the retention volume increases approximately exponentially with molar mass[19]. For homopolymers, with an increase in molar mass the number of interacting groups increases. This increases the possibility of adsorption of the molecules on the stationary phase. The distribution coefficient increases accordingly, resulting in large elution volumes even though the interaction

of a single repeating unit with the stationary phase is very weak. This phenomenon can be explained by the multiple attachment mechanism proposed by Glöckner[20]. Polymers with higher molar masses will be strongly adsorbed on the stationary phase and will elute later than lower molar masses[21]. The molar mass dependence in LAC is opposite to that in SEC. The strength of interaction between the analyte molecules and the stationary phase can be controlled by the eluent composition and/or the temperature[7].

3.4 Liquid Chromatography at Critical Conditions (LC-CC)

The transition between the two chromatographic modes of SEC and LAC is observed under special conditions, known as critical conditions. At critical conditions the entropy loss due to the exclusion of the polymer molecules from the pore walls of the stationary phase are exactly compensated by the enthalpy gain due to interactions of the molecules with the stationary phase[22-23]. The distribution coefficient is given by:

$$K_d = \exp\left(\frac{\Delta S}{R} - \frac{\Delta H}{RT}\right) \quad (7)$$

The change in interaction energy is zero i.e. $\Delta G = 0$ and $T\Delta S = \Delta H$. Accordingly, $K_d = 1$. At the critical point of adsorption the Gibbs free energy is constant and the distribution coefficient of a polymer chain becomes unity ($K_d = 1$), irrespective of the molar mass of the macromolecules and the pore size of the stationary phase. Chromatography at these conditions is known as liquid chromatography at critical conditions of adsorption (LC-CC) where molar mass dependence of retention time vanishes[19,24-29].

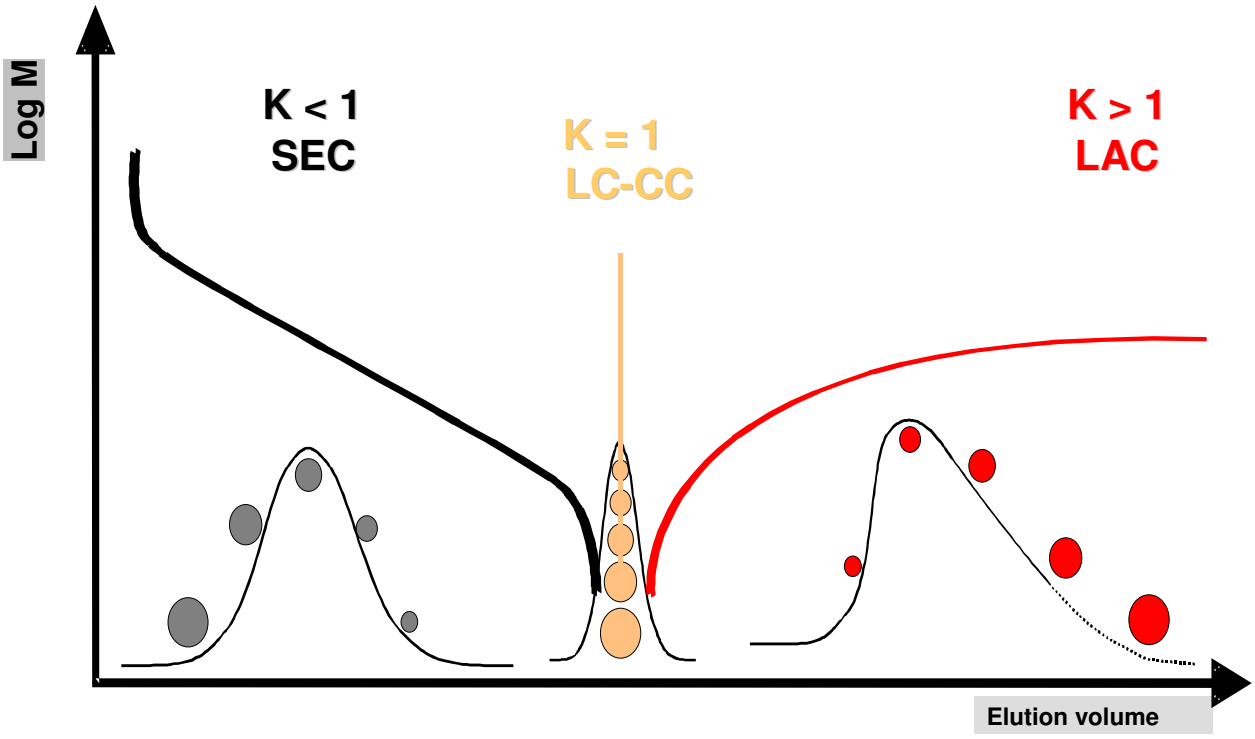

Figure 1: Schematic representation of the dependences of the elution volume on the molar mass for size exclusion, adsorption and chromatography at critical conditions of adsorption

At critical conditions, non-functionalised homopolymers elute at the same elution volume irrespective of the chain length and molar mass. The critical conditions for a given type of polymer depends crucially on the nature and type of stationary phase, eluent composition, temperature and the flow rate[30]. Since at critical conditions, the elution volume of a complex polymer is not affected by the molar mass of the homopolymer chain, separations according to endgroups, topology[31-41] or segments of different chemistry as in block[42-48] or graft copolymers[49-50] have been realised. Separations of blends[51-54] and even separations based on tacticity[55] have been reported. For the separation of block copolymers chromatography at critical conditions has been employed. By using critical chromatography it is possible to make one block of the copolymer chromatographically invisible. This means that homopolymers of the block elute at the same elution volume irrespective of the molar mass. The block copolymer can then be separated with respect to the block length of

the second block. Critical conditions have been established for a number of polymers[56]. Inspite of this, the application of LC-CC might be limited due to the difficulties in the determination of the critical eluent composition.

3.4.1 Analysis of block copolymers by LC-CC

In general, the analysis of block copolymers is rather complicated due to the simultaneous distributions in molar mass and chemical composition. The chemical composition may be expressed as an average number, characterising the total amount of each monomer in the reaction product. However, more detailed information is obtained when the chemical composition distribution is determined, characterising the sequence distribution of the different monomer units along the polymer chain. Depending on the sequence of incorporation of different monomers into the polymer chain, alternating and random copolymers, or graft and block copolymers are obtained. In addition, homopolymers of the different monomers are formed as unwanted by-products.

The analysis of block copolymers by chromatography at critical conditions is based on the concept of invisibility which assumes that if one establishes critical conditions for one block of the copolymer the repeating units of this block are chromatographically invisible and do not contribute to retention[57]. The chromatographic behaviour of the block copolymer is then dependent on the characteristics of the second block of the copolymer. The application of liquid chromatography at the critical point of adsorption to block copolymers is based on the consideration that Gibbs free energy ΔG_{AB} of a block copolymer A_nB_m is the sum of the distributions of block *A*, block *B*, ΔG_A and ΔG_B respectively.

$$\Delta G_{AB} = \Sigma n_A \Delta G_A + n_B \Delta G_B + \chi_{AB} \quad (8)$$

where χ_{AB} describes the interactions between blocks *A* and *B*. Assuming no specific interactions between *A* and *B* ($\chi_{AB} = 0$), the change in Gibbs free energy is only a function of the contributions of *A* and *B*.

$$\Delta G_{AB} = \Sigma n_A \Delta G_A + n_B \Delta G_B \quad (9)$$

By the use of chromatographic conditions, corresponding to critical point of homopolymer *A*, block *A* in the block copolymer will be chromatographically invisible, and the block copolymer will elute solely with respect to block *B*. Here $\Delta G_A = 0$, so Equation (9) becomes

$$\Delta G_{AB} = \Sigma n_B \Delta G_B \quad \text{.....(10)}$$

At the chromatographic conditions corresponding to critical point of homopolymer *B*, the opposite phenomenon is observed.

By using this concept of invisibility it is possible to analyse the second block of the copolymer regarding chemical heterogeneity and molar mass distribution independent of the first block.

The analysis of block copolymers by using chromatography at critical conditions can be divided into two groups:

1) The critical conditions for one component are established in such a way that the second component elutes in adsorption mode. By using this method it is possible to characterise the second component not only according to size but also according to the chemical composition, for example end groups[58]. It is also possible to characterise the size of the macromolecules, but this method is limited to macromolecules with smaller molar mass because retention is dependent exponentially on the size of the macromolecules[57].

2) The second component elutes in the SEC mode, before the first component elutes at the critical point of adsorption. This method is used for determining the block length of the second component. By choosing stationary phases having different polarities it is possible to establish critical conditions for the respective block. By using these critical conditions it is possible to determine the molar mass distribution of both the blocks.

In the present case the second method is used for determining the molar mass distribution of the block copolymers under study. For the analysis of PS-*b*-PMMA copolymers the polarities of different block components have to be considered. It is seen that the PS and PMMA blocks of the copolymer have different polarities. The

PMMA block is the polar block. By using a polar stationary phase it is seen that PMMA is strongly adsorbed as compared to PS and will elute at higher elution volume. By establishing the critical conditions for PMMA, PS will elute at lower elution volume, i.e. in the SEC region. Thus it is possible to determine the molar mass distribution of the PS block.

By using a non-polar stationary phase the opposite phenomenon is seen. PS elutes earlier as compared to PMMA. By establishing critical conditions for PS, it is seen that PMMA elutes in the SEC region and the block length of PMMA can be determined.

Pasch et al. analysed PS-*b*-PMMA copolymers by operating at the critical conditions of both the blocks[42,44]. Falkenhagen et al. characterised both blocks of poly(methyl methacrylate)-*b*-poly(tert-butyl methacrylate) by operating at the critical conditions for the corresponding homopolymers[47]. Triblock copolymers of poly(ethylene oxide-*b*-propylene oxide-*b*-ethylene oxide) were characterised by operating at critical conditions of the inner block as well as both the outer blocks[45,59].

3.5 Basic principles of NMR and direct coupling of HPLC and NMR

3.5.1 Basic principles of NMR

Nuclear magnetic resonance (NMR) is one method which belongs to the field of high frequency spectroscopy. The resonance absorption of electromagnetic energy takes place through the nuclei of solids, liquids and gases which are affected by strong and constant magnetic field. Basic principle of NMR is paramagnetism of the nucleus. A number of nuclei have spin and due to that a permanent dipole moment. It is known in general that nuclei with spin quantum number $I>0$ possesses a magnetic moment. Three cases can be possible. (a) Nuclei with even number of protons and even number of neutrons have $I=0$ (for example ^{12}C, ^{16}O) these nuclei are magnetically inactive. (b) Nuclei with odd number of protons and even number of neutrons and vice versa have $I=1/2$ *to* $9/2$ (for example ^{1}H, ^{13}C, ^{15}N, ^{31}P) these nuclei can be measured with NMR. (c) Nuclei with odd number of protons and odd number of neutrons have $I=1$ *to* 7 (for example ^{14}N, ^{2}H) these nuclei are magnetically active.

When a sample is placed in static magnetic field of strength B_0, it gives rise to a magnetic moment which rotates at some speed around the applied field; this is referred to as the Larmor frequency of the nucleus ω_0. In order to achieve resonance condition we irradiate perpendicular to the static magnetic field. The oscillating magnetic field then gives the condition that Larmor frequency is equal to the resonance frequency. This results into free induction decay *(FID)* which can be detected[63]. The constant of proportionality is the gyromagnetic ratio γ. It is a characteristic constant of the nuclear isotope.

$$\omega_0 = \gamma B_0 \quad \text{.....(11)}$$

In the first few decades all spectrometers, used a technique called the continuous wave spectroscopy (CW). By using this technique NMR spectra could be obtained using a fixed magnetic field and sweeping the frequency of the electromagnetic radiation, this more typically involved using a fixed frequency source and varying the current (and hence magnetic field) in an electromagnet to observe the resonant absorption signals[64]. Since the 70^s Fourier transform NMR was introduced with different pulsed techniques. By using these tecniques in addition to ^{1}H-NMR and ^{13}C-NMR a number of 2-D NMR experiments such as homonuclear and heteronuclear correlations can be performed. 3-D and 4-D NMR can be used for the determination of protein structure.

The NMR frequency is determined by the magnetic field at the site of the nucleus. In molecules the atomic nuclei are surrounded by electrons. When an atom is placed in a magnetic field, its electrons circulate about the direction of the applied magnetic field. This circulation causes a smaller magnetic field at the nucleus which opposes the externally applied field. Therefore at the nucleus the effective magnetic field is not same as the applied magnetic field. The electron density affects the applied magnetic field. Stronger electron density weakens the applied magnetic field. Thus the effective magnetic field at the nucleus is generally less than the applied magnetic field by a quantity σ, which is the magnetic shielding constant for a given chemical group. This shielding constant is a dimensionless quantity.

$$B_{eff} = B_0 (1 - \sigma) \quad \text{.....(12)}$$

The applied magnetic field and the effective magnetic field at each nucleus will vary depending on how strong or weak is the magnetic shielding. This gives rise to the chemical shift phenomenon. The chemical shift is defined as the nuclear shielding divided by the applied magnetic field. The chemical shift is only a function of the nucleus and its environment. It is always measured from a suitable reference compound. This may be an external reference, for example, a compound in a capillary tube placed in the sample tube or more commonly the reference compound added to the solution investigated. Sometimes the solvent peak itself may be used as reference. These are internal references.

The chemical shift is now defined as

$$\delta = {(\nu_{Substance} - \nu_{Reference})} \Big/ {\nu_{observe}[ppm]} \quad \text{.....(13)}$$

where $\nu_{Substance}$ – Resonance frequency of the substance

$\nu_{Reference}$ – Resonance frequency of the reference

$\nu_{observe}$ – Spectrometer frequency

The chemical shift is reported in parts per million (ppm). The chemical shift is a dimensionless quantity.

By using this equation it is possible to compare spectra measured with spectrometers having different frequencies as the chemical shifts are expressed in ppm and it is not necessary every time to measure the frequency of the signals. In NMR spectroscopy, the standard reference substance for protons is tetramethylsilane (TMS). TMS has a chemical shift of 0 ppm. The chemical shift is a very precise metric of the chemical environment around the nucleus. The nuclei of different elements have different ranges of chemical shifts. The ranges exhibit the variety of electronic environments of the nuclei in molecules. The proton chemical shifts span a range of 20 ppm for most of the compounds, whereas the carbon chemical shifts span a much broader range of 300 ppm. For ^{13}C, the reference frequency is the ^{13}C resonance in TMS. Structure elucidation of unknown organic compounds is usually performed by the combined use of ^{1}H and ^{13}C NMR spectroscopy.

3.5.2 ^{1}H-NMR experiment

Protons are the most widely studied nuclei because they are ubiquitous and they have a high sensitivity. The conventional way of recording NMR spectra is to dissolve the sample of interest in a 5 mm cylindrical glass tube by adding about 0.5 ml of deuterated solvent. The sample dissolved in the solvent is available during the entire experiment for the registration of NMR spectra. By applying the pulse Fourier transform acquisition mode, a gain in signal to noise ratio (*S/N*) of the acquired NMR spectrum can be obtained by co adding the Free Induction Decays (*FIDs*) resulting from pulse excitation. The *FID* is dependent upon the transverse relaxation time T_2, which affects the line shape and the resolution of a spectrum. The recovery of equilibrium magnetisation is determined by the spin lattice relaxation time T_1. After pulse excitation, it takes a time period of three to five times the T_1 to establish the full Boltzmann distribution, together with full magnetisation of the nuclei. Then a new excitation pulse can be applied. The signal to noise ratio is defined by the square root of the number of the number of transients (*NS*). The pulse relaxation time for a new excitation of fully relaxed nuclei is dependent upon the spin lattice relaxation time T_1. The range of proton chemical shifts is between 0 and 15 ppm[60-61]. In case of very complex mixtures there may be overlap of different structures which cannot be resolved and quantified by proton NMR experiments. To solve such problems carbon NMR experiments (^{13}C) have to be performed. These experiments provide direct information about the carbon skeleton of the investigated molecule, thus revealing valuable structural features such as carbonyl and carboxyl moieties, which cannot be deduced by ^{1}H-NMR spectroscopy.

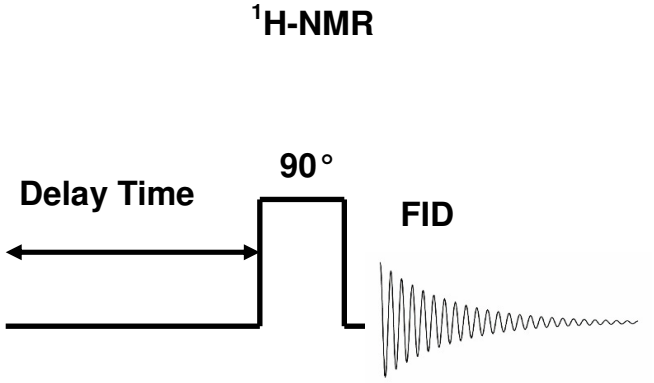

Figure 2: The pulse diagram to read the NMR signal while performing a ^{1}H-NMR experiment [62]

3.5.3 ^{13}C- NMR experiment

The big disadvantage of ^{13}C-NMR spectroscopy is its low sensitivity. Due to the natural abundance of 1.1 % of the ^{13}C isotope and due to long spin-lattice relaxation times (T_1) of the order of seconds to minutes, the acquisition of a routine ^{13}C NMR spectrum of a 0.1 M solution of an organic compound takes several minutes.

Since carbon is a low sensitivity nucleus it is better to dissolve the sample of interest in a 10 mm tube, so that the active volume of the NMR coil contains more of the nucleus of interest. High concentrations are often required for the low sensitivity nucleus. ^{13}C-NMR spectra are very complex and one observes a number of signals as they are coupled to protons. The signals of ^{13}C distribute themselves into multiplets. To get rid of this negative effect it is necessary to decouple protons from carbons while performing the experiment. In the decoupled spectra one then observes singlets. Since all the protons are decoupled from carbon this experiment is called ^{1}H-Broadband-Decoupling. In order to perform this experiment one uses composite pulses. Therefore, it is also called composite pulse decoupling. As the decoupler is on during the entire experiment protons are decoupled from carbon continuously[63].

The advantage of using this experiment is that due to the heteronuclear overhauser effect the intensity of the signal can be increased (a maximum NOE factor of 2.98 can be reached depending on the number of attached protons).

However, the signals intensities cannot be quantified anymore. Another experiment which can be performed is Inverse gated decoupling experiment. Here the decoupler is on in the ^{13}C-channel only at the time of pulse excitation and during the acquisition of spectra. As a result no NOE^{s} build during the experiment and the intensities of the ^{13}C-NMR signals are not falsified.[51] This method is a quantitative one. The integration of the signals provides information about the number of carbons present in the compound.

Carbon NMR is often used to study polymers because of the large chemical shift range and resolution. Although ^{13}C is not very sensitive compared to protons, the carbon spectrum is spread over a much larger range, so there is a greater chance that the carbon spectrum will be well resolved. The range of carbon chemical shifts is between 0 and 200 ppm. ^{13}C chemical shifts are of interest in polymer studies because they are very sensitive to molecular structure and conformation. The correlation between carbon chemical shift and molecular structure has been extensively investigated and empirical correlations between the structure and chemical shift have been reported[65-66].

Solution NMR is an important method for polymer characterisation, especially the microstructure of the polymers such as tacticity, branching, stereochemical isomerism, geometric isomerism, end groups, chain architecture and chemical composition of copolymers[67].

In the study of block copolymers NMR spectroscopy cannot distinguish between blocks and blends of homopolymers formed during the synthesis of the copolymers. It gives us no information about the molar mass distribution as well as the chemical composition distribution of the total block copolymer and the individual blocks. NMR spectroscopy gives no information on the amount and molar mass of homopolymers formed. In order to completely characterise the block copolymers the hyphenation of chromatographic separation techniques with NMR spectroscopy is one of the most powerful and time-saving methods for the separation and structural elucidation.

Coupling of chromatographic techniques with continuous flow ^{13}C-NMR would be the ideal choice. But since the ^{13}C-isotope is not sensitive there are not many applications in this field. It is possible to monitor electro-chemical reactions of high concentration compounds (0.1 M solutions)[68], or even to use diluted samples with ^{13}C-labelled positions[69-71]. However, this technique is not feasible for recording continuous flow ^{13}C-NMR spectra of chromatographic peaks. The only choice for

recording spectra in the continuous-flow mode is the coupling of chromatographic techniques with ^{1}H-NMR. In order to get ^{13}C chemical shift information, indirect detection 2D experiments such as ^{1}H-^{13}C-NMR spectra can be performed in the stop-flow mode.

3.5.4 NMR spectroscopy in a flowing liquid

In the conventional measuring mode, the NMR experiments are carried out with probe heads holding NMR tubes. In case of flow NMR, however, the probe head contains a flow cell which allows a continuous flow through the entire probe. The NMR detection coil covers usually an active volume of 60-120 µL. Depending on the flow rate the sample remains only for some seconds within the active volume. This residence time τ is dependent upon the volume of the detection cell and the employed flow rate. A shorter residence time τ within the NMR measuring coil results in a reduction of the effective lifetime of the particular spin states. Thus the effective relaxation rates, $1/T_n$ are increased by $1/\tau$:

$$1/T_{n\ effective} = \sum 1/T_i + 1/\tau \quad \text{..... (14)}$$

In the following system, the reciprocal relaxation rates, the relaxation times T_{1flow} and T_{2flow} are reduced according to the following:

$$1/T_{1flow} = 1/T_{1static} + 1/\tau \quad \text{..... (15)}$$
$$1/T_{2flow} = 1/T_{2static} + 1/\tau \quad \text{..... (16)}$$

In a net effect, the pulse repetition times in flowing systems can be reduced to the decrease in the apparent spin-lattice relaxation times T_{1flow}, whereas at a given detection volume an increase in flow rate leads to an increase in the signal half-width W due to the decrease of T_{2flow}.

$$W = (1/\pi)\ T_2 \quad \text{..... (17)}$$
$$W_{flow} = W_{stationary} + 1/\tau \quad \text{..... (18)}$$

Thus, the resolution of a continuous flow ^{1}H-NMR spectrum is strongly dependent upon the flow rate/detection volume ratio.

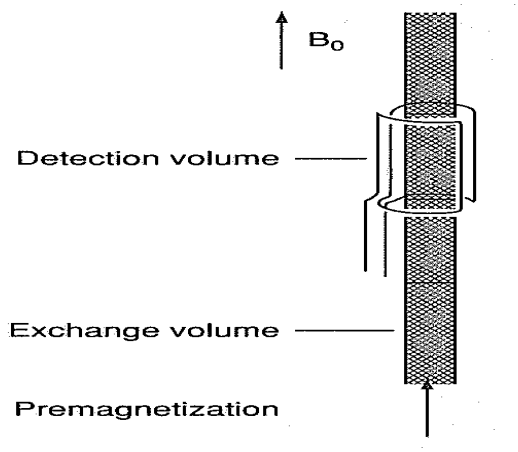

Figure 3: Continuous-flow NMR detection principle

In an on-flow NMR experiment, the excited nuclei leave the flow cell whereas fresh nuclei enter. Due to the decrease of the apparent T_{1flow} rates, faster pulse repetition rates can be used and more transients can be accumulated in a distinct period of time. The theoretical maximum sensitivity is obtained when the pulse repetition time (*PRT*) is equal to the residence time τ in the NMR flow cell. To achieve this we should have optimum values of acquisition time and relaxation delay.

$$PRT = (Acquisition\ time\ AQ + Relaxation\ delay\ D1)\ optimum = \tau \quad \ldots\ldots\ldots \quad (19)$$

If the fresh incoming nuclei are fully magnetised upon entering the flow cell, the Boltzmann distribution is established, an increase in sensitivity can be obtained[72-75].

3.5.5 Design of continuous NMR flow probes

The first approach for continuously recording NMR spectra was to use the conventional existing probe for the registration of NMR spectra. The spectra are usually recorded under rotation of the NMR tube with a rotational speed of 20 Hz in order to remove magnetic field inhomogeneities. Watanabe and Niki[76] modified the NMR probe to make it more sensitive, introducing a thin-wall Teflon tube transforming it into a flow through structure. The main problem with this design was that no

complete transfer of the mobile phase is guaranteed by the employment of the tube. Peak mixing and memory effects will occur at the bottom of the rotating NMR tube. Thus, it would be more straightforward to employ a bubble cell design of a widened glass tube. This approach was used for the registration of the first continuous flow NMR spectra with iron magnets[77-81] and also together with cryomagnets[82-90].

This design which was introduced in the early 1980s is still used today. Such a design combines the bubble cell characteristics together with a U-type design of the glass tube employed as the NMR detector. For on-line HPLC-NMR and GPC-NMR coupling a vertically oriented flow cell with a directly fixed double-saddle coil is used[91-96]. The whole arrangement is centered in the glass Dewar of a conventional probe body, in which a thermocouple is inserted, allowing the execution of temperature dependent measurements. By fixing a U-type glass tube in the Dewar of a NMR probe body, the central symmetry of the magnetic field in the z-direction of the cryomagnet is broken and the rotation of the glass tube is not possible.

The internal diameter of the glass tube is either 2, 3, or 4 mm resulting in detection volumes of 60, 120 and 180 µL, respectively. The glass walls of the flow-cell are parallel at least within the length of the proton detection coil (18 mm) and taper at both ends to fit PTFE tubing (i.d. 0.25 mm). PTFE tubing and glass tube are connected by shrink-fit tubing. Inverse continuous flow probes contain an additional coaxial coil (matched to the ^{13}C resonance frequency) surrounding the ^{1}H detection coil for heteronuclear $^{1}H/^{13}C$ shift correlated experiments. However, in contrast to the conventional probe design, the filling factor i.e. the ratio of sample volume to the NMR detection volume is much higher. As both the inlet and outlet of the continuous flow detection cell are at the bottom of the cylindrical NMR probe, the whole probe body can be inserted into the room temperature bore of the cryomagnet. No problems with air bubbles exist because the NMR detection cell is filled from the bottom to the top against the gravity of earth. Within this design the radiofrequency coil is positioned parallel to the z-direction of the magnetic field of the cryomagnet, magnetic field homogeneity can be readily achieved, because the device for the correction of the magnetic field, the so called shim system is optimised for correcting inhomogeneities in the z-direction. Thus, the U-type flow cell shows very good NMR characteristics, despite the non-rotation of the cell.

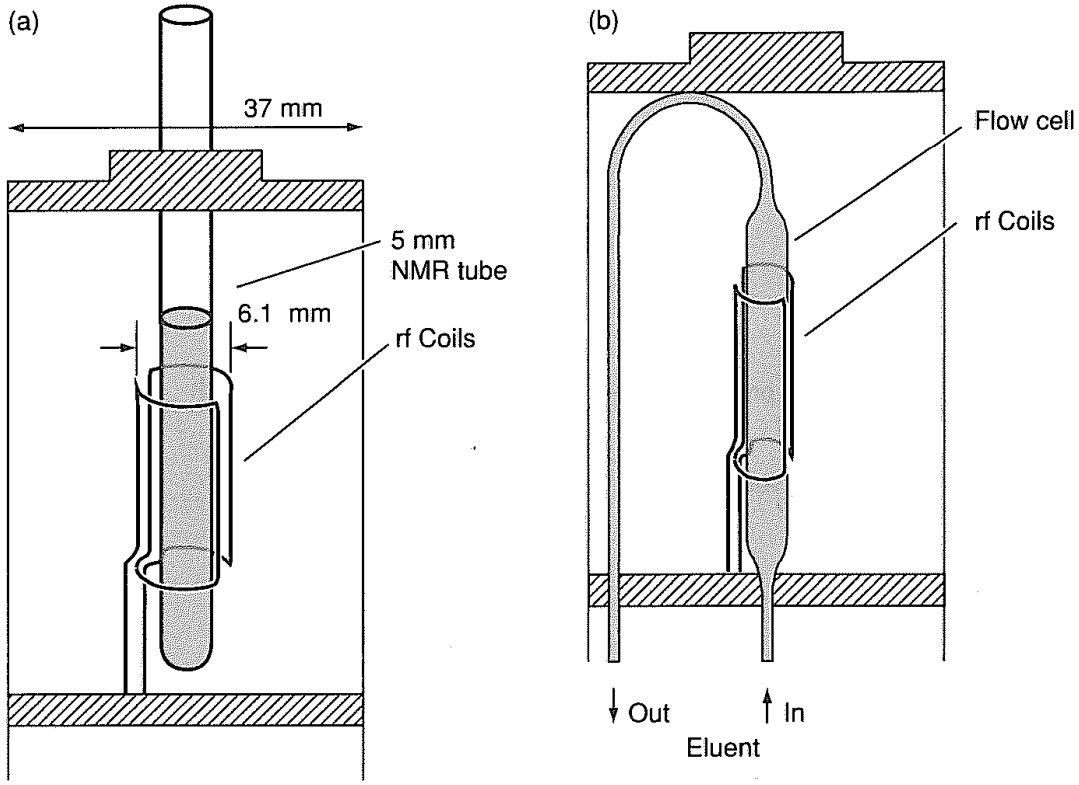

Figure 4: Schematics of (a) conventional and (b) continuous flow NMR probes used for cryomagnets

3.5.6 Solvent suppression

Solvent suppression is necessary while performing HPLC-NMR and GPC-NMR for observing small analyte signals in the presence of much larger signals from the mobile phase. Solvent signal suppression is performed by using the techniques mentioned below:

3.5.6.1 Presaturation (NOESY presaturation)[97-98]

The principle of presaturation relies on the phenomenon that nuclei which are unable to relax, because their population in the ground state α and the excited state β is the same, do not contribute to the free induction decay after pulse irradiation. A highly selective low-power pulse irradiates the desired solvent signals for 0.5 to 2 s, prior to data acquisition, thus leading to saturation of the solvent signal frequency. NOESY-

type presaturation is an effective pulse sequence of presaturation. It can be combined with shifted laminar pulses[99] for multiple solvent suppression. This technique is especially suitable for stop-flow measurements but can also be used for on-flow measurements.

3.5.6.2 WATERGATE (WATER by GrAdient Tailored Excitation)[100-102]

The WATERGATE technique, one of the most promising techniques, relies on a refocusing pulse flanked by two symmetrical pulsed field gradients (PFGs) to attenuate the water resonance. This method evolved from the realisation that echo techniques provided superior phase properties compared with conventional selective excitation. The WATERGATE technique is restricted to refocusing elements that are antisymmetric in time or that have a net rotation axis that is stable as a function of offset.

It would be an alternative for use in stop-flow experiments. It can also be easily combined with ^{13}C satellite decoupling during the shaped pulses.

3.5.6.3 BPPSTE (BiPolar gradient Pulsed Stimulated Echo)[103]

This technique is derived from diffusion-ordered spectroscopy. After the first 90° radio frequency (RF) pulse, the magnetisation is located in the x-y plane, then a pair of gradient pulses is applied to dephase the signals. The second pair of gradient pulses is used to rephase the magnetisation. The large molecule diffuses slowly and thus remains in exactly the same B_o magnetic field throughout the diffusion period. In contrast, the small molecules, such as solvent, diffuses rapidly and thus is not refocused later, resulting in zero net magnetisation. It is based on the large differences of the diffusion coefficients of the solvents as compared to those of the macromolecules.

Wu and Beshah have successfully applied it for the eliminating solvent signals in SEC-NMR[104]. It is applicable for both on-flow and stop-flow experiments.

3.5.6.4 WET (water suppression enhanced through T_1 effects)[106,108]

The WET sequence uses four selective shaped pulses of variable lengths and different flip angles. Each selective pulse is followed by a dephasing field gradient pulse having a certain ratio to each other. The read pulse of the sequence can be a rectangular pulse, a composite hard pulse or a shaped composite pulse. In practice, SEDUCE[105] is the favoured pulse shape because of its high selectivity at rather short pulse lengths, in comparison with other shapes. By varying the flip angle of the selective shaped pulse, the WET sequence can be optimised. On an average, the suppression duration will be less than 100 ms. ^{13}C-decoupling is applied during the shaped pulses and the acquisition period, for eliminating the ^{13}C satellites. If several ^{13}C resonances need to be decoupled, band-selective ^{13}C-decoupling should be applied including adiabatic decoupling schemes such as WURST[107].

By the combination of shaped RF pulses, pulsed-field gradients (PFG) and selective ^{13}C-decoupling the acquisition of high quality spectra at on-flow conditions with HPLC gradients is also possible. This technique is superior in the on-flow mode but can also be used in the stop-flow mode.

However, all the solvent suppression techniques mentioned above have the big disadvantage that compound signals lying under the solvent signal are also suppressed. Thus valuable information may be lost. This is the reason why multiple solvent suppression is only useful to a limited extent because too much spectroscopic information may be lost after eliminating too many signals. Therefore, solvents should be chosen in such a way that they do not overlap with the compound signals of interest.

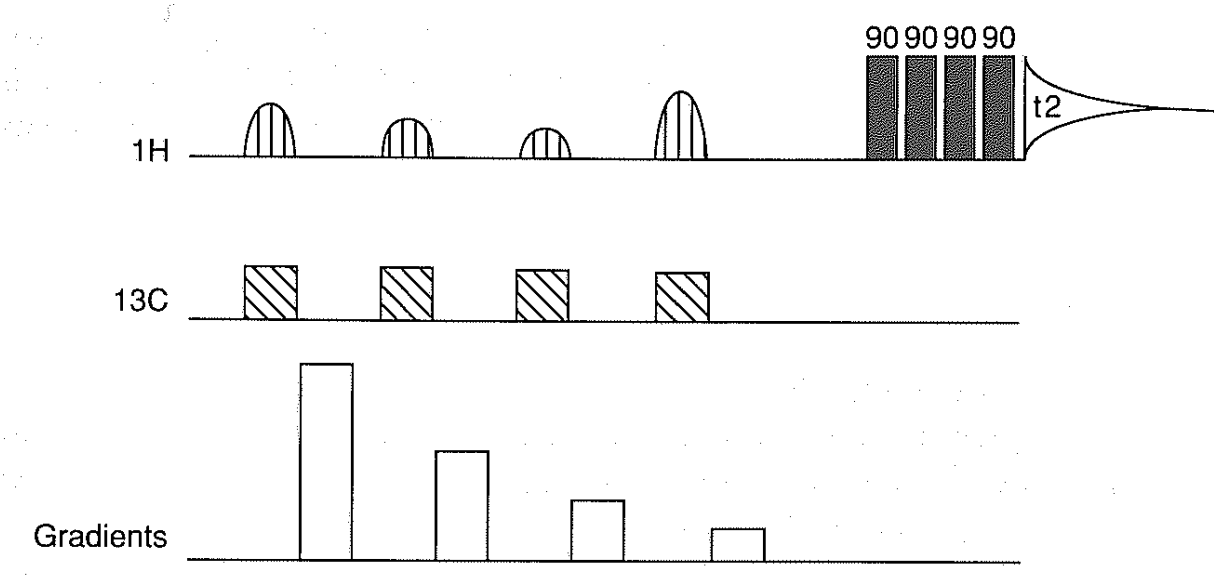

Figure 5: Representation of the WET pulse sequence for multiple solvent suppression used for the HPLC-^{1}H-NMR experiment

3.5.7 Different working modes in HPLC-NMR

For carrying out LC-NMR coupled experiments special interfaces with switching valves under software control are required for reliable and reproducible results. The working modes can be first differentiated by the status of the sample during the measurement. The four different working modes in LC-NMR are:

1. On-flow or continuous-flow
2. Direct stop-flow
3. Time-slice
4. Loop storage/loop transfer

1. On-flow or continuous-flow

The outlet of the chromatographic system is directly connected to the NMR detection flow cell. NMR spectra are acquired continuously while the sample is flowing through the flow cell. The result is a set of one-dimensional (1D) NMR spectra which cover the whole chromatogram and are typically displayed as a two-dimensional (2D) contour plot showing chemical shift of the NMR spectrum on the X-axis versus the

retention time on the Y-axis. The chromatography and NMR system perform independently of each other. The only necessary link between the two is the liquid capillary connection between the column and the NMR flow cell. The NMR spectrometer can perform the function as a detector for the chromatographic system, so no conventional LC detector in the chromatographic system is necessary.

2. Direct stop-flow

In this mode, the eluent is directly flowing from the chromatographic system into the NMR flow probe. Stop-flow requires the calibration of the delay time, which is the time required for the sample to travel from the LC detector (typically a UV detector) to the NMR flow cell. The delay time in turn depends on the flow rate, the volume of the flow cell and the length of the capillary connecting HPLC with the NMR. As only selected peaks are measured in the NMR spectrometer the separation is monitored in parallel with an UV detector. The separation is interrupted when the chromatographic peak of interest reaches the centre of the NMR flow cell. Different types of 1D and 2D experiments can be performed. In order to measure further peaks, the separation is continued until the next peak is positioned in the NMR flow cell. The result is a set of NMR spectra for certain selected peaks of the chromatogram. The samples remain static in the flow cell and the conditions should remain static during the whole NMR experiment.

3. Time-slice

Time-slice involves a series of equidistant stops during the elution of the chromatographic peak of interest. Time-slice is used when two analytes elute together or with close retention times, or when the separation is poor. For carrying out this experiment an interface such as peak sampling unit is connected between the chromatographic system and the NMR flow probe[109].

4. Loop storage/loop transfer

In this mode, the eluent is directly flowing from the chromatographic system into the storage device. As only selected peaks are measured in the NMR system the

separation is monitored, in parallel, with an LC detector. A peak is selected from the chromatogram recorded by the LC detector. The time taken for the peak to move from the LC detector into the storage loop is recorded. Now the selected peak is stored in the storage loop. Without interrupting the separation, further peaks can be trapped in the subsequent storage loops.

At a later stage, after the separation is completed, the loop contents are transferred into the NMR flow probe. Different types of 1D and 2D NMR measurements can be carried out. The result is a set of NMR spectra for certain selected peaks of the chromatogram. As the separated peaks are collected in storage loops, it is not influenced by start and stop disturbances as well as diffusion due to long waiting times. The transfer process is completely independent from the NMR measurements. This means that the samples can be prepared for the NMR measurements while the NMR spectrometer can be used for other purposes. Once the peaks are stored and isolated in the loops, the measurement times for the individual experiments are not limited by diffusion effects.

The contamination of samples with previously eluted peaks can be avoided. The volume of the storage loops is similar to that of the NMR flow cell, but as the volume is formed by a capillary rather than by a cavity with a large inner diameter, the broadening effects are dramatically reduced. In addition, the peaks are first stored in separate, previously washed loops so that they contain the clearly separated peaks. Between measurements of the samples, the NMR flow cell can be washed with an arbitrary amount of solvent. The technique is very useful for the measurement of closely eluting peaks and systems with large concentration differences.

3.5.8 Purity of HPLC grade solvents

Most of the solvents used contain small amounts of impurities due to the presence of added stabilising chemicals. The HPLC grade solvents are supposed to be especially pure but NMR measurements show that these solvents also contain small amounts of impurities. NMR detection is much more sensitive to smaller amounts of individual chemicals due to solvent suppression of the main solvent peaks. The most commonly used solvents, such as D_2O and acetonitrile are available with high NMR purity. For all other solvents, the amount of impurity present has to be examined by using a

reference spectrum. In some cases it is feasible to distill the HPLC grade solvents before performing the HPLC-NMR experiments.

4. Results and Discussion

4.1. Analysis of PS-*b*-PMMA copolymers and blends of PS and PMMA

4.1.1 Method development for establishing the critical conditions of PMMA

For separating PS-*b*-PMMA copolymers critical conditions were established for the PMMA block. In order to select appropriate eluents for LC-CC, attention should be paid to evaluate the polarities of the stationary and mobile phases in comparison to the polarities of the monomer units. Since PMMA is the polar part of PS-*b*-PMMA copolymer critical conditions were established by using a polar and non polar solvent mixture and a set of normal phase Si columns. It has been shown in Ref.[42] that mixtures of MEK-cyclohexane as the mobile phase are well suited for establishing the critical conditions. Using a set of polar stationary phases Si 300-5 and Si 1000-7 with column dimensions of 200x4.6 mm inner diameter, PMMA will elute at critical conditions whereas PS will elute in size exclusion chromatography (SEC) mode. Thus separation takes place in the order of increasing polarity. The molar masses of the copolymers and polymer blends under investigation are summarised in Table 1.

Sample	PS-b-PMMA M_w (kg/mol)	Sample	Blend PS/PMMA M_w/M_w (kg/mol)
1	20.5	6	4.05/84.9
2	65	7	15/84.9
3	108	8	35/84.9
4	158	9	65/84.9
5	610	10	145/84.9
		11	470/84.9

Table 1: Molar masses of the block copolymers and the blends of homopolymers as given by the supplier (blends were prepared by 50/50 wt %)

Fig. 6 shows the critical diagram obtained by using normal phase Si columns at ambient temperature (22°C). The PMMA standards were used for establishing the

critical conditions. At a mobile phase composition of MEK/cyclohexane 100:0 v/v SEC mode is seen. The critical conditions correspond to a mobile phase composition of MEK/cyclohexane 74.3:25.7 v/v which is in agreement with Ref.[42]. Liquid adsorption chromatography is seen at a mobile phase composition of MEK/cyclohexane 70:30 v/v.

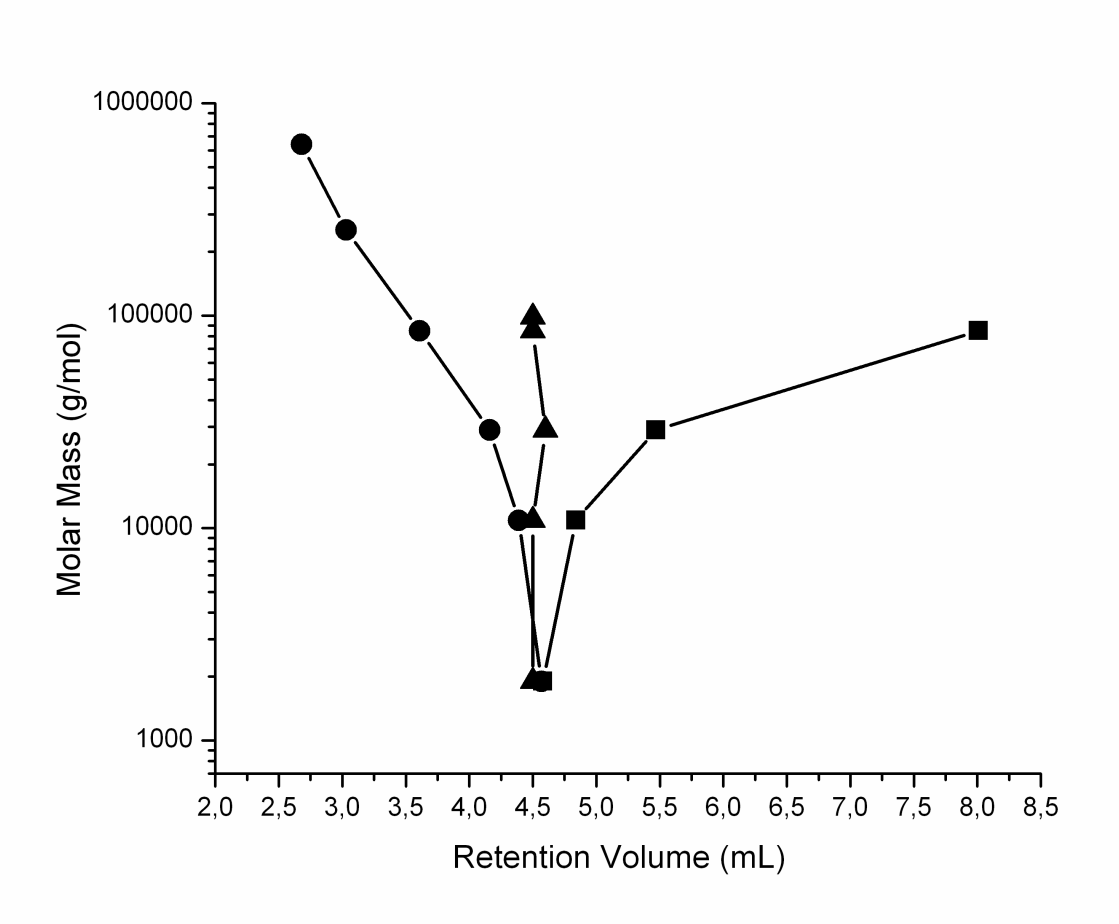

Figure 6: Critical diagram of PMMA showing molar mass versus retention volume, mobile phase MEK/cyclohexane ● = 100:0, ▲= 74.3:25.7, ■ = 70:30 v/v; stationary phase: Si 300-5 and Si 1000-7

The critical conditions established for PMMA are used for the analysis of PS-*b*-PMMA copolymers.

4.1.2 LC-CC-^{1}H-NMR of PS-*b*-PMMA copolymers at critical conditions of PMMA

When LC-CC is coupled to NMR one major problem has to be taken into account. The positions of the solvent signals relative to the signals of the analytes have to be considered. It is important that signals of interest in both monomer units of the block copolymers can be detected via proton signals. These signals should not overlap with the mobile phase signals. Fig. 7 shows the ^{1}H-NMR spectra of a PS-*b*-PMMA copolymer dissolved in a mixture of MEK and cyclohexane without adding deuterated solvents [Fig. 7 (a)] and in deuterated dichloromethane [Fig. 7 (b)]. WET solvent suppression is applied to the signals of both MEK and cyclohexane. Four solvent signals were suppressed. It is evident from Fig. 7 (a) that the OCH_3 group of the PMMA block and the aromatic protons of the PS block are unaffected by solvent signals and can be used for determining the chemical composition distribution. Fig. 7 (b) also indicates that the tacticity of the PMMA block can be calculated from the α-CH_3 groups when a deuterated solvent is used. The syndiotactic, heterotactic and isotactic triads are represented by rr, mr and mm respectively. When one uses MEK/cyclohexane only the syndiotactic signal is visible.

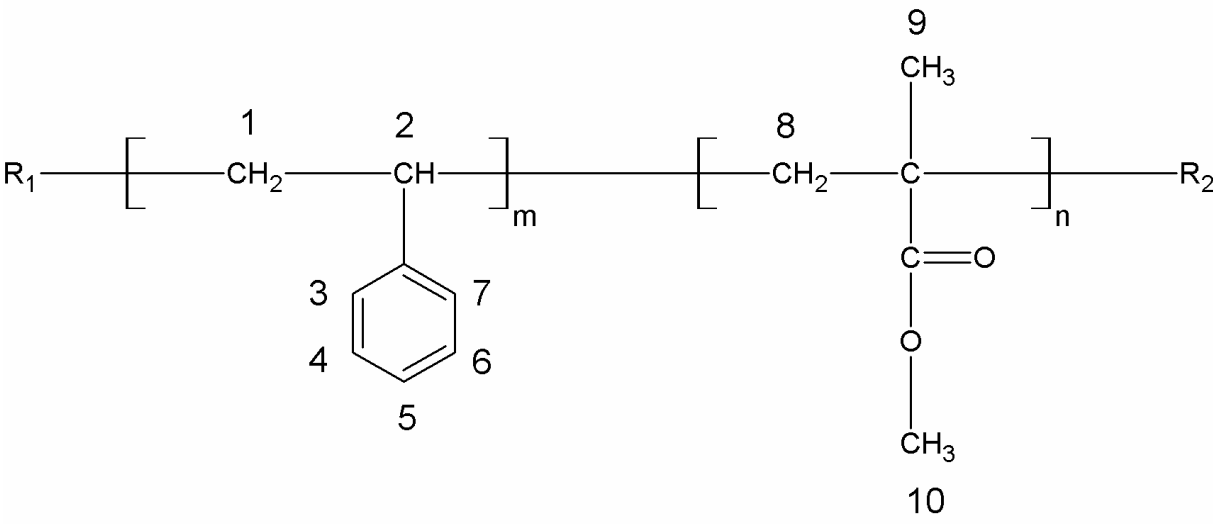

Scheme 1: Structure of PS-*b*-PMMA

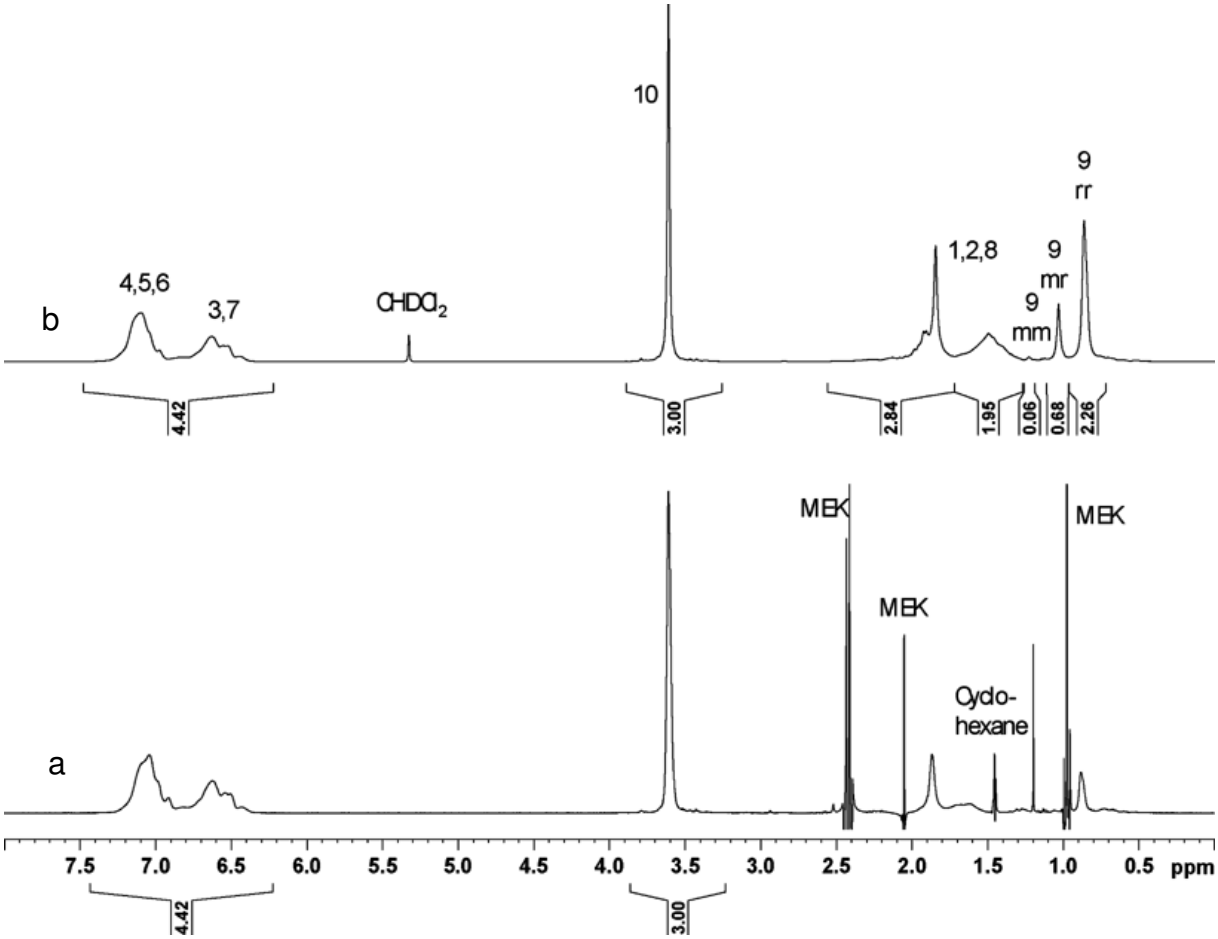

Figure 7: ^{1}H-NMR spectra of PS-*b*-PMMA copolymer (sample 1) in (a) non-deuterated MEK/cyclohexane with WET solvent suppression and (b) in $CHDCl_2$ respectively. The assignments are given according to Scheme 1.

The present critical conditions are used for the analysis of blends of PS and PMMA as well as for PS-*b*-PMMA copolymers. The samples given in Table 1 are used for the analysis.

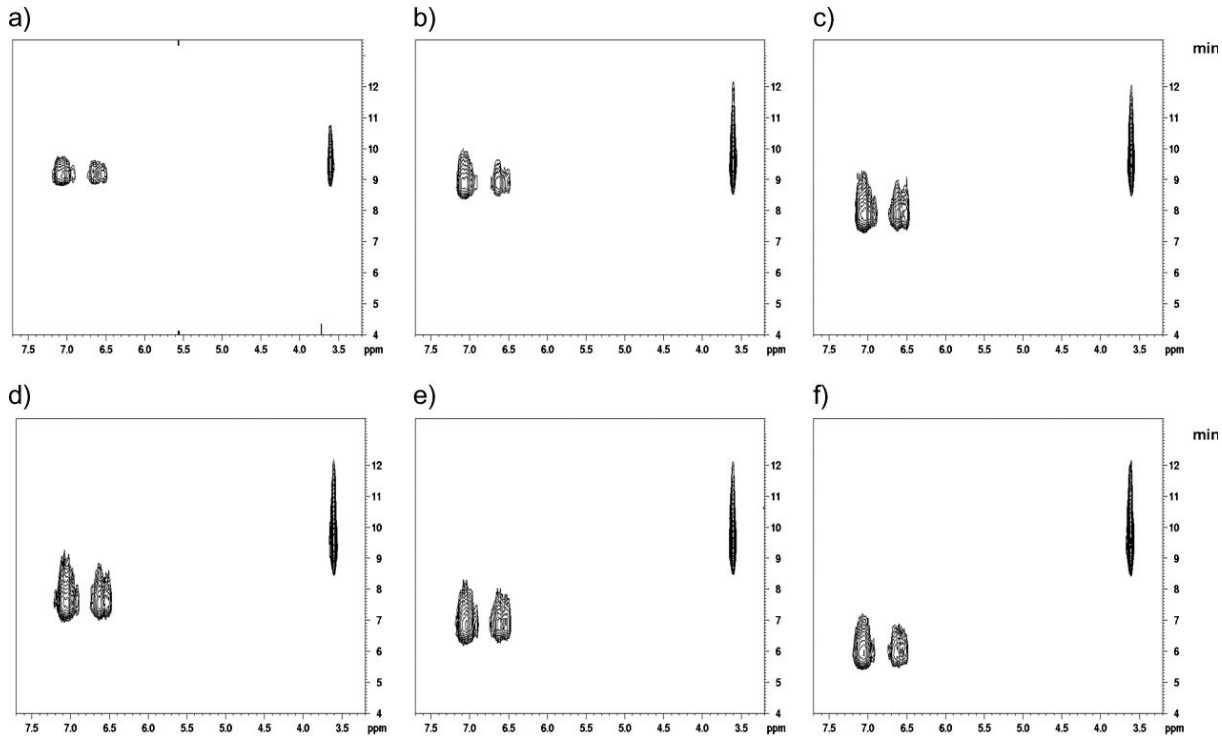

Figure 8: LC-CC-NMR (400 MHz) on-flow runs of samples 6 (a), 7 (b), 8 (c), 9 (d), 10 (e), 11 (f) (blends of PS and PMMA of different molar masses) at the critical point of adsorption of PMMA

Fig. 8 shows the HPLC-NMR on-flow runs of blends of PS and PMMA. The on-flow runs are presented as contour plots which are processed as two-dimensional NMR spectra. Fourier transformation is performed on the series of free induction decays (FIDs) and displayed as the contour plot of retention time versus chemical shift. Two different regions can be differentiated in Fig. 8. The region of 6.3-7.3 ppm shows the aromatic protons of PS and the signal at 3.6 ppm belongs to the OCH_3 group of PMMA. According to Fig. 8, the PS homopolymers elute in the order of their molar masses. Regarding SEC conditions it can be stated that the higher the molar mass the earlier the elution. This behaviour indicates that PS is eluting in the SEC mode. Since critical conditions of PMMA are chosen, PMMA is always eluting as the last component. These on-flow runs can already be used to derive a molar mass calibration curve for PS. In this case the vertical projections of the on-flow runs are taken for the calibration curve. The peak maximum molar masses (M_P) of the aromatic protons will then be plotted versus the retention volume. For a higher precision, all nine PS standards are measured separately with LC-CC-NMR and plotted as a calibration curve in Fig. 9.

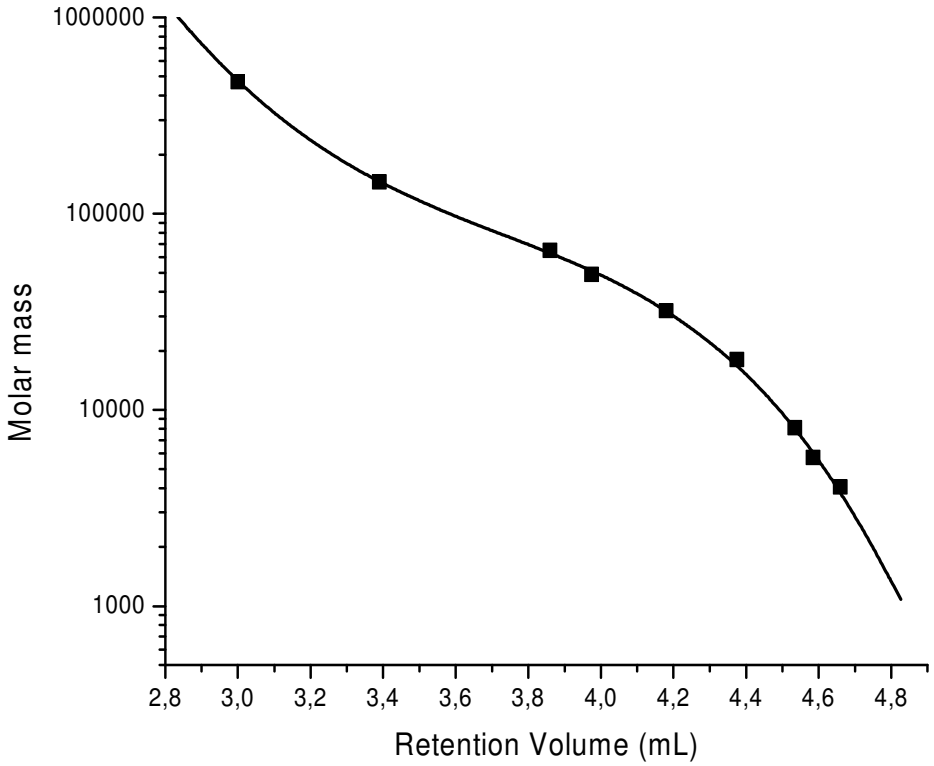

Figure 9: Calibration curve of PS showing molar mass versus retention volume at critical point of adsorption of PMMA, solid line = curve fitted with fifth order polynomial

This curve will then be used to determine the block length of PS of the block copolymers. Fig. 10 shows the HPLC-NMR on-flow run of sample 1. It is evident from this Fig. that two different regions of the eluting samples can be found. Again the aromatic protons of the PS block and the OCH_3 group of the PMMA block can be observed. The projections towards the elution time axis present the concentration profiles of the styrene (full line) and MMA units (dotted line). If one considers all the block copolymers a general tendency can be seen: the elution time of the copolymer peaks decreases with increasing molar mass which is in agreement with the SEC mode of the PS block.

As a consequence the molar mass of the PS blocks of the copolymers can be determined by using HPLC-NMR on-flow data of the PS calibration (Fig. 9).

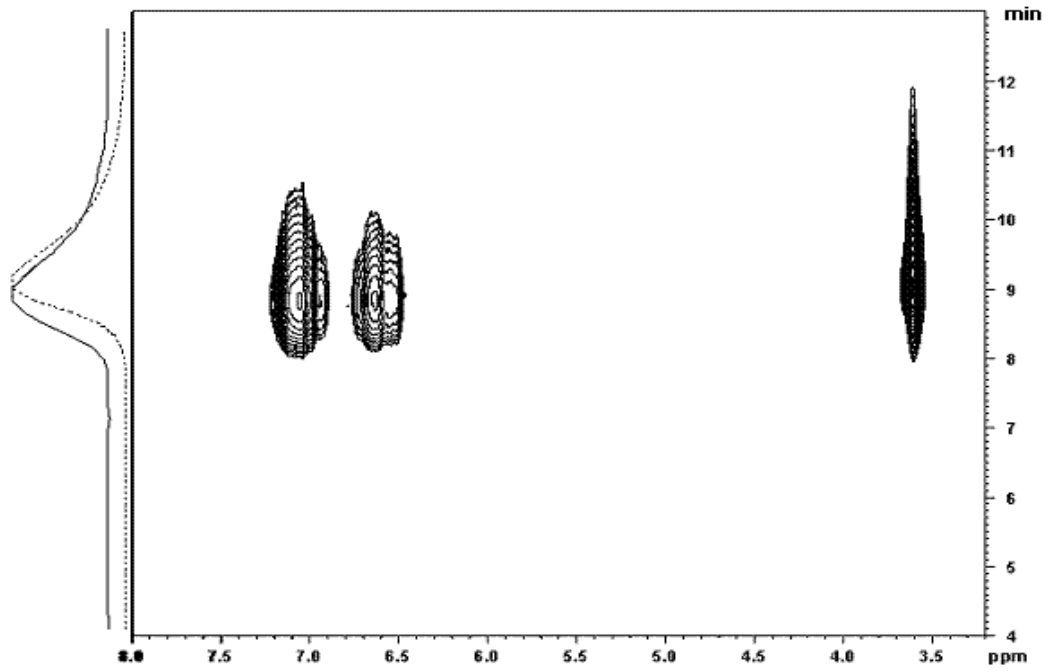

Figure 10: LC-CC-NMR on-flow run of PS-*b*-PMMA copolymer (sample 1) at critical conditions of PMMA, vertical projections are taken from the aromatic (solid line) and OCH_3 proton signals (dashed line)

Table 3 shows the molar masses of the PS blocks of the copolymers determined by LC-CC-NMR. In order to compare with the LC-CC-NMR data, the bulk samples are also analysed by conventional SEC and off-line ^{1}H-NMR. The SEC calibration is based on PS. Using the chemical compositions and the SEC data of Table 2, the molar masses of the blocks of the samples can be calculated according to the following equations:

$$M_{copol} = N_S M_S + N_{MMA} M_{MMA} \quad (20)$$

Where M_{copol} is the molar mass of the copolymer, N_S and N_{MMA} are the number of styrene and MMA units in the copolymer chain, M_S the molar mass of one styrene unit (104 g/mol) and M_{MMA} the molar mass of one methyl methacrylate unit (100

g/mol). Accordingly, the molar content of styrene (x_{mol}) and MMA ($1-x_{mol}$) can be calculated from N_S and N_{MMA}.

$$M_{PS} = N_S M_S \quad (21)$$

$$M_{PMMA} = N_{MMA} M_{MMA} \quad (22)$$

$$X_{mol} = N_S/(N_S + N_{MMA}) \quad (23)$$

$$1 - x_{mol} = N_{MMA}/(N_S + N_{MMA}) \quad (24)$$

Using equations (21)-(24), the molar masses of the PMMA and PS blocks can be obtained as follows:

$$M_{PMMA} = M_{copol} /\{1+ M_s x_{mol}/[(1-x_{mol}) M_{MMA}]\} \quad (25)$$

$$M_{PS} = M_{copol}/\{1+ M_{MMA} (1-x_{mol})/[x_{mol} M_s]\} \quad (26)$$

These equations will be further used in the other chapters in modified form for the calculations.

Sample	Nominal M_w (kg/mol)	M_w by SEC (kg/mol)	M_P by SEC (kg/mol)	Styrene/MMA by NMR (mol%)
1	20.5	20.5	17.6	47.1/52.9
2	65	75	69	45.1/54.9
3	108	132	121.5	48.1/51.9
4	158	164	100	47.4/52.6
5	610	668	571	64.8/35.2

Table 2: SEC and ^{1}H-NMR analyses of the block copolymers

The calculated molar masses of the PS blocks of the bulk samples are summarised in Table 3 and compared to the molar masses that were obtained by LC-CC-NMR.

Sample	M_p (PS block) by LC-CC-NMR (kg/mol)	M_P (PS block) by SEC and NMR (kg/mol)
1	11.5	8.5
2	25.4	31.8
3	56.8	59.6
4	58.2	48.4
5	177	375

Table 3: Molar masses of the PS block of the copolymers determined by SEC and off-line NMR with Equation (26) or LC-CC-NMR with the peak maximum of the aromatic proton signals

In case of LC-CC-NMR, the maximum intensity of the aromatic signals was used for determining the retention time. The calculation of the molar mass is based on Fig. 9. It turns out from Table 3 that the molar masses of the PS blocks determined with both methods are almost the same for samples 1 to 4. This result gives the impression of a good consistency between the off-line measurements of the bulk samples and LC-CC-NMR. Only the highest molar mass shows strong deviations.

Furthermore, the chemical compositions should be compared between the bulk samples and LC-CC-NMR. The main advantage of HPLC-NMR is that it provides the individual concentrations of both monomer units. Thus, it is possible to determine also the chemical composition distribution (CCD) of the copolymers without using standards. Based on the on-flow run of Fig. 10, the CCD can be determined at different elution times. Fig. 11 shows these CCDs. It also shows the vertical projections taken from these on-flow runs. The individual NMR chromatograms are presented as solid lines for the PS and as dashed lines for the PMMA blocks. Fig. 11 also allows the determination of an average chemical composition by adding all polymer containing traces of the on-flow runs of Fig. 10. The results are presented in Table 4. These data show a very good agreement with the chemical composition of the bulk samples (see Table 2).

Sample	M_p (PS block) by LC-CC-NMR (kg/mol)	Styrene/MMA of copolymer by LC-CC-NMR (mol %)	M_p of block copolymer (kg/mol) calculated
1	11.7	45.2/54.8	25.3
2	25.4	43.9/56.1	56.6
3	56.8	48.2/51.8	115.5
4	58.2	48.5/51.5	117.6
5	177	67.3/32.7	259.7

Table 4: The molar masses of the PS block of the copolymers, chemical compositions and calculated total molar masses of the block copolymers

The following general conclusions can be derived from Fig. 11:

(i) Samples 1 and 2 show a monomodal molar mass distribution (MMD). There is no indication of homopolymer. Samples 3-5 show PMMA homopolymer indicated either by shoulders of the dashed lines or a second smaller maximum at the region of 9-11 min. The solid line always shows a monomodal distribution for PS.

(ii) The molar mass of both monomer blocks can be determined by LC-CC-NMR. Indeed, LC-CC-NMR is a very useful tool for determining the molar masses of the blocks. Since LC-CC-NMR can be used as a concentration detector for both monomer units simultaneously, it can provide the total molar mass of the copolymer. The molar mass of the PS block is obtained directly from the peak maximum of the elution of the aromatics. In order to calculate the molar mass of the PMMA block, the chemical composition at different elution volumes was determined. Due to the fact that critical conditions of PMMA cannot separate the copolymer form PS homopolymer, the determination of the molar mass of the PS block will not be correct. The method will actually deliver higher block lengths of PS. Therefore, most of the molar masses are the same as for the bulk sample. In addition, the block length of PS is also affected by the interruption of the living polymerisation process. If chain transfer stops the process then the homopolymer PS has the same length as the block copolymer. If recombination of two chains takes place then homopolymer PS is two times as long as the block. Sample 5 shows differences for the molar masses determined by LCCC-NMR and off-line measurements of the bulk sample which cannot be explained by critical conditions of PMMA.

In this case a significant amount of PS homopolymer has shifted the maximum elution of the aromatics to lower molar masses and delivers an artificial molar mass of the PS block. The correct determination of the PS block can only be executed via critical conditions of PS.

(iii) The agreement of the chemical compositions between LC-CC-NMR and off-line measurements of the bulk sample is strongly connected to the fact that the copolymer and the PS homopolymer are eluting together. Therefore, the chemical composition of LC-CC-NMR calculated as the sum of all contributions of the elution will finally result into the same amount as for the bulk.[114]

a)

M_P = 11700

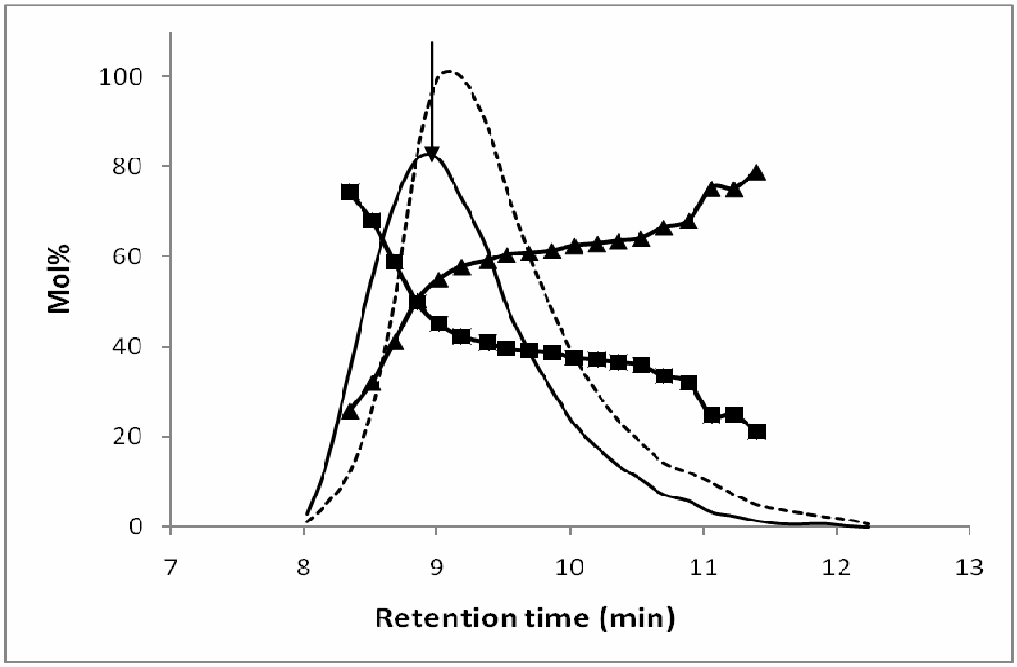

b)

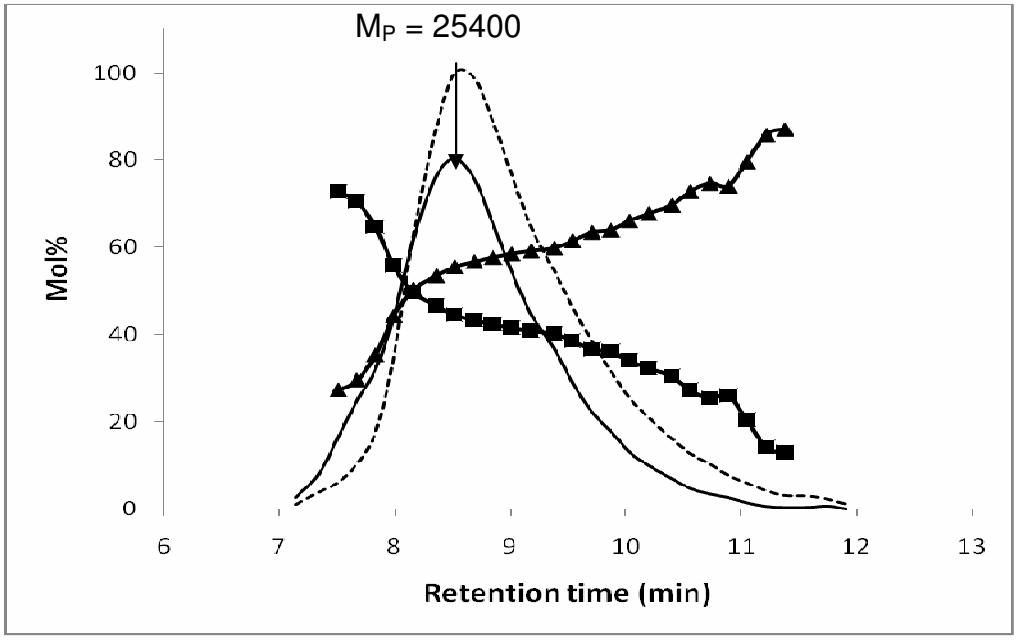
MP = 25400
100
80
60
40
20
0
Mol%
6
7
8
9
10
11
12
13
Retention time (min)

c)

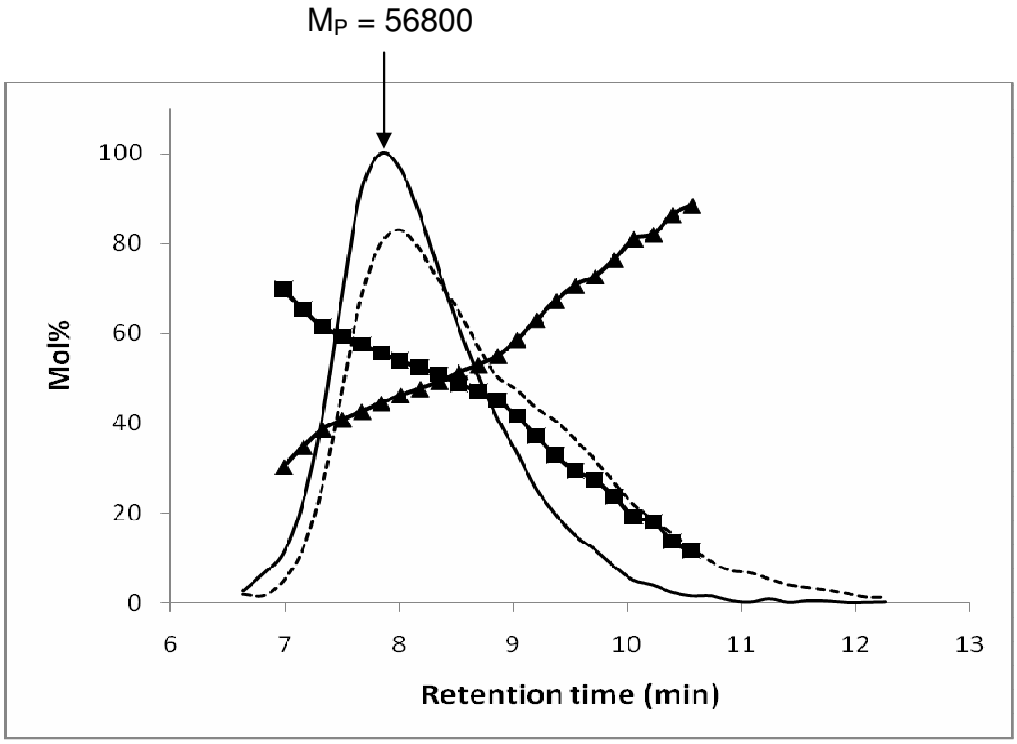
MP = 56800
100
80
60
40
20
0
Mol%
6
7
8
9
10
11
12
13
Retention time (min)

d)

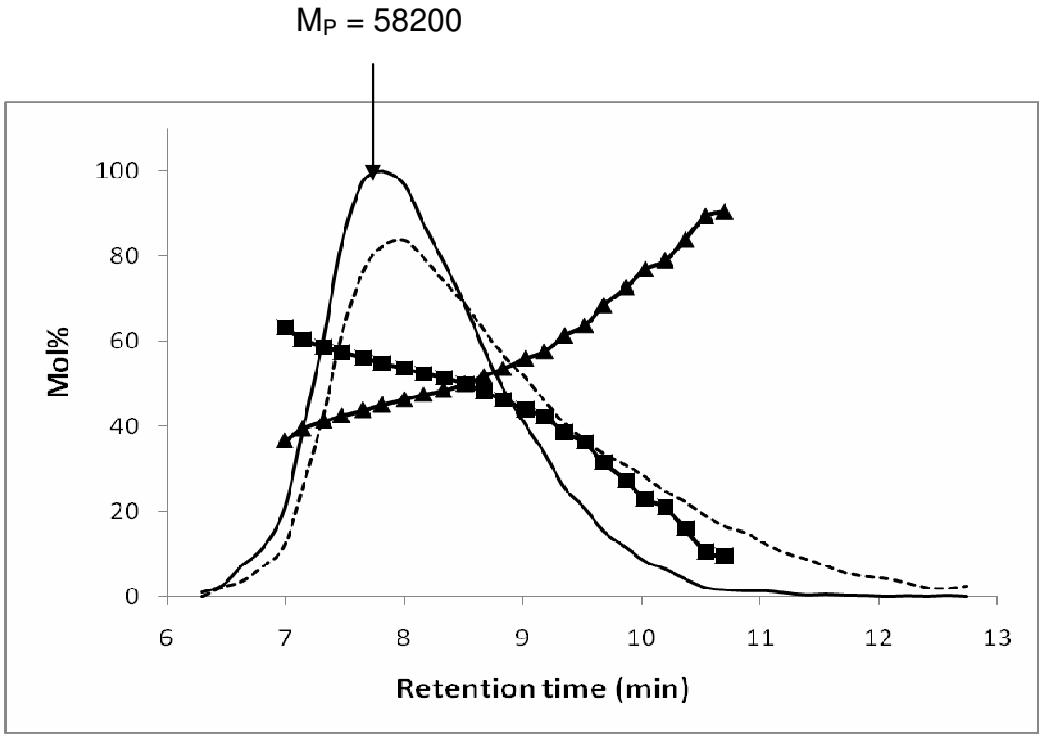
M_P = 58200
100
80
60
40
20
0
Mol%
6
7
8
9
10
11
12
13
Retention time (min)

e)

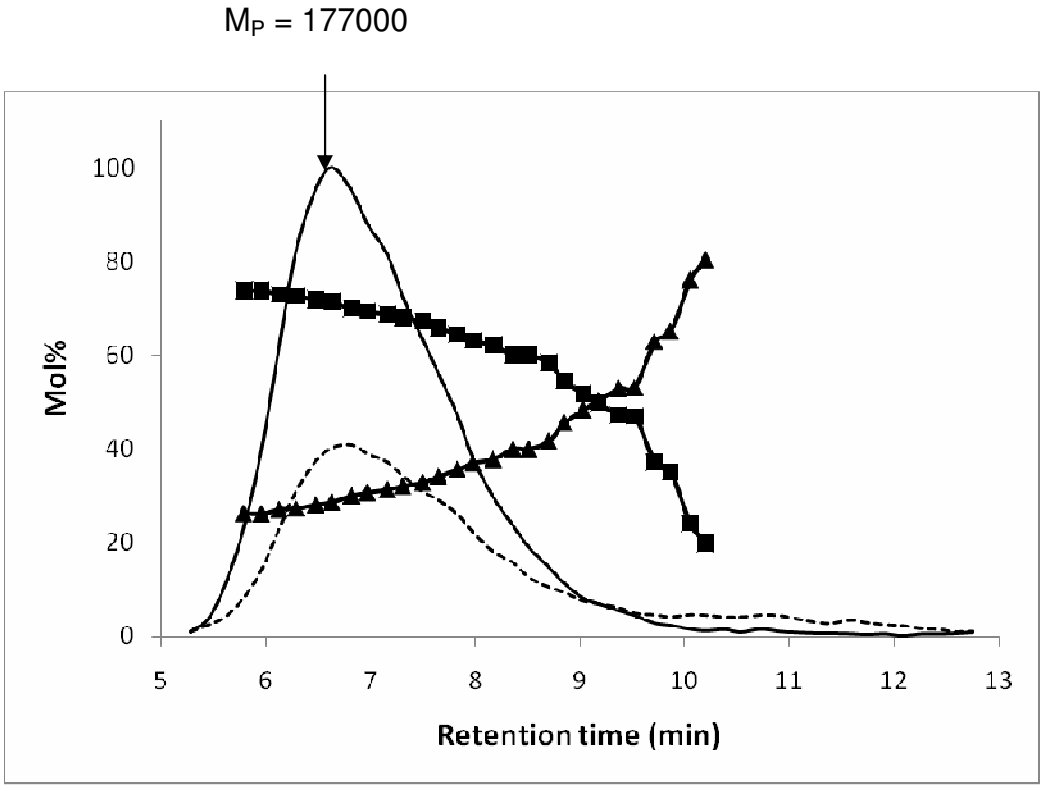
M_P = 177000
100
80
60
40
20
0
Mol%
5
6
7
8
9
10
11
12
13
Retention time (min)

Figure 11: Chemical composition of PS-*b*-PMMA copolymers versus retention time (■ = mol% PS, ▲= mol% MMA), dashed line = NMR projection of the OCH_3 group, solid line = NMR projection of the aromatic region, samples 1 (a), 2 (b), 3 (c), 4 (d), 5 (e)

4.1.3 Method development for finding the critical conditions of PS

For separating PS-*b*-PMMA copolymers critical conditions were established for the PS block. It has already been shown in Ref.[44] that mixtures of THF-acetonitrile as mobile phases are well suited for establishing critical conditions. Using a set of non-polar stationary phases C_{18} 300-5, 1000-7 with column sizes of 250x4 mm inner diameter, PS will elute at critical conditions whereas PMMA will elute in the SEC mode. Thus separation takes place in order of decreasing polarity. For establishing the critical conditions for PS same experimental procedures were used as that for the critical conditions of PMMA. The PS and PMMA calibration standards mentioned for establishing the critical conditions for PMMA were used.

Fig. 12 shows the critical diagram obtained by using reversed phase columns at ambient temperature (22°C). PS standards were used for establishing the critical conditions. At a mobile phase composition of THF/ACN 50:50 and 49:51 v/v size exclusion chromatography is seen. The critical conditions correspond to a mobile phase composition of THF/ACN 48:52 v/v which is in agreement with Ref.[44]. Liquid adsorption chromatography is seen at a mobile phase composition of THF/ACN 47:53 v/v.

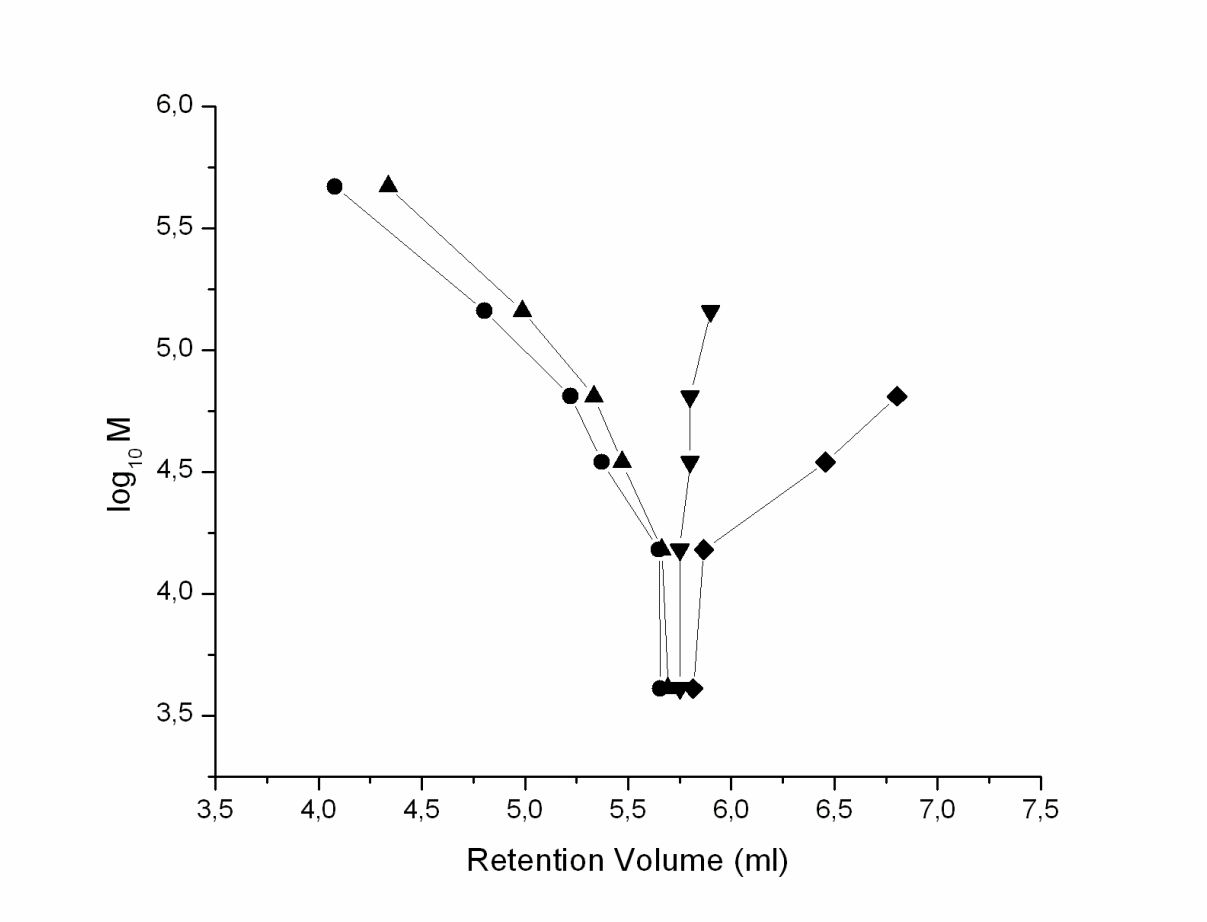

Figure 12: Critical diagram of PS showing molar mass versus retention volume, mobile phase THF/ACN ● = 50:50, ▲= 49:51, ▼= 48:52, ■ = 47:53 v/v, stationary phase: C_{18} 300-5, 1000-7

The critical conditions established for PS are used for the analysis of PS-*b*-PMMA copolymers.

4.1.4 LC-CC-^{1}H-NMR of PS-*b*-PMMA copolymers at critical conditions of PS

The coupling of LC-CC with NMR is a complicated process. The solvents should be chosen in such a way that they separate the block copolymers. In addition the solvent signals should not overlap with the signals of interest of the monomer units and can be detected by proton signals. Fig. 13 shows the ^{1}H-NMR spectra of a PS-*b*-PMMA copolymer dissolved in a mixture of THF and ACN without adding deuterated solvents [Fig. 13 (a)] and in deuterated dichloromethane [Fig. 13 (b)]. WET solvent

suppression is applied to the signals of both THF and ACN. It is evident from Fig. 13 that the α-CH_3 group of the PMMA block and the aromatic protons of the PS block are unaffected by solvent suppression. These signals can be used for determining the chemical composition distribution. This Fig. also indicates that the tacticity of the PMMA block can be calculated from the α-CH_3 group. The syndiotactic, heterotactic and isotactic triads are represented by rr, mr and mm respectively.

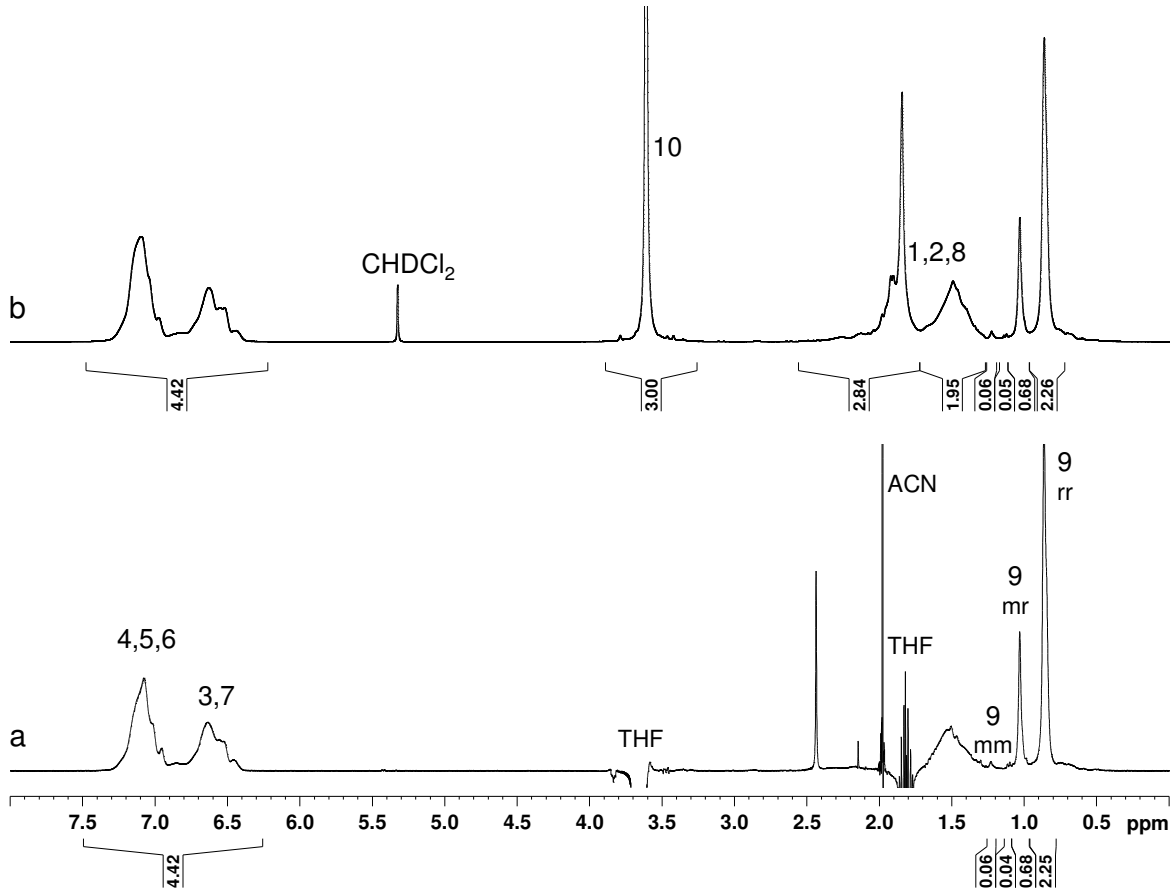

Figure 13: ^{1}H-NMR spectra of PS-*b*-PMMA copolymer (sample 1) with sample in (a) non-deuterated ACN/THF with WET solvent suppression and (b) in $CHDCl_2$, respectively. The assignments are given according to Scheme 1.

These critical conditions are used for the analysis of blends of PS and PMMA as well as for PS-*b*-PMMA copolymer. For performing the HPLC-NMR measurements, same experimental conditions were used as in the case for the critical conditions of PMMA. Fig. 14 shows the HPLC-NMR on-flow run of a blend of PS, PMMA and PS-*b*-PMMA copolymer. According to Fig. 14, the block copolymer elutes first (a) (retention time

(RT) = 8.1 min), (b) followed by PMMA (RT = 9.9 min) and (c) PS (RT = 12.7 min). Since critical conditions of PS are chosen, PS is eluting as the last component. The other components are eluting in the SEC mode. Therefore, the block copolymer with the larger PMMA block elutes first followed by the PMMA homopolymer.

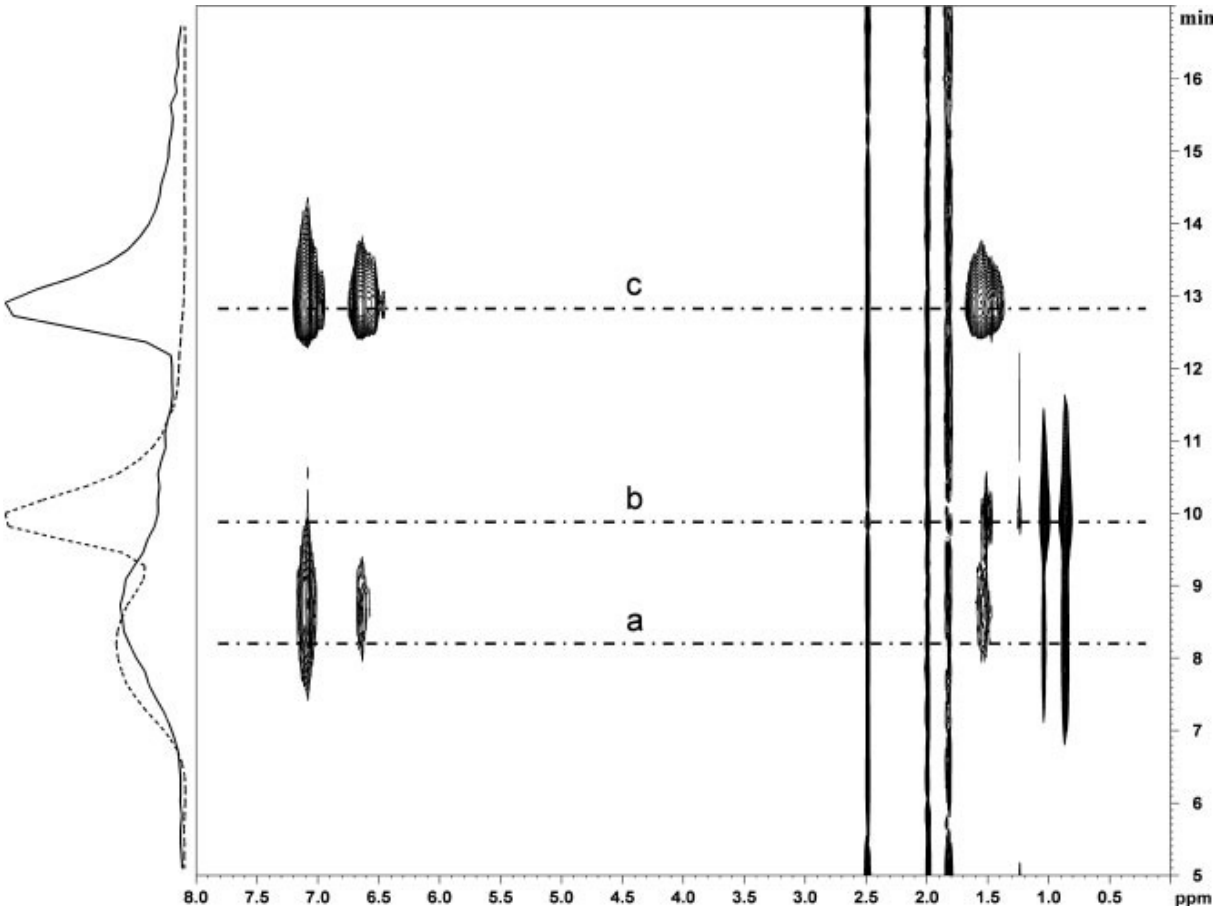

Figure 14: LC-CC-NMR on-flow run of the blend of (a) PS-*b*-PMMA copolymer (M_w = 610 kg/mol), (b) PMMA (M_w = 29 kg/mol) and (c) PS (M_w = 65 kg/mol) at the critical point of adsorption of PS. Projections taken from the vertical traces (solid line = aromatic region, dashed line = α-CH_3 group).

Instead of presenting a contour plot, Fig. 14 could also be displayed as a stacked plot, where each spectrum is displayed separately with its individual signal intensities. These spectra would correspond to the traces of the contour diagram. The projections towards the elution time axis present the concentration profiles of the styrene (solid line) and MMA units (dotted line). Fig. 15 represents the most intense traces of the separated components. Fig. 15 (a) shows the typical chemical shifts of the copolymer as indicated in Fig. 13. However, the OCH_3 group of the PMMA block

overlaps with THF signal and is suppressed. The second eluting peak can be assigned to PMMA (M_w = 29 kg/mol) [Fig. 15 (b)]. The homopolymer is mainly represented by the α-CH_3 groups at 0.8-1.1 ppm. This trace also contains some residual aromatic signals belonging to the copolymer. The OCH_3 group is again suppressed. The third trace belongs to PS (M_w = 65 kg/mol) and is represented by the aromatic signals at 6.4-7.3 ppm and the aliphatic region around 1.5 ppm.

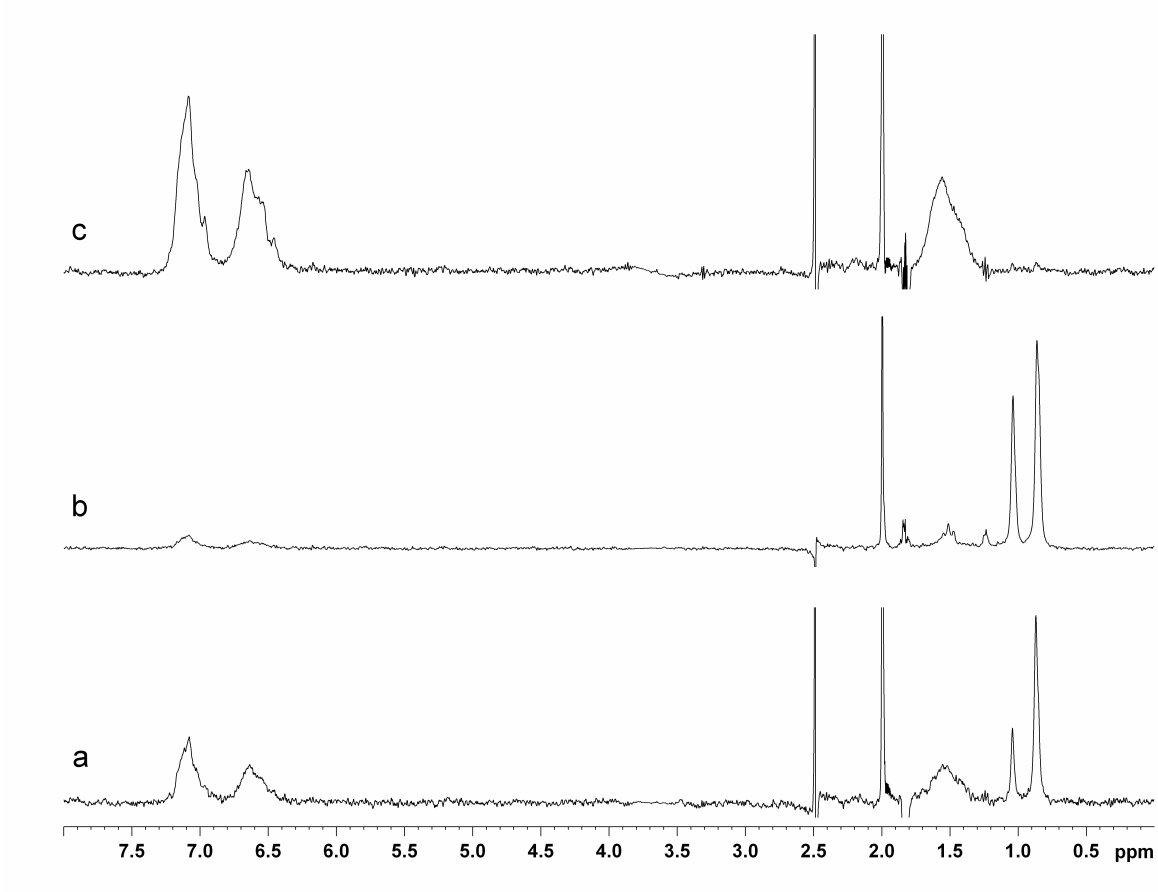

Figure 15: ^{1}H-NMR traces of the on-flow run of Fig. 14 (a) PS-*b*-PMMA (M_w = 610 kg/mol, RT = 8.1 min; (b) PMMA (M_w = 29 kg/mol, RT = 9.9 min); (c) PS (M_w = 65 kg/mol, RT = 12.7 min)

Fig. 16 shows the HPLC-NMR on-flow run of sample 1. It is seen from this Fig. that a separation into two different components takes place. The first component shows different retention times and is eluting in the order of their molar masses. According to SEC conditions it can be stated that the higher the molar mass the earlier the elution which indicates that PMMA is eluting in SEC mode. The second component elutes near the critical retention time of PS. The identification of the two components

can be done by assigning the observed chemical shifts. Since the first eluting peak shows coexisting signals at the aromatic and aliphatic regions, this peak can be assigned to the copolymer. The peak eluting later can be assigned to PS homopolymer based on the typical NMR chemical shifts of PS and the critical elution time of PS. The solid line represents the distribution of the aromatic protons that are present both in the copolymer and the PS homopolymer; the dashed line represents the distribution of the α-CH_3 groups only due to the copolymer. Consequently, the molar mass of the PMMA blocks in the copolymers can be determined by the HPLC-NMR on-flow data of PMMA calibration standards.

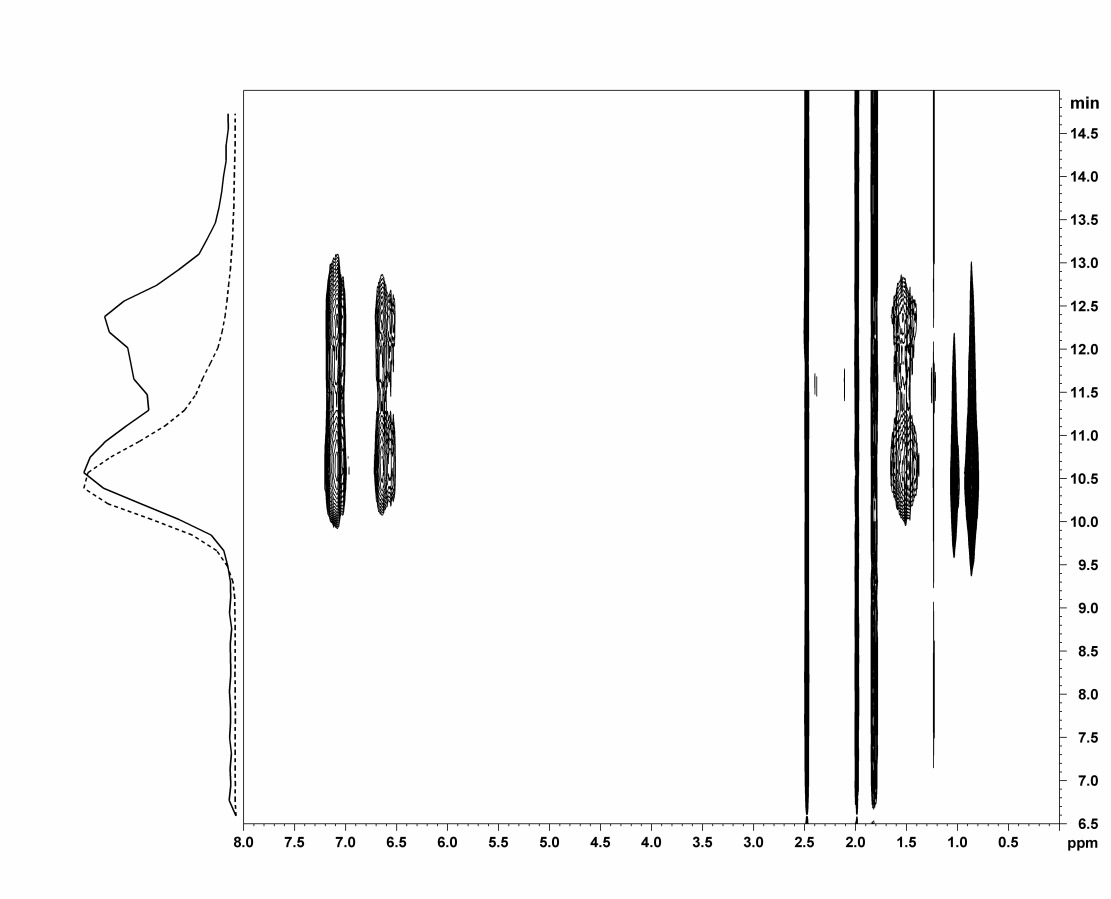

Figure 16: LC-CC-NMR on-flow run of PS-*b*-PMMA copolymer (sample 1), vertical projections are taken from the aromatic (solid line) and α-CH_3 proton signals (dashed line)

For the evaluation of the LC-CC-NMR data, the block copolymers are also analysed by conventional SEC and off-line ^{1}H-NMR. The conventional SEC data are obtained in THF using cross-linked polystyrene (PS) as the stationary phase. The calibration is

based on PS. As can be seen from Table 2, the SEC molar mass data are in good agreement with the nominal molar masses given by the producer. Off-line ^{1}H-NMR is used to determine the chemical composition of the samples. From the signal intensities of the aromatic protons (styrene) and the α-CH_3 protons (methyl methacrylate) the average composition of the block copolymers can be calculated, see Table 2.

One has to keep in mind that the values given in Table 2 are related to the total samples. These contain, in addition to the true block copolymer, certain amounts of PS homopolymer. In the next step the molar masses of the PMMA blocks are calculated from SEC and off-line NMR data. The calculations were done using Equation 25.

The calculated molar masses of the PMMA blocks are summarised in Table 5 and compared to the molar masses that were obtained by LC-CC-NMR. In the case of LC-CC-NMR, the maximum intensity of the α-CH_3 signals was used for determining the retention time. Similar to standard chromatographic procedures, the determination of the molar mass versus elution volume function can be derived. The PMMA calibration standards mentioned in the case for establishing the critical conditions of PMMA are used for the construction of the calibration curve.

Sample	**M_p (PMMA block) by SEC and NMR (kg/mol)**	**M_p (PMMA block) by LC-CC-NMR (kg/mol)**
1	9.1	14.2
2	30.4	27.1
3	61.9	48.1
4	51.8	48.1
5	196	196

Table 5: Molar masses of the PMMA block of the copolymers determined by SEC and off-line NMR with Equation (25) or LC-CC-NMR with the peak maximum of the α-CH_3 group

Using the calibration curve given in Fig. 17, the molar masses of the PMMA blocks in the block copolymers were determined.

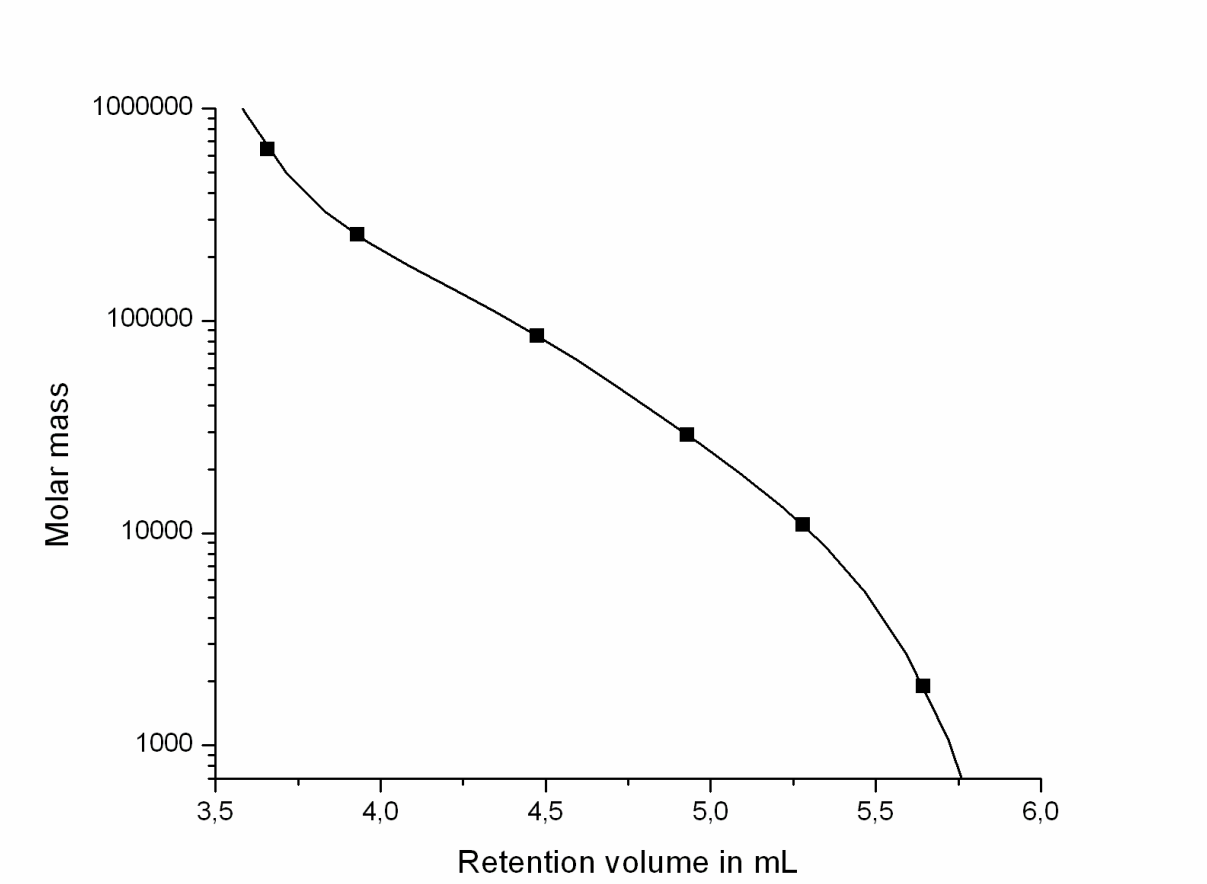

Figure 17: Calibration curve of PMMA showing molar mass versus retention volume at the critical point of adsorption of PS, solid line = curve fitted with fifth order polynomial

Considering the complexity of the experiments and the size of the NMR flow cell (60 µL), the PMMA molar masses obtained by both approaches agree quite well. There are different sources of error that can affect the results. First of all, the accuracy of establishing the critical conditions will influence the results. A second source of error is the accuracy of the molar mass analysis by off-line SEC. PS calibration was used to determine the molar masses of the samples. In addition, SEC does not separate the block copolymers from the detected PS homopolymers and accordingly the presence of these homopolymer fractions will affect the molar mass analysis. SEC sees the peak maximum of the copolymer whereas LC-CC sees the peak maximum of the PMMA block. To the same extent this is true for the chemical composition that

was analysed by off-line ^{1}H-NMR. These values were obtained for the total samples and may deviate from the chemical composition of the true block copolymers.

The total volume of the NMR flow cell, which is about twice the active volume, can cause tailing during the elution and can finally result in spreading out the eluted peak. Nevertheless, the 60 µL flow cell is already a very good compromise between LC resolution and NMR sensitivity.

One of the significant benefits of HPLC-NMR is the ability to determine the CCD of the copolymers without using standards. Using the on-flow data presented in Fig. 16, it is possible to calculate the chemical composition at different elution volumes. Based on the calibration curve given in Fig. 17, the CCD can be determined as a function of molar mass at critical conditions of PS. Fig. 18 shows the plots of CCD versus retention time for the different block copolymers. The Fig. also shows the NMR projections of the aromatic region (solid line, normalised to one proton) and the α-CH_3 (dashed line, normalised to one proton).

a)

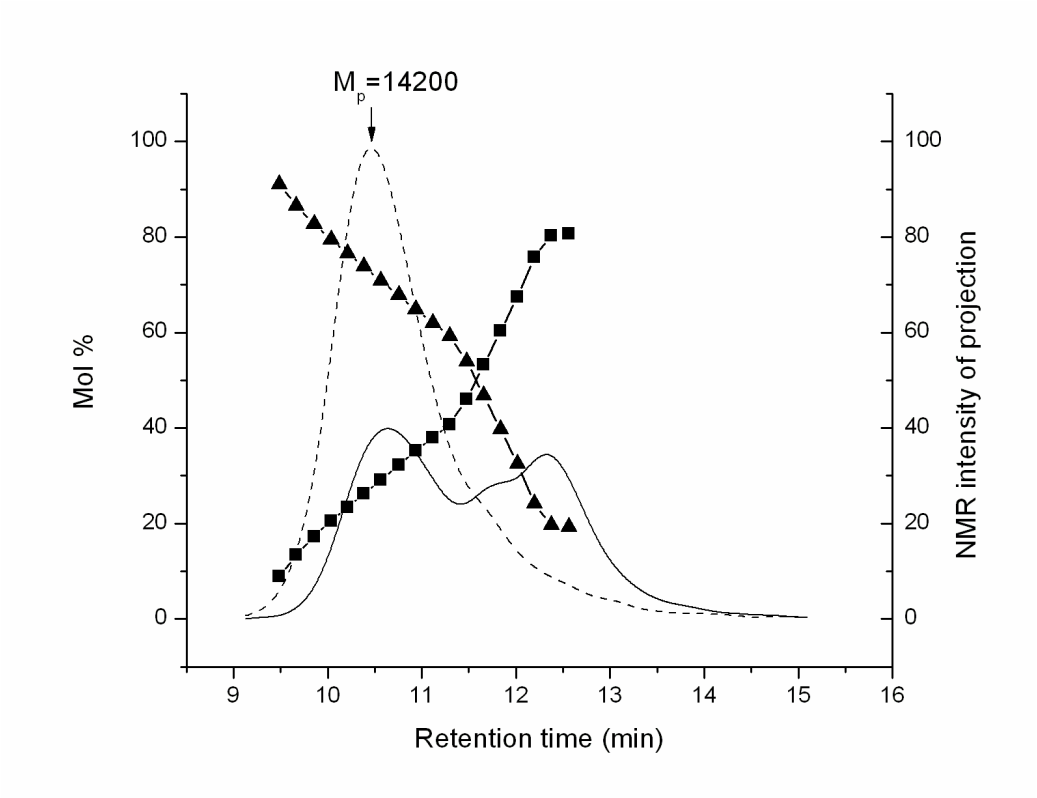

b)

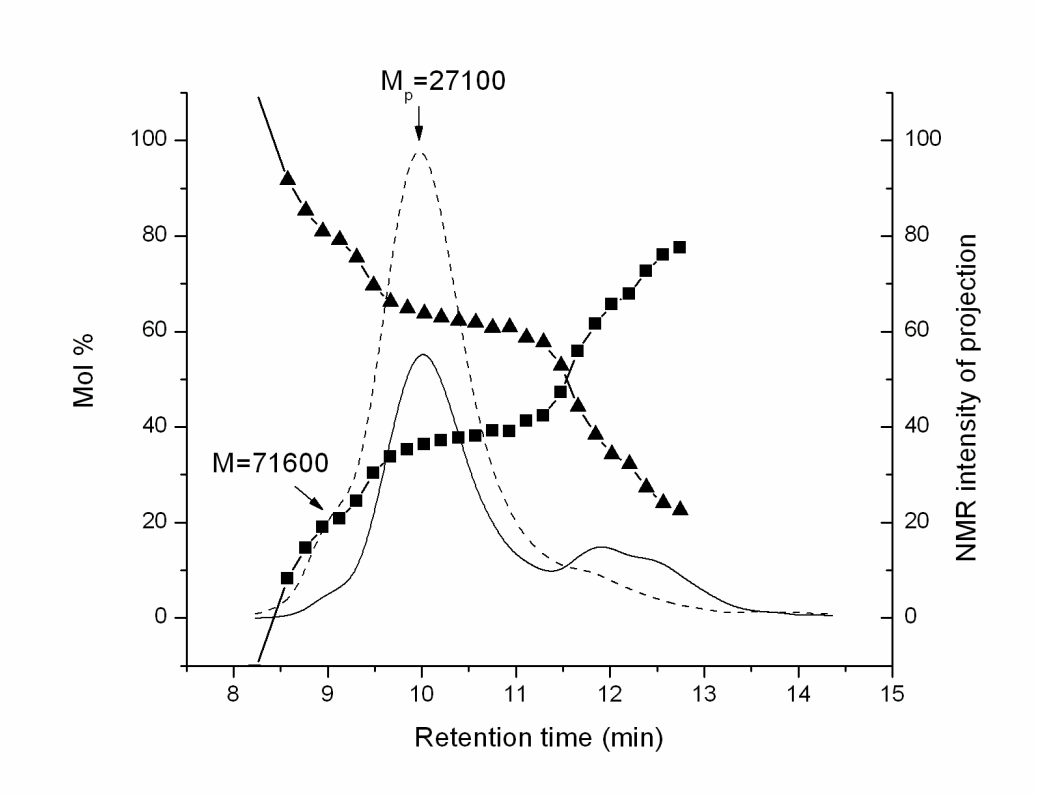
M_p=27100
M=71600
Mol %
NMR intensity of projection
Retention time (min)

c)

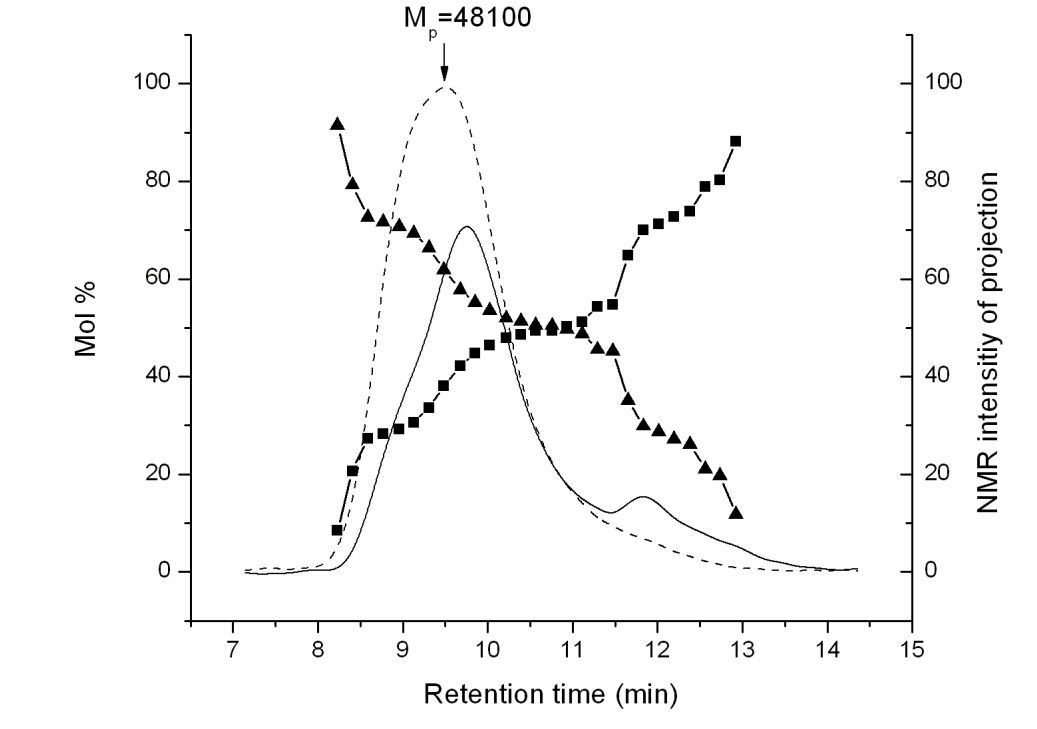
M_p=48100
Mol %
NMR intensitiy of projection
Retention time (min)

d)

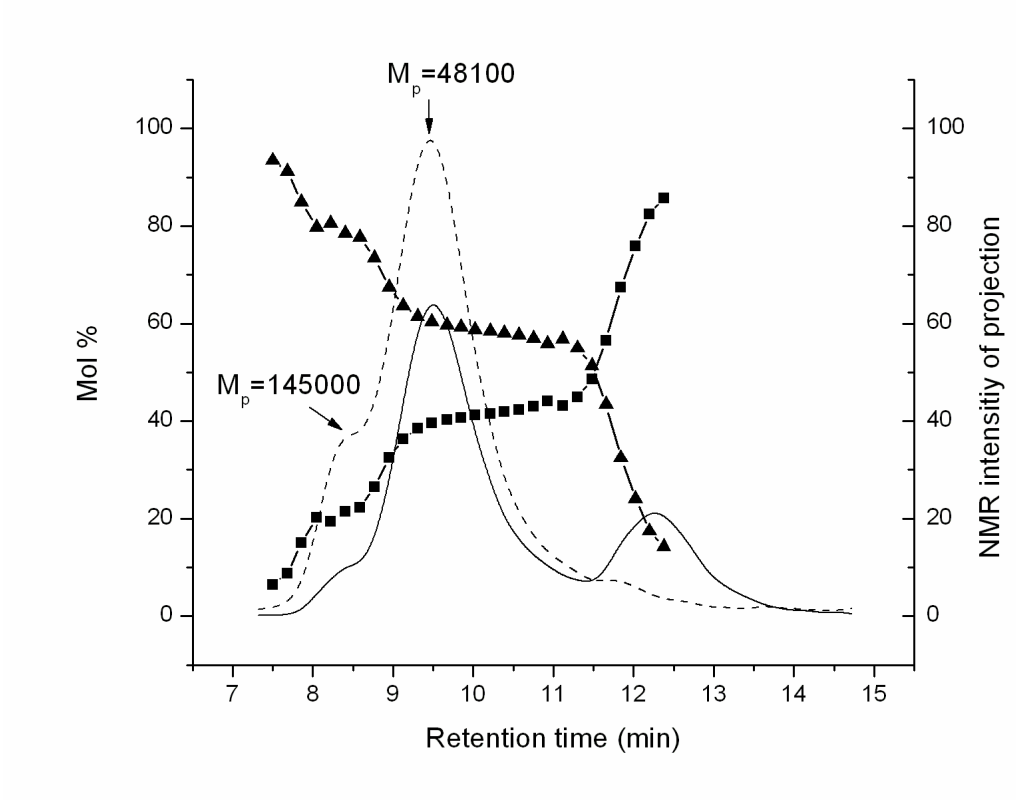
M$_p$=48100
M$_p$=145000
Mol %
NMR intensitiy of projection
Retention time (min)
0
20
40
60
80
100
7
8
9
10
11
12
13
14
15

e)

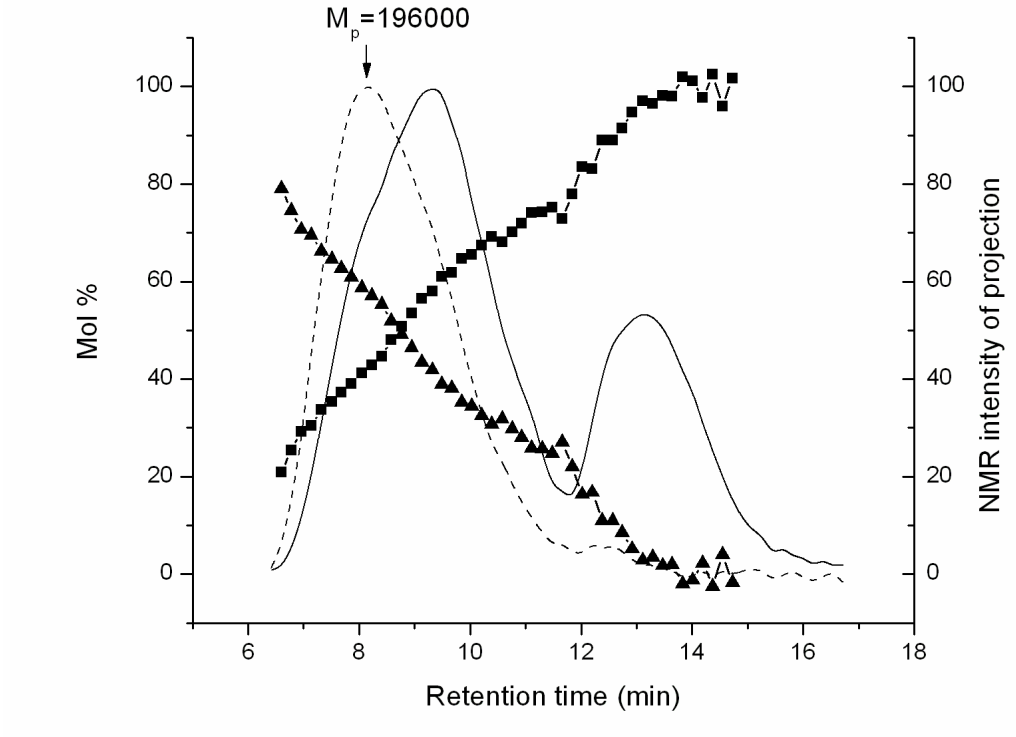
M$_p$=196000
Mol %
NMR intensity of projection
Retention time (min)
0
20
40
60
80
100
6
8
10
12
14
16
18

Figure 18: Chemical composition of PS-*b*-PMMA copolymers versus retention time (■ = mol% PS, ▲= mol% MMA), dashed line = NMR projection of the α-CH_3 group, solid line = NMR projection of the aromatic region, samples 1 (a), 2 (b), 3 (c), 4 (d), 5 (e)

The following general conclusions can be derived from Fig. 18 (a-e):

(i) All samples show a bimodal molar mass distribution (indicated by the solid line). The distribution at lower retention times represents the copolymer and at higher retention time the distribution belongs to PS homopolymer.

(ii) It was found that all block copolymers show a significant chemical heterogeneity. Samples 1, 3 and 5 [Fig. 18 (a, c, e)] are very broadly distributed with regard to CCD while samples 2 and 4 [Fig. 18 (b, d)] show a more moderate dependence of the CCD versus retention time in the region of the copolymer. The more pronounced chemical heterogeneity of samples 1, 3 and 5 may have two reasons: (A) the PMMA block in the block copolymers may have a higher polydispersity or (B) the chemical composition of the block copolymer may exhibit a larger drift.

(iii) The retention time of the PMMA projection profiles (α-CH_3) can be used for calculating M_p of the PMMA block.

In addition to these general statements, further structural peculiarities can be obtained from the CCD plots. First of all, the plots indicate that all samples are mixtures of the block copolymer and PS homopolymer. Accordingly, the average chemical composition given in Table 2 does not correspond to the true chemical composition of the block copolymer fractions. As can be seen in Fig. 18 (a), the true block copolymer has a composition of roughly 70 mol% MMA and 30 mol% styrene. This is quite different from the average sample composition being 53:47 mol% MMA/styrene. The samples 2 and 4 show shoulders towards very low retention times that have a chemical composition different from the composition of the main copolymer fraction. In both cases, these shoulders indicate fractions that have a higher PMMA content. Assumingly, these fractions are the result of coupling reactions that are taking place during the living polymerisation. Coupling can take

place between two living chain ends when a suitable coupling component is present in the reaction mixture as an impurity. The formation of coupling products is well documented for anionic polymerisation. The molar masses of the PMMA blocks of these coupling products are roughly double than the molar masses of the PMMA blocks in the diblock copolymers. This could indicate the formation of multiblock fractions.

Based on the data that are obtained by LC-CC-NMR, the chemical structure and molar mass of the true block copolymer fractions of samples 1-5 can be determined. As has been shown from LC-CC with PMMA calibration, the molar masses of the PMMA blocks of the block copolymers are obtained. It should be noted that for this analysis NMR is a much more suitable detector than any concentration detector because it selectively detects the concentration profile of the MMA units instead of the total concentration profile. The true chemical compositions of the block copolymers are determined from the MMA and styrene concentration traces given in Fig. 18. As can be seen in Table 6, the chemical compositions of the block copolymer fractions are significantly different from the data for the total samples. Taking now the true PMMA block molar masses and the true copolymer compositions, the total molar masses of the block copolymers can be calculated, see Table 6. A comparison with the average molar masses of the total samples shows significant differences; compare Tables 4 and 6.

Sample	M_p (PMMA block) by LC-CC-NMR (kg/mol)	Styrene/MMA of copolymer by LC-CC-NMR (mol%)	M_p of block copolymer (kg/mol)
1	14.2	30.0/70.0	20.3
2	27.1	34.8/65.2	41.6
3	48.1	40.3/59.7	80.6
4	48.1	38.4/61.6	78.1
5	196	52.2/47.8	410

Table 6: True molar masses of the PMMA blocks of the copolymers, true copolymer chemical compositions and calculated total molar masses of the block copolymers

Finally, the tacticity of the PMMA blocks shall be investigated. For a first overview on the tacticity of the total samples, the PMMA calibration standards and the PS-*b*-PMMA copolymers were measured and the tactic compositions were determined. The corresponding results are summarised in Table 7.

PMMA Mw (kg/mol)	mm (%)	mr (%)	rr (%)		Sample	mm (%)	mr (%)	rr (%)
1.9	11.3	39.5	49.2		1	2.4	23.0	74.6
10.9	4.7	36.8	58.5		2	1.7	21.1	77.2
29	4.8	36.6	58.6		3	3.0	26.1	70.9
84.9	4.0	48.0	48.0		4	1.4	20.7	77.9
253	1.0	19.7	79.3		5	2.3	24.3	73.4
640	4.6	49.7	45.7					

Table 7: Tacticity of the PMMA calibration standards and the PMMA blocks of the copolymers

Due to the fact that the α-CH_3 groups in the ^{1}H-NMR spectra reveal also the syndiotactic, heterotactic and isotactic triads (see Fig. 13), the tacticity is determined from the on-flow data of Fig. 16. The on-flow data, however, do not show the isotactic signals because of overlapping impurities. Therefore, the isotactic part was estimated by average data taken from Table 7 and supposed to be constant during the on-flow run. Fig. 19 presents the calculated tacticities of the PMMA blocks as a function of the molar mass for the critical conditions of PS. It shows that the tacticity of the PMMA blocks is constant and does not depend on the molar mass. The blocks are predominantly syndiotactic[115]. This behaviour was found for all copolymers.

a)

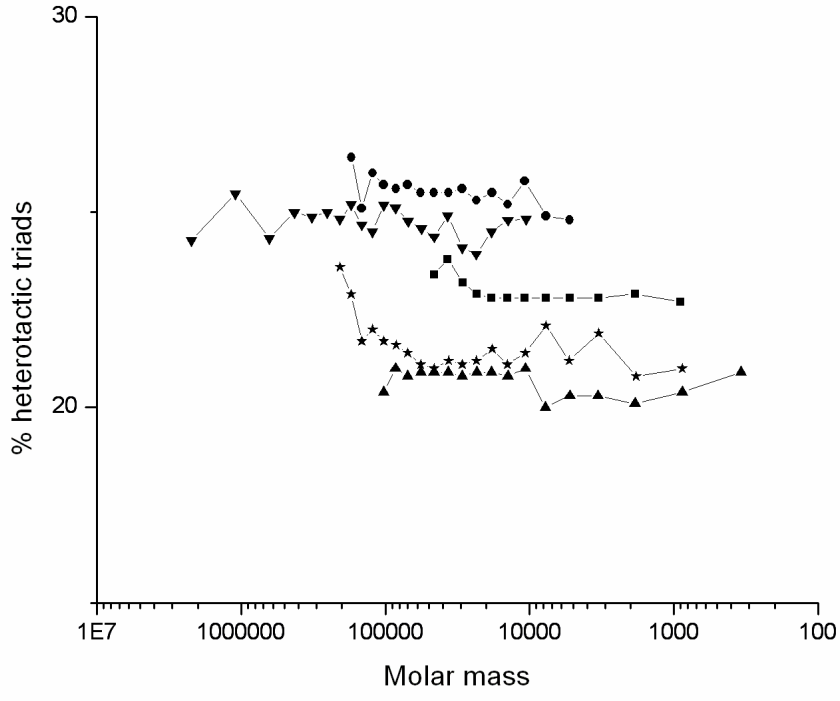

b)

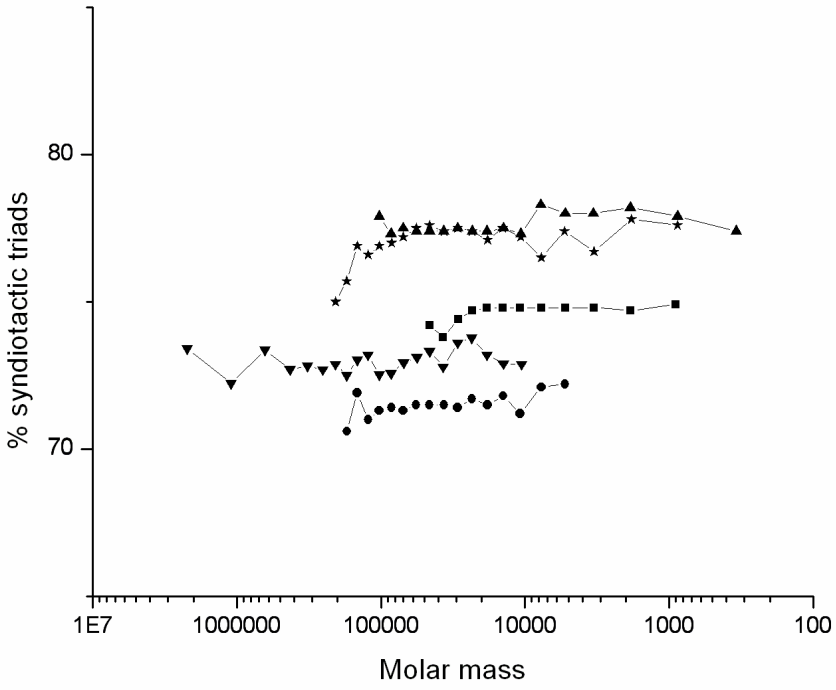

Figure 19: Tacticity of the PMMA block of PS-*b*-PMMA copolymers versus molar mass, heterotactic (a) and syndiotactic (b), (■ = sample 1, ▲ = sample 2, ● = sample 3, * = sample 4, ▼ = sample 5)

5. Analysis of 1,4-polyisoprene and 3,4-polyisoprene by using chromatography at critical conditions

5.1 Development of critical conditions for 1,4-polyisoprene by using solvent mixtures

Critical conditions for 1,4-polyisoprene were established by using solvent mixtures of MEK-cyclohexane. Fig. 20 shows the critical diagram obtained by using two C_{18} 300-5 reversed phase columns, with column sizes of 250x4.6 mm inner diameter. The 1,4-PI standards were used for establishing the critical conditions. At a mobile phase composition of MEK/cyclohexane (70:30) v/v size exclusion chromatography is seen. The critical conditions correspond to a mobile phase composition of MEK/cyclohexane (90:10) v/v in which all the 1,4-PI homopolymers elute at the same elution volume irrespective of their molar mass. Liquid adsorption behaviour is seen at a mobile phase composition of MEK/cyclohexane (95:5) v/v.

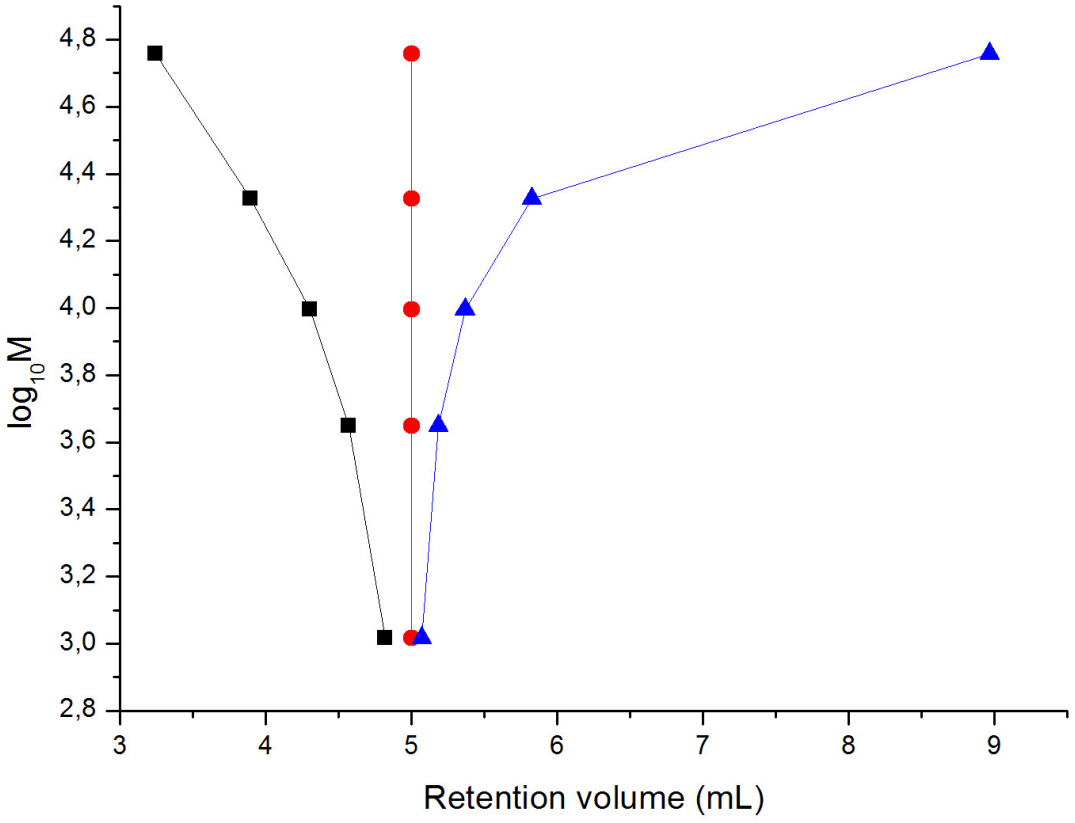

Figure 20: Critical diagram of 1,4-PI showing molar mass versus retention volume at a mobile phase composition of MEK/cyclohexane ■ = 70:30, ● = 90:10, ▲= 95:5; stationary phase: two columns of C_{18} 300-5

5.2 On-line coupling of LC-CC-NMR for the analysis of blends of 1,4-PI and 3,4-PI by operating at the critical conditions of 1,4-PI

The chromatographic system was coupled directly on-line to NMR and on-flow LC-CC-NMR experiments were performed at the critical conditions of 1,4-PI. The mobile phase for performing LC-CC-NMR should be chosen in such a way that they do not overlap with signals of interest of the homopolymers. The signals of interest can then be used for quantification. Fig. 21 shows the ^{1}H-NMR spectra of 3,4-PI dissolved in protonated MEK/cyclohexane [Fig. 21 (a)] and in deuterated chloroform [Fig. 21 (b)]. Fig. 22 shows the ^{1}H-NMR spectra of 1,4-PI dissolved in protonated MEK/cyclohexane [Fig. 22 (a)] and in deuterated chloroform [Fig. 22 (b)]. It is evident from Fig. 21 that the olefinic protons (chemical shift range between 4.3 ppm and 6.1 ppm) as well as from Fig. 22 the olefinic protons (chemical shift range between 4.6 and 5.4 ppm) can then be used for calculating the chemical composition as they do not overlap with the signals of the mobile phase. WET solvent suppression was applied to the signals of both MEK and cyclohexane. Four solvent signals were suppressed. The signals in the aliphatic region (chemical shift range 0.8-2.5 ppm) cannot be used for quantification because they are suppressed by the solvent signals. Therefore it is not possible to distinguish between cis-1,4-PI and trans-1,4-PI.

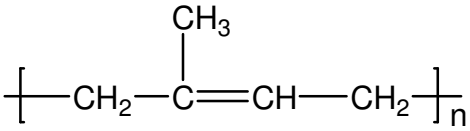

(1) 1,4-PI

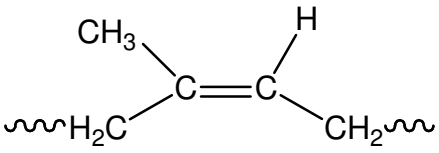

(1a) cis-1,4-PI

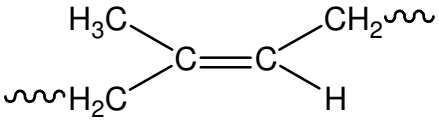

(1b) trans-1,4-PI

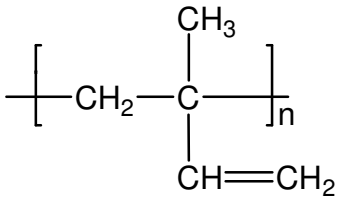

(2) 1,2-PI

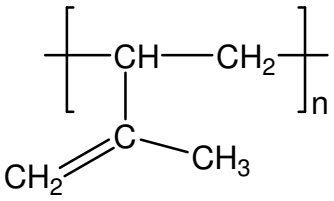

(3) 3,4-PI

Scheme 2: Different microstructures of PI

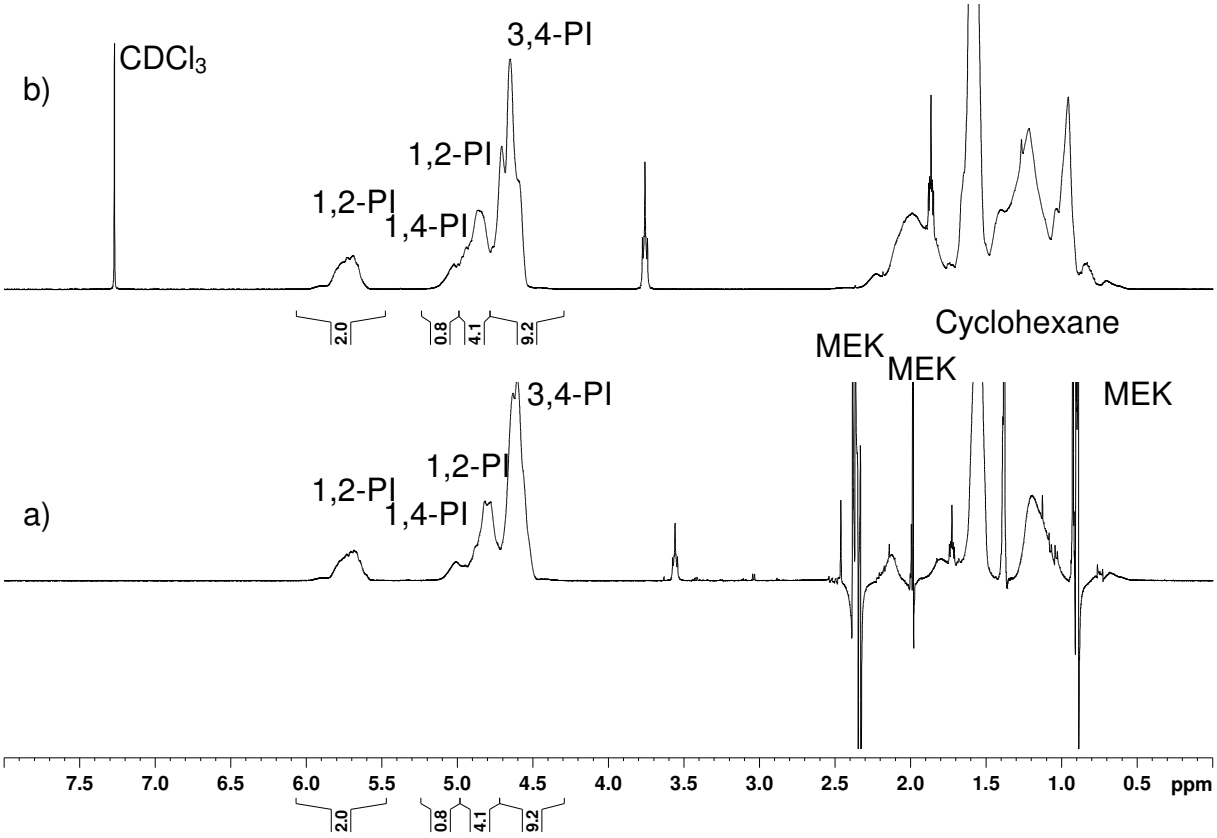

Figure 21: ^{1}H-NMR spectra of 3,4-PI (M_w = 9.4 kg/mol) in (a) non-deuterated MEK/cyclohexane with WET solvent suppression and (b) in $CDCl_3$, respectively. The assignments of the olefinic protons are given according to Scheme 2.

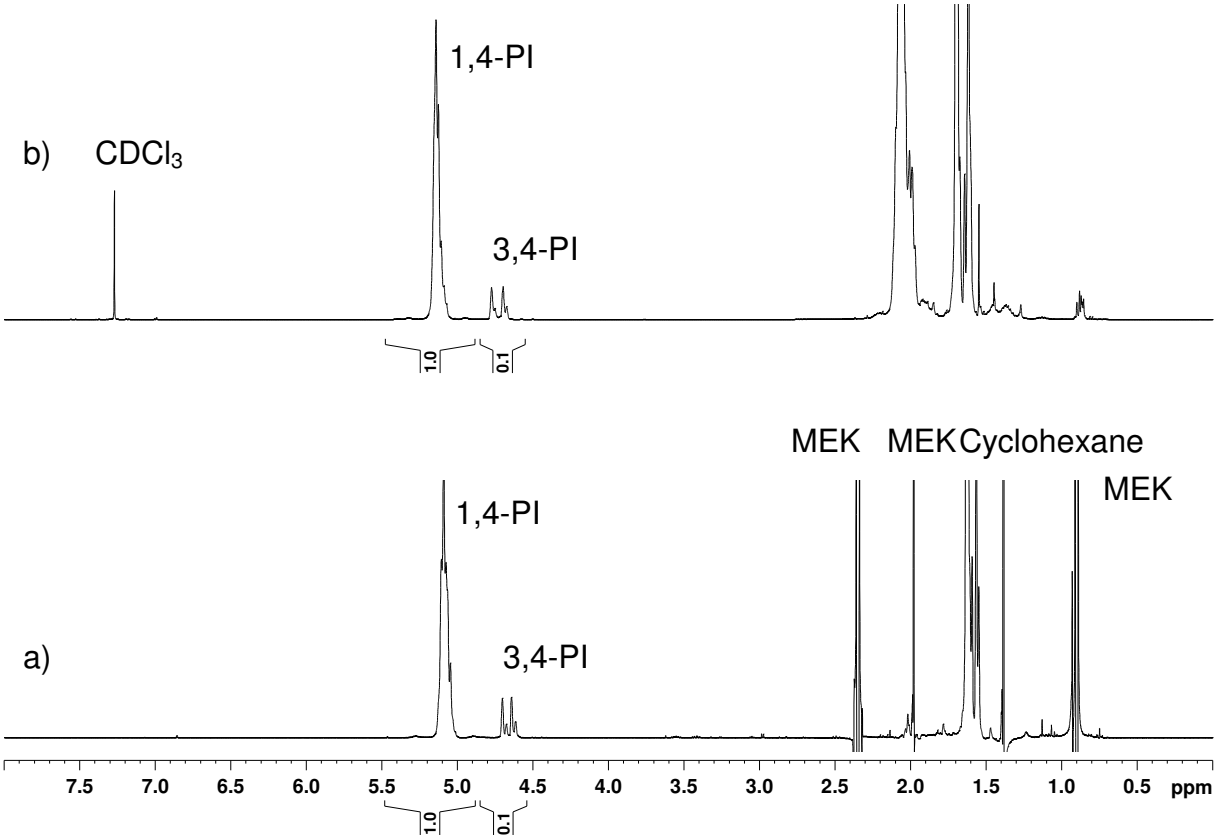

Figure 22: ^{1}H-NMR spectra of 1,4-PI (M_w=9.9 kg/mol) in (a) non-deuterated MEK/cyclohexane with WET solvent suppression and (b) in $CDCl_3$ respectively. The assignments are given according to Scheme 2.

To get a general overview on the microstructure of the samples 1,4-PI and 3,4-PI standards were measured by ^{1}H-NMR and the stereochemical compositions were determined. The corresponding results are summarised in Tables 8 and 9.

1,4-PI M_w (kg/mol)	**1,4-PI units (mol%)**	**3,4-PI units (mol%)**
1.0	94.3	5.7
4.5	93.1	6.9
9.9	94.2	5.8
21.2	94.3	5.7
57.4	94.5	5.5

Table 8: ^{1}H-NMR of 1,4-PI

3,4-PI M_w (kg/mol)	1,4-PI units (mol%)	3,4-PI units (mol%)	1,2-PI units (mol%)
1.1	11.6	64.0	24.4
9.4	11.0	62.5	26.5
33.9	13.2	58.5	28.3
53.3	16.1	50.4	33.5
76.7	17.2	48.8	34.0

Table 9: ^{1}H-NMR of 3,4-PI

It is evident from Tables 8 and 9 that 1,4-PI and 3,4-PI are not pure samples but contain some amount of the other tactic species.

The critical conditions of 1,4-PI is used for separating and analysing blends of 1,4 and 3,4-PI. The samples given in Table 10 are used for the analysis. Fig. 23 shows a HPLC-NMR on-flow run of a blend of 1,4-PI and 3,4-PI. The X-axis corresponds to the proton chemical shift and the Y-axis to the retention time in minutes. In this case, the region from 4 to 6.1 ppm is displayed. The olefinic protons of 1,4 and 3,4-PI can be observed. These on-flow runs can then be used to produce NMR chromatograms by taking the vertical projections of both regions together. Fig. 24 shows these projections. From this Fig. it is evident that 1,4-PI elutes at the same retention time as critical 1,4-PI at 10.38 min whereas 3,4-PI elutes in SEC mode. The lower the molar mass of 3,4-PI, the later is the elution. The blend having the lowest molar mass of 3,4-PI has a retention time of 9.5 min. The on-flow plot shows that 1,4-PI does not exist as a pure homopolymer. It consists of 1,4-PI as the main component and a small amount of 3,4-PI in the homopolymer chain. The same is true for the samples containing predominantly 3,4-PI. This homopolymer is rather a terpolymer consisting of 1,2-PI, 1,4-PI and 3,4-PI.

Thus we can separate blends of homopolymers of 1,4-PI and 3,4-PI by using chromatography at critical conditions of 1,4-PI.

Sample	Blend 1,4-PI/3,4-PI M_w/M_W (kg/mol)
12	21.2/33.3
13	21.2/53.3
14	21.2/76.7

Table 10: Molar masses of the blends of 1,4-PI and 3,4-PI (blends were prepared by 50/50 wt %)

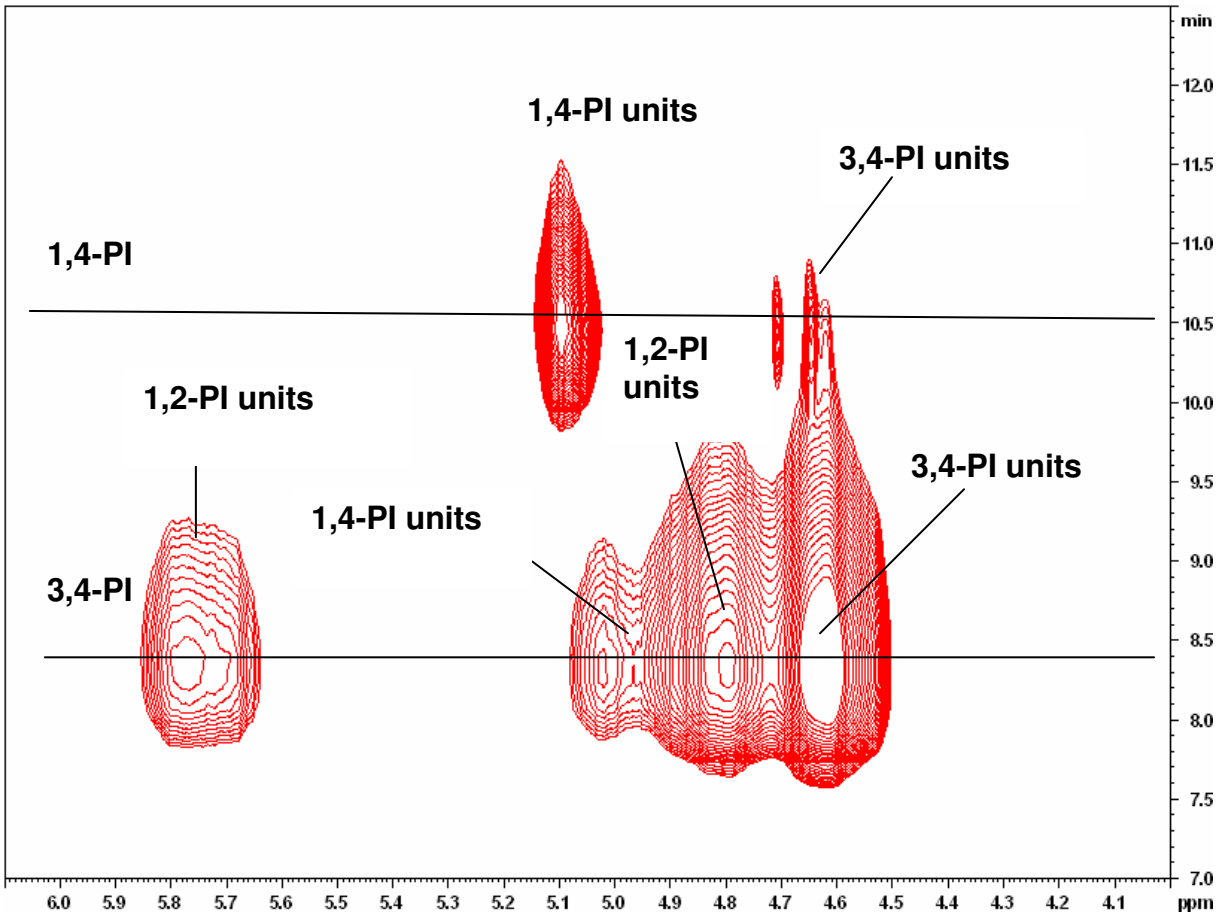

Figure 23: On-flow contour plot of a blend of 1,4-PI (M_w=21.2 kg/mol) and 3,4-PI (M_w=76.7 kg/mol) measured at the critical conditions of 1,4-PI

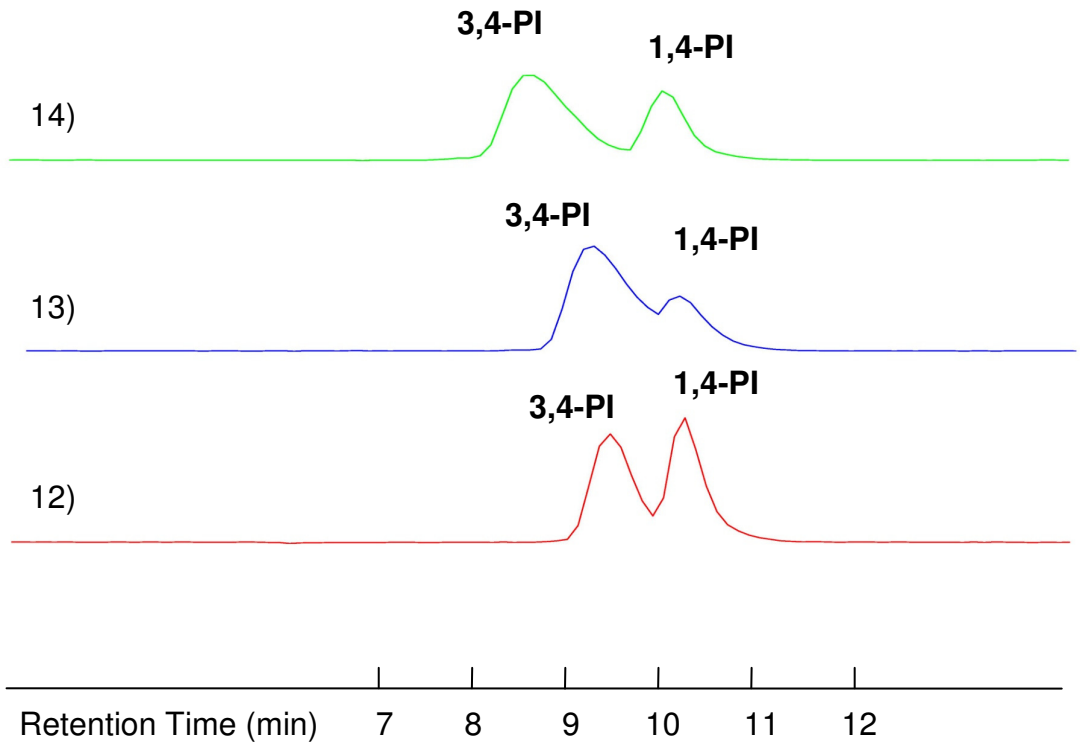

Figure 24: Vertical projections of the on-flow runs of blends of 1,4-PI and 3,4-PI; (blend 12) 1,4-PI M_W=21.2 kg/mol/3,4-PI M_W=33.3 kg/mol, (blend 13) 1,4-PI M_W= 21.2kg/mol/3,4-PI M_W=53.3 kg/mol and (blend 14) 1,4-PI M_W=21.2 kg/mol/3,4-PI M_W=76.7 kg/mol

3,4-PI was also measured at the critical conditions of 1,4-PI by using on-flow HPLC-NMR. From the peak maximum of the olefinic protons between 4.5 and 5 ppm the retention time of the different 3,4-PI standards can be calculated (see Fig. 21). Also from the on-flow runs NMR chromatograms can be produced by taking the vertical projections of the olefinic protons of 3,4-PI. These vertical projections are displayed in Fig. 25. From the Fig. it can be seen that as the molar mass of the 3,4-PI standards increases, the retention time decreases indicating SEC behaviour.

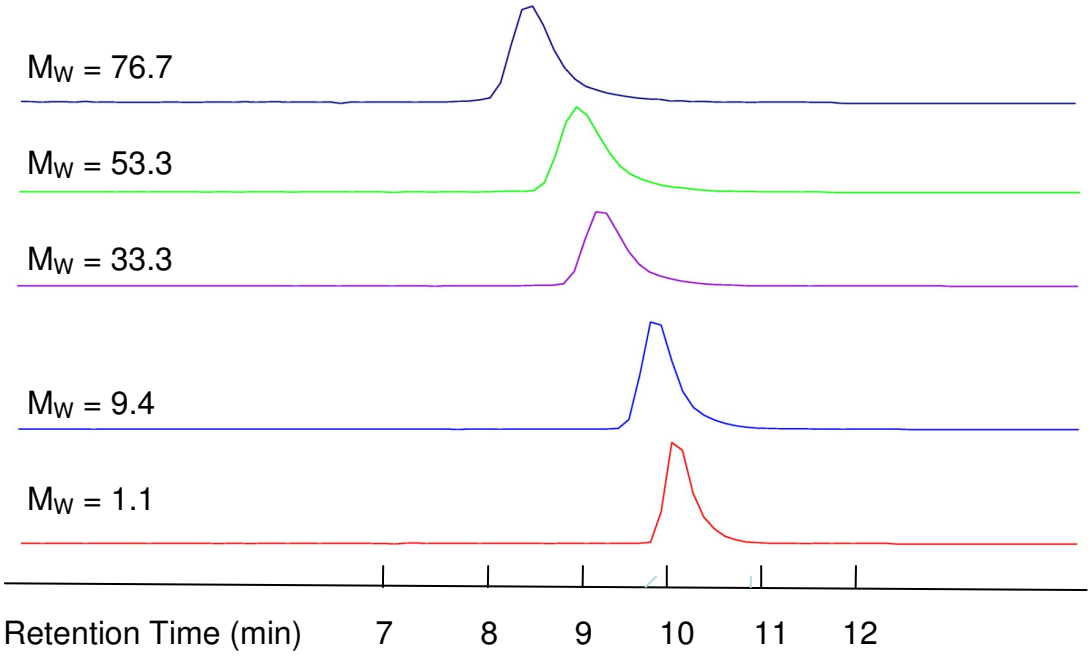

Figure 25: Vertical projections of the LC-CC-NMR on-flow runs of 3,4-PI calibration standards; samples M_W = 1.1; M_W = 9.4; M_W = 33.3; M_W = 53.3; M_W = 76.7 kg/mol

The 3,4-PI calibration standards mentioned above are then used for the construction of the calibration curve (see Fig. 26).

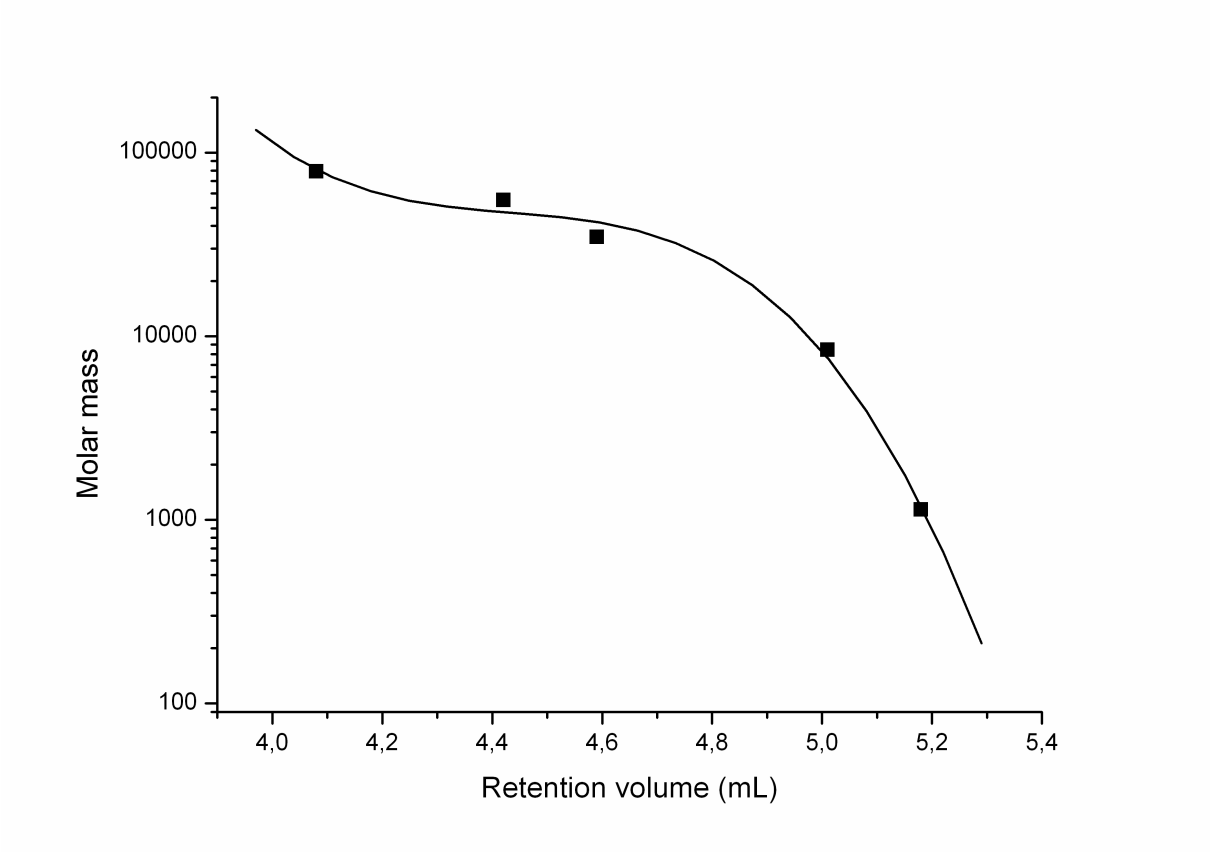

Figure 26: Calibration curve of 3,4-PI showing molar mass versus retention volume at critical point of adsorption of 1,4-PI, solid line = curve fitted with third order polynomial

All the 1,4-PI calibration standards were measured by on-flow HPLC-NMR at the critical conditions of 1,4-PI. From the typical chemical shift of 3,4-PI between 4.6 to 4.7 ppm it is seen that 1,4-PI standards are copolymers of 1,4-PI and 3,4-PI. These measurements were performed in order to verify whether the small amount of 3,4-isoprene units present in 1,4-PI calibration standards shows SEC behaviour based on the molar mass dependence at critical conditions of 1,4-PI. Since 1,4-PI standards are random copolymers of 1,4-PI and 3,4-PI it is not possible to calculate the molar mass of the 3,4-PI units since the block copolymer approach does not work.

The chemical composition of the different samples can also be calculated by adding the proton NMR traces of the on-flow runs.

The values of the chemical compositions are summarised in Table 11. The chemical compositions of 1,4-PI is nearly similar to those given in Table 8.

M_p of 1,4-PI (kg/mol)	1,4-PI units by LC-CC-NMR (mol%)	3,4-PI units by LC-CC-NMR (mol%)
1.1	93.5	6.5
4.5	92.5	7.5
9.9	93.8	6.2
21.6	93.7	6.4
58.8	94.8	5.2

Table 11: Chemical composition of 1,4-PI calibration standards by LC-CC-NMR measured at the critical conditions of 1,4-PI

Now the stereochemistry of PI will be investigated. The olefinic protons of PI reveal different stereochemistry in the ^{1}H-NMR spectra. Fig. 27 presents the stereochemistry of 3,4-isoprene units present in 1,4-PI as a function of retention time measured at the critical conditions of 1,4-PI. The 1,4-PI standards 1.1 kg/mol, 9.9 kg/mol and 21.6 kg/mol show 6-7 % of 3,4-PI units. The 4.5 kg/mol standard shows about 8% of 3,4-PI units whereas the 58.8 kg/mol standard shows less than 6% of 3,4-PI units. Fig. 27 shows that the stereochemistry is nearly constant.

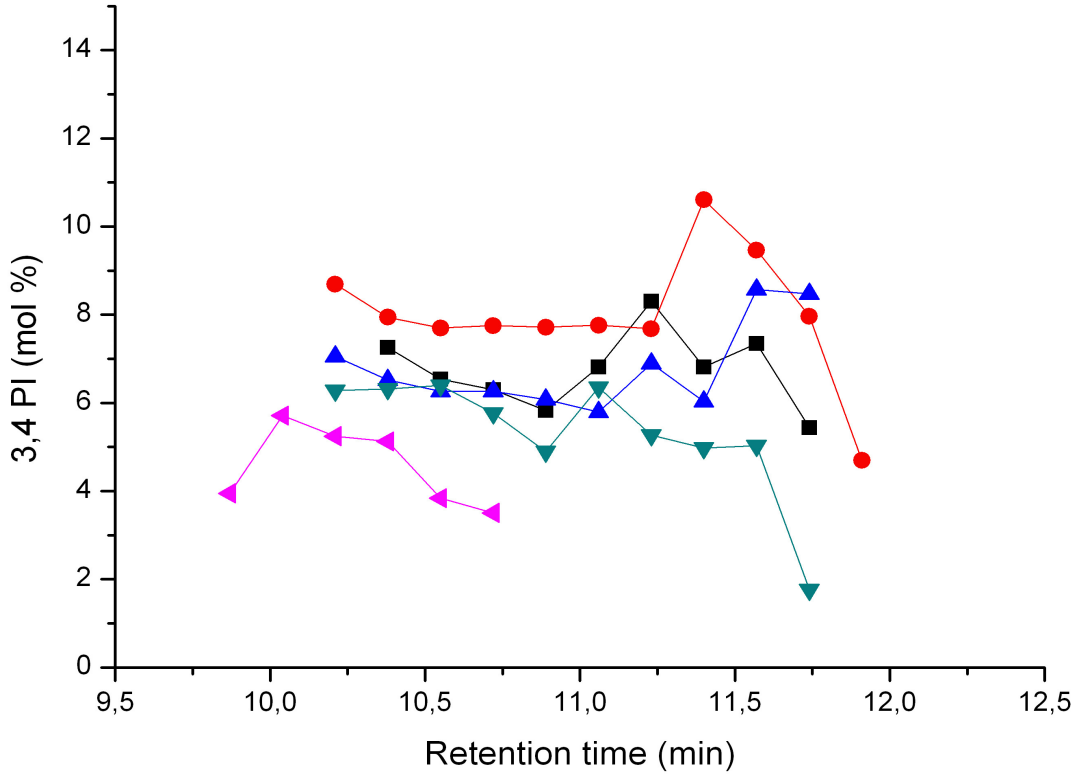

Figure 27: Stereochemistry of 3,4-PI units present in 1,4-PI versus retention time at critical conditions of 1,4-PI, (■ = 1.1, ● = 4.5, ▲ = 9.9, ▼ = 21.6, ◀ = 58.8 kg/mol)

6. Analysis of PS-*b*-PI copolymers

6.1 Method development for establishing the critical conditions of PS by using solvent mixtures

Mixture of THF-cyclohexane as mobile phase is well suited for establishing the critical conditions. Fig. 28 shows the critical diagram obtained by using a set of normal phase columns. The PS homopolymers were used for establishing the critical conditions. SEC is seen at a mobile phase composition of THF/cyclohexane less than 17.8/82.2 for example (20:80) v/v. The critical conditions correspond to a mobile phase composition of THF/cyclohexane (17.8:82.2) v/v and at a mobile phase composition of THF/cyclohexane (15:85) v/v liquid adsorption chromatography is observed.

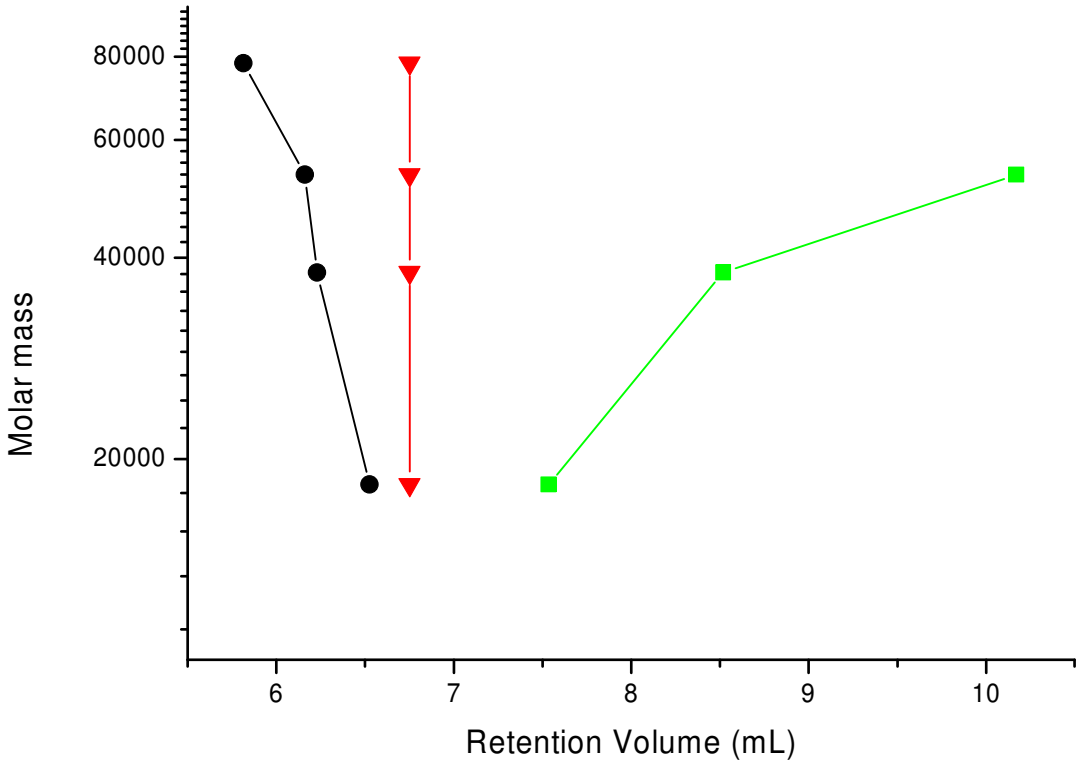

Figure 28: Critical diagram of PS showing molar mass versus retention volume, mobile phase THF/cyclohexane ● = 20:80, ▼= 17.8:82.2, ■ = 15:85 v/v; stationary phase: two columns of Si 300-5

6.2 LC-CC-^{1}H-NMR of PS-*b*-PI copolymers at critical conditions of PS

Fig. 29 shows the ^{1}H-NMR spectra of a PS-*b*-PI copolymer dissolved in a mixture of THF and cyclohexane without adding deuterated solvents [Fig. 29 (a)] and in deuterated tetrahydrofuran [Fig. 29 (b)]. WET solvent suppression is applied to the signals of both THF and cyclohexane. Three solvent signals are suppressed. It is evident from Fig. 29 that the olefinic protons of the PI block and the aromatic protons of the PS block are unaffected by suppression. These signals can be used for determining the chemical composition distribution. This Fig. also indicates that the stereochemistry of the PI block can be calculated from the olefinic protons. PI shows different types of microstructure cis-1,4-PI, trans-1,4-PI, 1,2-PI and 3,4-PI. Since the methyl groups of 1,4-PI are present in the downfield region of the proton NMR spectrum they are suppressed by the solvent signals. But from the olefinic protons one can differentiate between the different microstructures of PI.

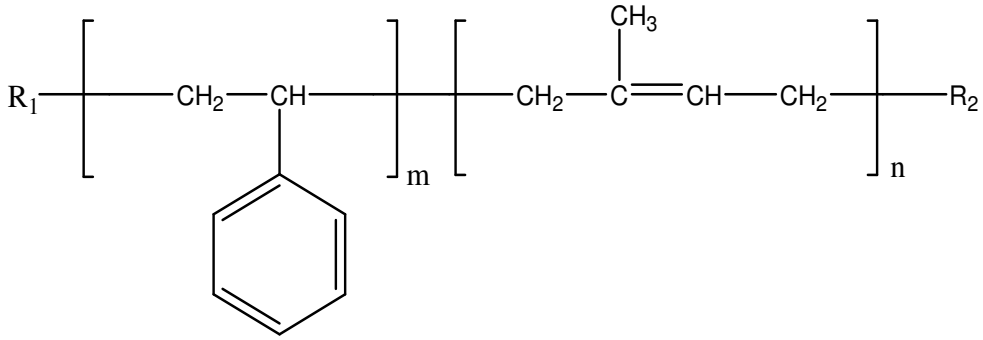

(1) PS-*b*-1,4-PI

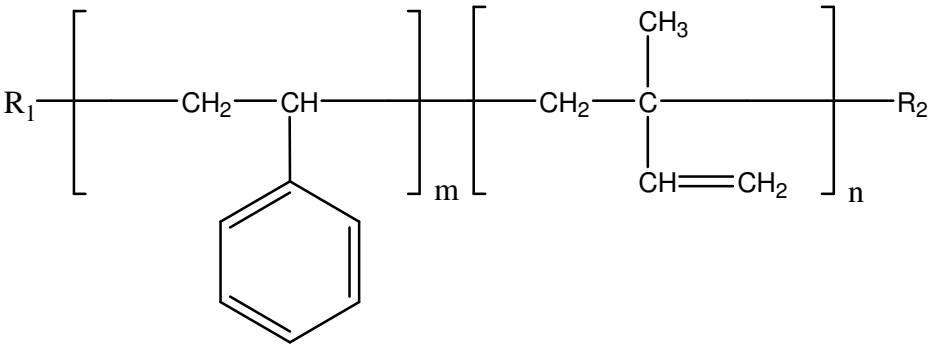

(2) PS-*b*-1,2-PI

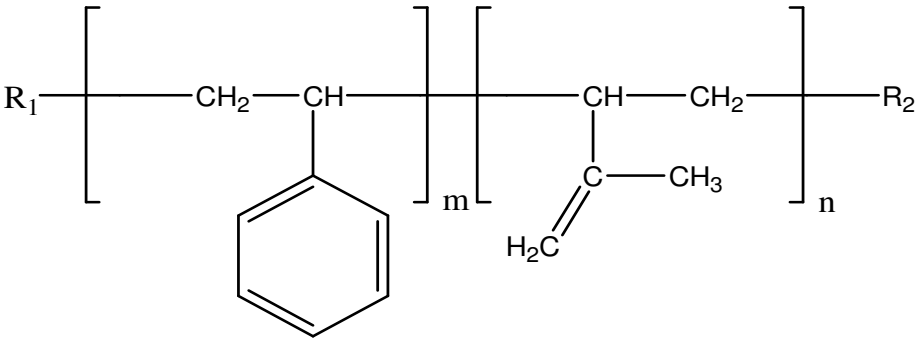

(3) PS-*b*-3,4-PI

Scheme 3: Structure of PS-*b*-PI copolymer showing different microstructures of the PI block: (1) PS-*b*-1,4-PI, (2) PS-*b*-1,2-PI and (3) PS-*b*-3,4-PI

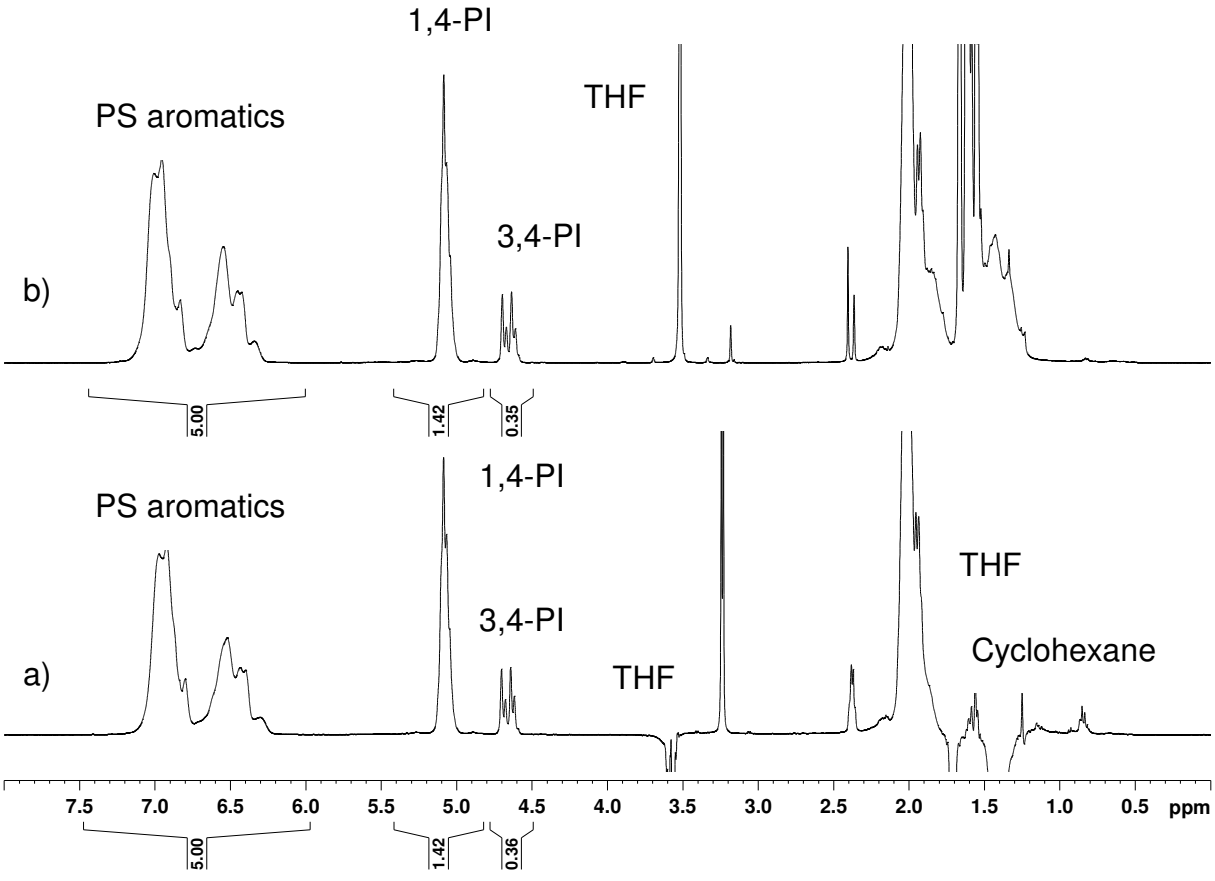

Figure 29: ^{1}H-NMR spectra of PS-*b*-PI copolymer in (a) non-deuterated THF/ cyclohexane with WET solvent suppression and (b) in deuterated THF respectively. The assignments are given according to Scheme 3.

Critical conditions of 17.8:82.2 v/v are then used for the analysis of PS-*b*-PI copolymers.

6.3 Comparison of sequential living anionic polymerisation and coupling of living precursor blocks for the analysis of PS-*b*-PI copolymers by on-line HPLC-NMR

For analysing PS-*b*-PI copolymers the samples given in Table 12 were used. These block copolymers are synthesised by sequential living anionic polymerisation and coupling of living precursor blocks. In the case of synthesis by sequential anionic polymerisation, first styrene was added at room temperature to a cyclohexene solution of butyllithium under vigorous stirring and the polymerization was allowed to proceed overnight. Then isoprene was introduced by smashing the break-seal of the corresponding ampoule and after 2 days the reaction was terminated with methanol. Cyclohexene was preferred as polymerisation solvent against cyclohexane, because the latter is a theta solvent for polystyrene at room temperature. In this case there is a possibility for formation of PS homopolymer as by-product.

The synthesis of PS-*b*-PI via the coupling procedure takes place in two steps. In the first step a cyclohexene solution of polystyryllithium, was added to a huge molar excess (typically 100-fold) of dichlorodimethylsilane under vigorous stirring, at room temperature. Under these conditions formation of chlorosilyl-terminated PS is favoured, whereas formation of PS-$SiMe_2$-PS is almost ruled out. Removal of the unreacted dichlorodimethylsilane takes place by distilling off all volatiles under high vacuum and redissolving the chlorosilyl-terminated PS in pure cyclohexene, three times. In the second coupling step, the purified chlorosilyl-terminated PS is reacted with a slight molar excess of polyisoprenyllithium for 3 days, at room temperature, whereupon methanol is added to deactivate the polyisoprenyllithium excess. There is a possibility of formation of both PS as well as PI homopolymers as by-products when synthesis is carried out by the coupling method.

The PS-*b*-PI copolymers synthesised by different methods were then analysed by HPLC-NMR. Figs. 30 and 32 shows HPLC-NMR on-flow runs of PS-*b*-PI copolymer synthesised by coupling of living precursor blocks and sequential living anionic polymerisation. The copolymer synthesised by coupling of living precursor blocks and sequential living anionic polymerisation shown in Figs. 30 and 32 shows separation

into two components. The first component elutes in SEC mode while the second component elutes at the critical retention time of PS. Since the first eluting peak shows coexisting signals at the aromatic and olefinic regions, this peak can be assigned to the copolymer. The peak eluting later can be assigned to PS homopolymer based on the typical NMR chemical shifts of PS between 6.4 and 7.3 ppm, and the critical elution time of PS. The resonance peak at 5.1 ppm is used to calculate the amount of 1,4-PI. The doublet at 4.65 and 4.75 ppm is used to calculate the amount of 3,4-PI. Fig. 32 does not show the presence of 3,4-PI since very little amount is present. The signals in the aliphatic region cannot be used for the quantification because these polymer signals overlap with the solvent signals and are suppressed when solvent suppression is performed. From these on-flow plots the most intense ^{1}H-NMR traces are extracted. Trace 1 in both the on-flow plots indicates the presence of copolymer and trace 2 in both the plots shows the presence of PS homopolymer (see Figs. 31 and 33).

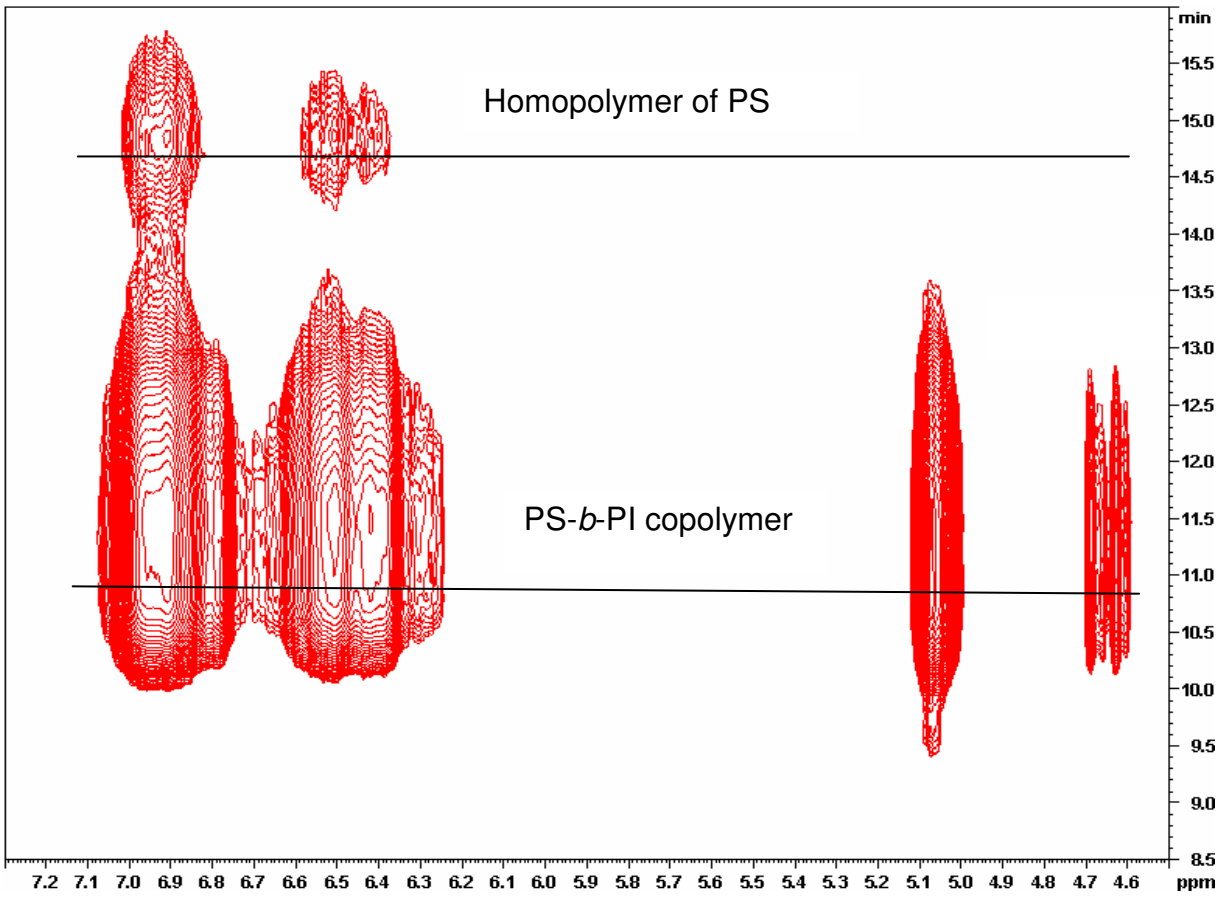

Figure 30: LC-CC-NMR on-flow run of PS-*b*-PI copolymer (sample 21) synthesised by coupling of living precursor blocks, critical conditions of PS

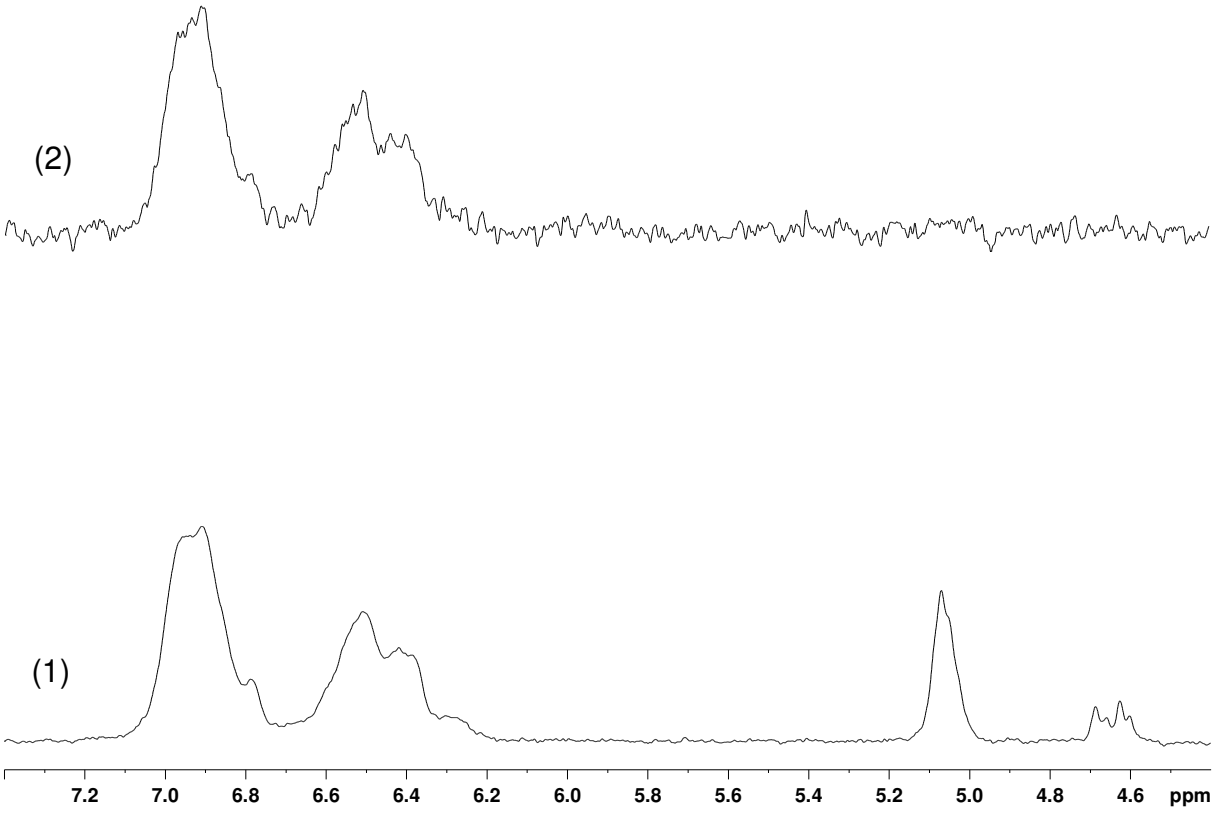

Figure 31: ^{1}H-NMR traces of the on-flow run; (1) PS-*b*-PI copolymer, (2) Homopolymer of PS

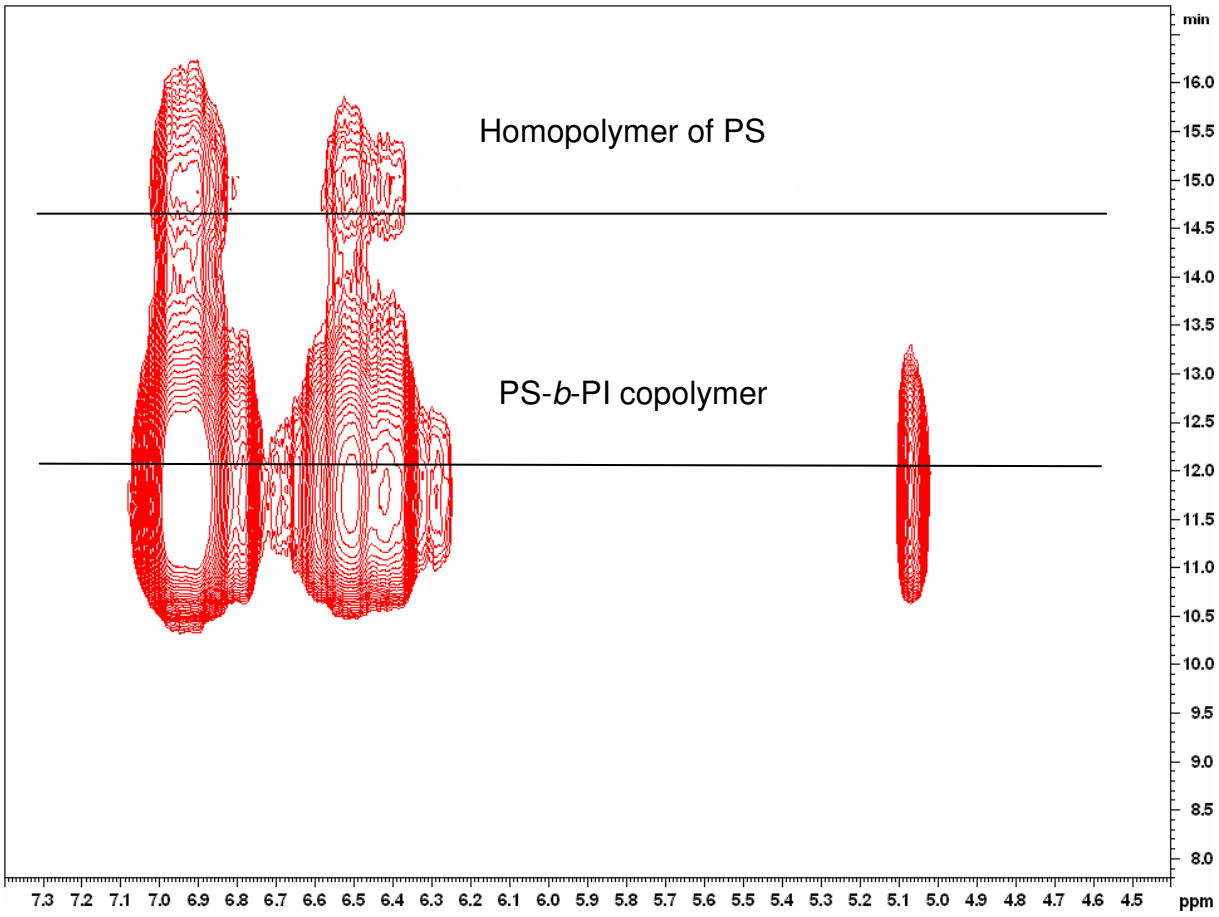

Figure 32: LC-CC-NMR on-flow run of PS-*b*-PI copolymer (sample 18) synthesised by sequential living anionic polymerisation, critical conditions of PS

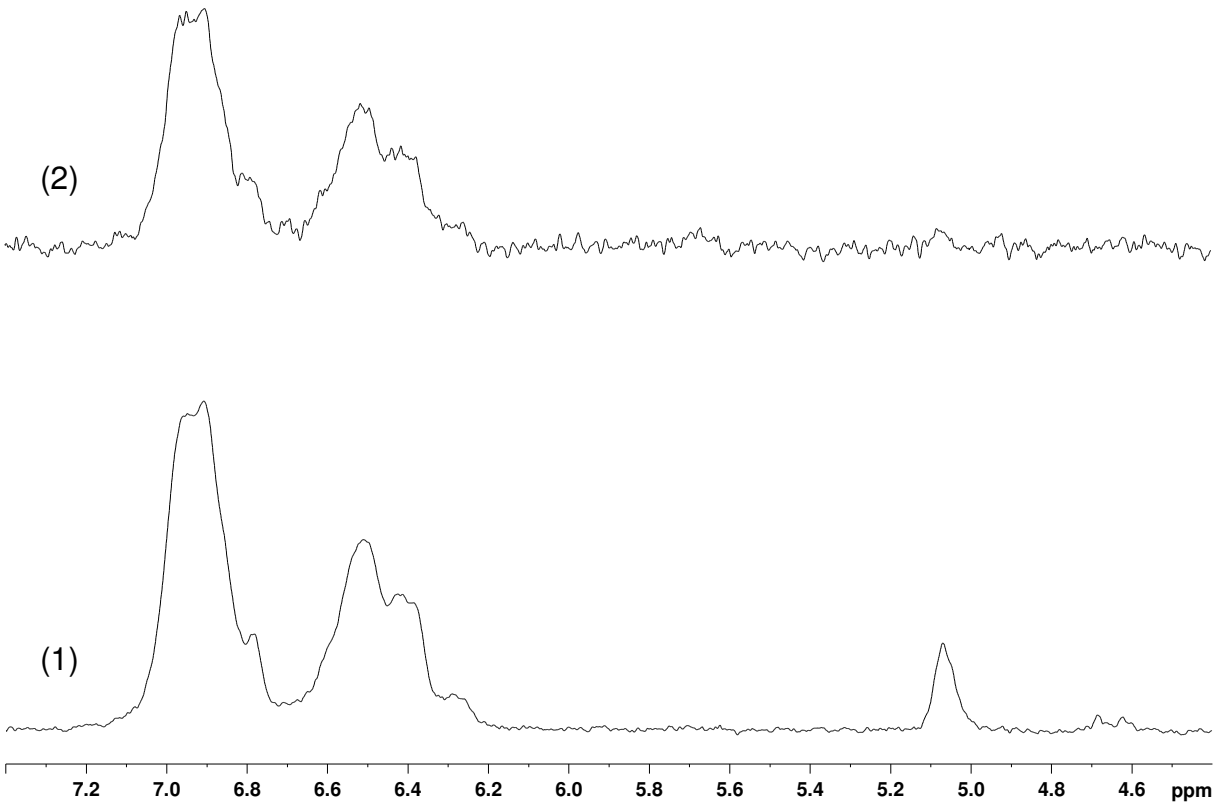

Figure 33: ^{1}H-NMR traces of the on-flow run; (1) PS-*b*-PI copolymer, (2) Homopolymer of PS

The block copolymers given in Table 12 are also analysed by conventional SEC and by off-line NMR. The conventional SEC data are obtained by using THF as solvent and cross-linked polystyrene as the stationary phase. The calibration is based on PS. Off-line NMR is used to determine the chemical composition of the samples. From the signal intensities of the aromatic protons (styrene) and the olefinic protons (isoprene) the average chemical composition of the block copolymers can be calculated, see Table 12.

Sample	Name	M_P by SEC (kg/mol)	styrene/isoprene by ^{1}H-NMR (mol%)
15	(38-44) sma	118.5	38.6/61.4
16	(54.3-25) sma	101.9	56.1/43.9
17	(18.5-57.8) sma	107.3	16.2/83.8
18	(78.2-11.3) sma	113.9	78.2/21.8
19	(37-36.7) coup	97.8	29.6/70.4
20	(18.7-50) coup	108.1	13.9/86.1
21	(53.2-25) coup	99.5	52.9/47.1

Table 12: SEC and ^{1}H-NMR analysis of the block copolymers (where sma means sequential living anionic polymerization and coup means coupling of living precursor blocks. The numbers in brackets refer to the assumed molar masses of each block)

Consequently, the molar mass of the PI blocks in the copolymers can be determined by on-flow HPLC-NMR and PI calibration standards. For calculating the molar masses of the PI block in PS-*b*-PI copolymer by LC-CC-NMR a calibration curve is constructed by using PI calibration standards. The molar mass is calculated by taking the peak maximum (M_P) of the olefinic protons. Using the calibration curve given in Fig. 34, the molar masses of the PI blocks in the block copolymers were determined.

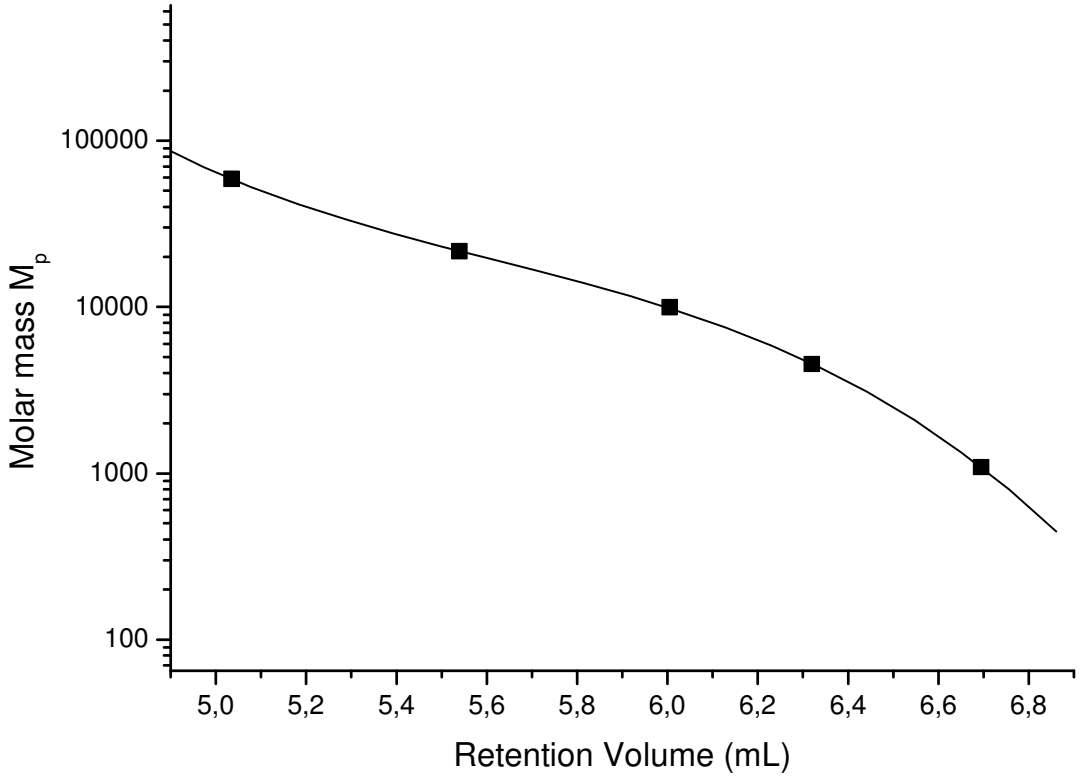

Figure 34: Calibration curve of PI showing molar mass versus retention volume at critical point of adsorption of PS, solid line = curve fitted with third order polynomial

Table 13 shows the molar masses of the PI blocks of the copolymers determined by LC-CC-NMR. These data are then compared to the molar masses of the block copolymers obtained by SEC and off-line NMR. Using the chemical compositions and the SEC data of Table 12, the molar masses of the blocks of the samples can be calculated according to the modified version of Equations (25-26).

The values of the molar masses obtained by SEC and off-line NMR are higher than the molar masses obtained by on-line LC-CC-NMR. Considering the complexity of the experiments different sources of error can occur. The accuracy of establishing the critical conditions will influence the results. The second source of error is the accuracy of the molar mass analysis by off-line SEC. PS calibration standards were used to determine the molar masses of the copolymers. In addition, SEC does not separate the block copolymers from the PS as well as PI homopolymers and therefore the presence of these homopolymer fractions will affect the molar mass analysis. To the same extent this is also true for the chemical composition that was analysed by off-line NMR. These values were obtained for the total samples and may deviate from the chemical composition of the true block copolymers.

Sample	**M_p (PI block) by LC-CC-NMR (kg/mol)**	**M_P of (PI block) by SEC and NMR (kg/mol)**
15	40.5	60.4
16	25.4	34.5
17	61.9	82.8
18	14.9	17.6
19	34.8	59.5
20	34.8	86.7
21	25.4	36.6

Table 13: Molar masses of the PI block of the copolymers determined by SEC and off-line NMR with modified version of Equation (26) or LC-CC-NMR with the peak maximum of the olefinic protons

Sample	M_p (PI block) by LC-CC-NMR (kg/mol)	Styrene/isoprene of copolymer by LC-CC-NMR (mol%)	M_P of block copolymer (kg/mol) calculated
15	40.5	33.4/66.6	71.6
16	25.4	55.9/44.1	74.6
17	61.9	16.2/83.8	80.2
18	14.9	76.7/23.3	89.9
19	34.8	29.6/70.4	57.2
20	34.8	13.9/86.1	43.4
21	25.4	49.3/50.7	63.2

Table 14: The molar masses of the PI block of the copolymers, chemical compositions and calculated total true molar masses of the block copolymers

Using the true molar mass of the PI block obtained by LC-CC-NMR and the true chemical composition obtained by adding all polymer traces of the on-flow runs the true molar mass of the block copolymer is calculated. The results are summarised in Table 14.

One of the major benefits of on-flow HPLC-NMR is the ability to determine the CCD of the copolymers. Using the on-flow data presented in Figs 30 and 32, it is possible to calculate the chemical composition at different elution volumes. Fig. 35 [samples 15 (a), 17 (b), 19 (c) and 21 (d)] shows the plots of CCD versus retention time for some of the block copolymers. The Fig. also shows the NMR projections of the aromatic region (solid black line, normalised to one proton), olefinic protons from 1,4-PI (solid red line, normalised to one proton) and olefinic protons from 3,4-PI (solid green line, normalised to one proton). The following general conclusions can be derived from Fig. 35 (samples 15, 17, 19 and 21):

(i) The samples (15 and 17) are synthesised by sequential living anionic polymerisation. In this case, in a first step styrene is polymerised to form the PS precursor block. After styrene is completely consumed, isoprene is added to the living system to form the second block. So there is a possibility for the formation of PS homopolymer. Sample 15 shows bimodal MMD (indicated by the black solid line) due to the presence of PS homopolymer. Sample 17 does not contain PS homopolymer. The PI block (indicated by the red solid line) contains shoulders at higher retention due to the formation of small amount of homopolymer of PI see samples (15

and 17) which cannot be separated from the copolymer. These shoulders indicate fractions that are results of coupling reactions that take place between two living block copolymer chain ends, i.e. $(PS\text{-}b\text{-}PI)_2$, presumably caused by the inadequately degassed methanol. The molar masses of the PI blocks of these coupling products are smaller than the molar masses of the PI blocks in the diblock copolymers. Lower retention times represents the copolymer and the higher retention time belongs to PS, since we are at critical conditions of PS.

(ii) The block copolymers show no significant chemical heterogeneity. The samples show a moderate dependence of CCD versus retention time in the region of the copolymer.

(iii) The samples (19 and 21) are synthesised by the coupling of living precursor blocks, so there is a possibility for the formation of PS homopolymer. All the samples show at least bimodal distribution. Samples 19 and 21 show shoulders at higher retention time indicating the presence of homopolymer of PI (indicated by the red solid line). In addition to the shoulder sample 21 indicates the presence of PS homopolymer (shown by the black solid line). The homopolymer elutes from 13.5-15.5 min. The shoulder seen in sample 19 between 8.5-9 min may have PI molar mass that is larger than the molar mass of PI block in the copolymer. This component is assigned to a coupling by-product that contains two PI blocks. This might happen due to incomplete removal of the unreacted Me_2SiCl_2 from the chlorosilyl-terminated PS and due to inadequately degassed methanol.

(iv) The samples synthesised by coupling of living precursor blocks show chemical heterogeneity. They show a moderate dependence of CCD versus retention time in the region of the copolymer.

(v) Sample 19 is rich in PI at low retention times which indicates that they have a higher molar mass whereas they are rich in PS at high retention times indicating that they have a lower molar mass. Sample 21 is rich in PS at low retention times and dominated by PI at higher retention times.

(a)

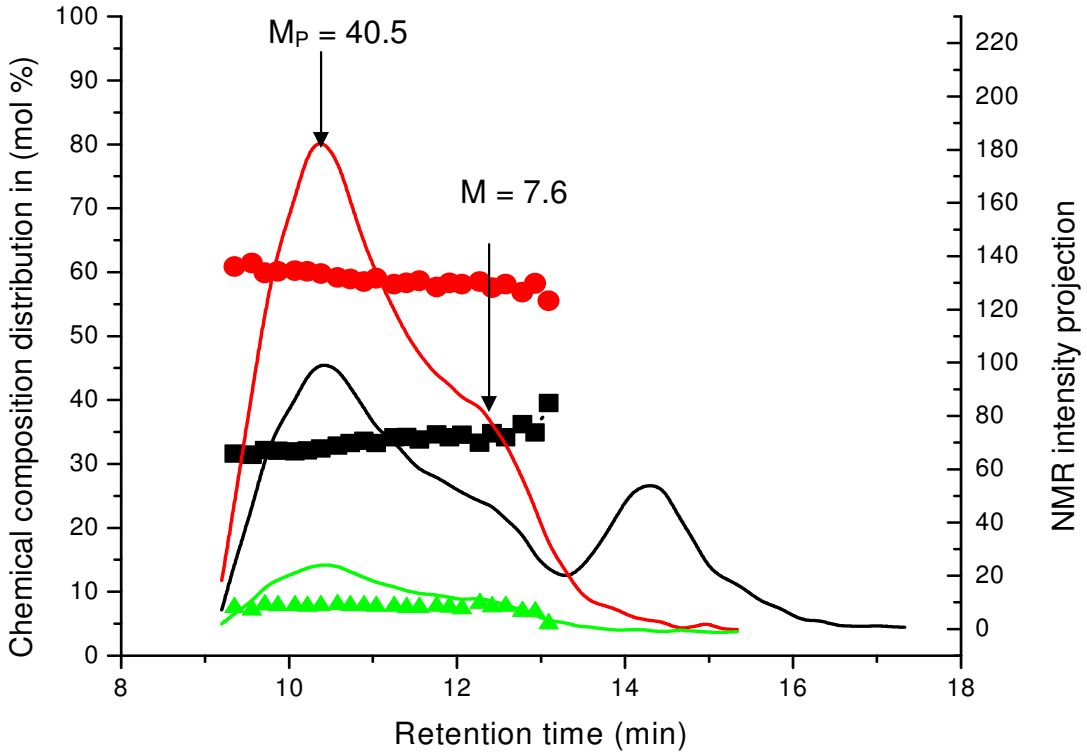
MP = 40.5
M = 7.6
Chemical composition distribution in (mol %)
NMR intensity projection
Retention time (min)

(b)

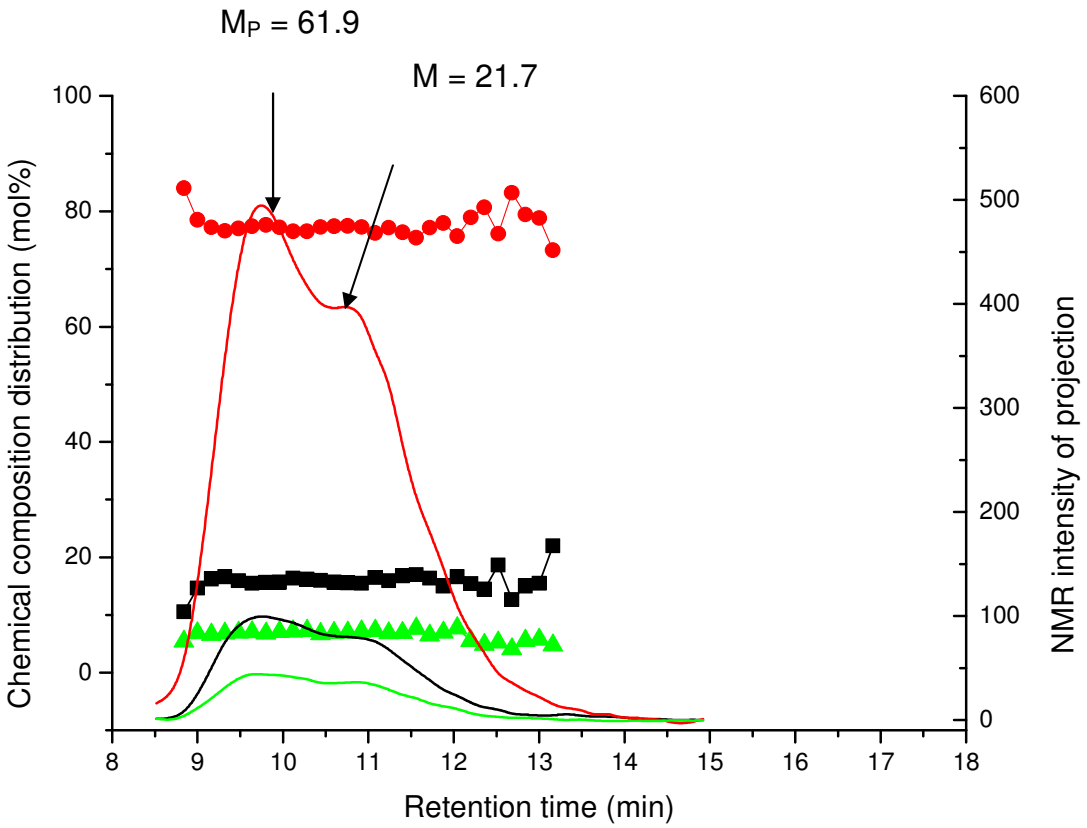
MP = 61.9
M = 21.7
Chemical composition distribution (mol%)
NMR intensity of projection
Retention time (min)

(c)

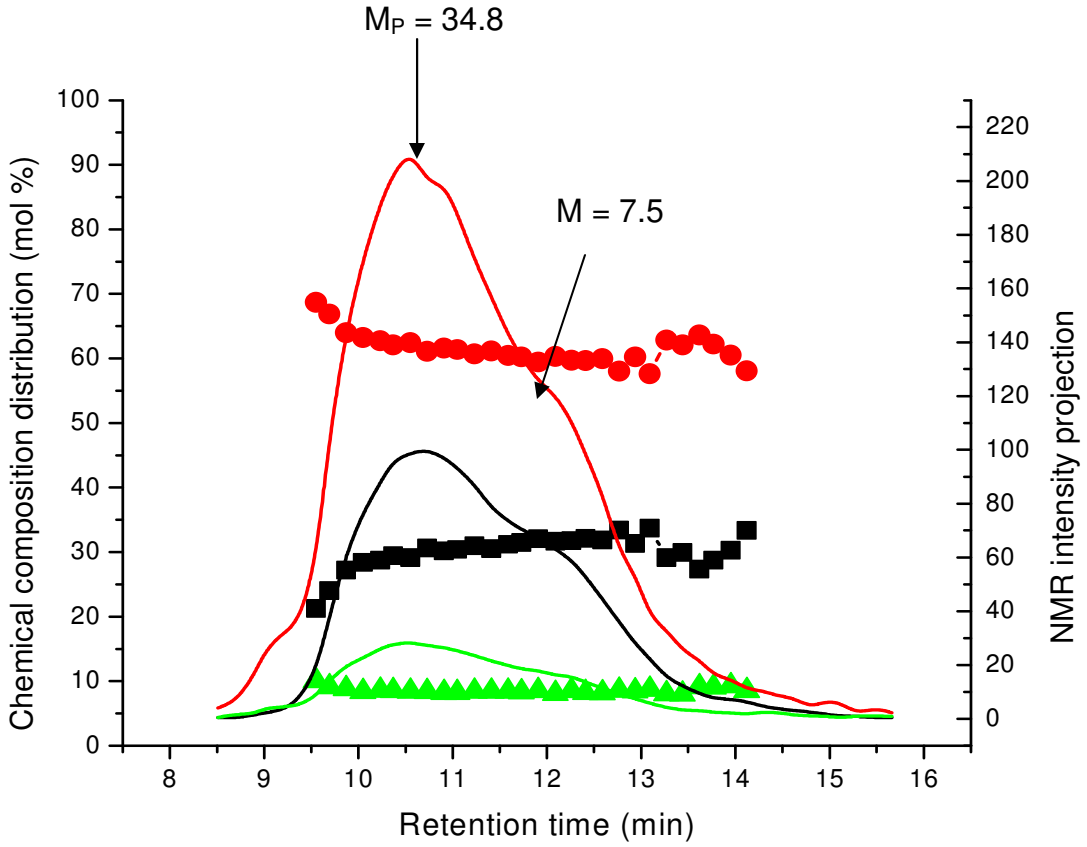
M_P = 34.8
M = 7.5
Chemical composition distribution (mol %)
NMR intensity projection
Retention time (min)

(d)

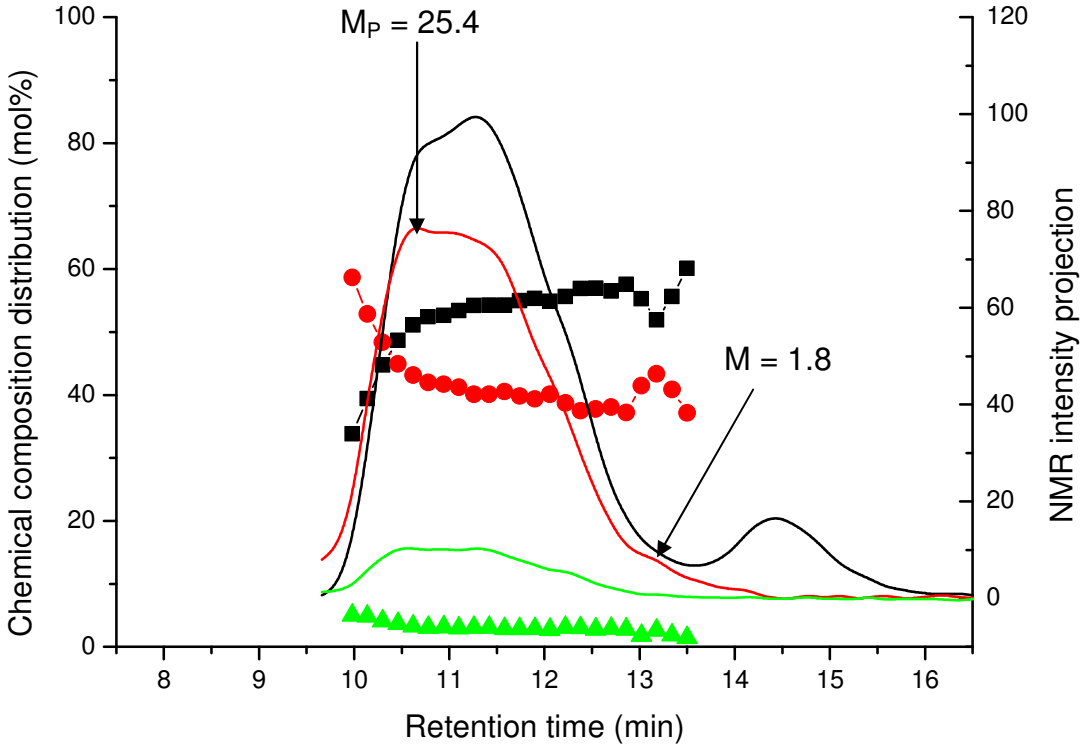
M_P = 25.4
M = 1.8
Chemical composition distribution (mol%)
NMR intensity projection
Retention time (min)

Figure 35: Chemical composition of PS-*b*-PI copolymers versus retention time (■ = mol% PS, ●= mol% 1,4-PI and ▲= mol% 3,4-PI), solid line black = NMR projection of the aromatic region, solid line red = NMR projection of 1,4-PI and solid line green = NMR projection of 3,4-PI [samples 15 (a), 17 (b), 19 (c), 21 (d)]

To get an overview on the stereochemistry of the total samples, the PI calibration standards and the PS-*b*-PI copolymers were measured by ^{1}H-NMR and the stereochemical compositions were determined. The corresponding results are summarised in Table 15.

Sample	**1,4-PI/3,4-PI by ^{1}H-NMR (mol%)**	**Sample M_W (kg/mol)**	**1,4-PI/3,4-PI by ^{1}H-NMR (mol%)**
15	88.97/11.03	1.04	94.26/5.74
16	87.64/12.36	4.46	93.07/6.93
17	91.94/8.06	9.91	94.18/5.82
18	91.19/8.81	21.2	94.26/5.74
19	89.13/10.87	57.4	94.53/5.47
20	92.25/7.75		
21	88.13/11.87		

Table 15: Stereochemistry of the PI blocks of the copolymers and PI calibration standards

Now, the stereochemistry of the PI blocks of the copolymers shall be investigated. Due to the fact that the olefinic protons in the ^{1}H-NMR spectra reveal different stereochemistry see Scheme 3, the stereochemistry is determined from the on-flow data of Figs. 30 and 32. Figs. 36 and 37 present the calculated stereochemistry of the PI blocks as a function of retention time for the critical conditions of PS. It shows that the stereochemistry of the PI blocks is constant and does not depend on the different retention times. The block copolymers synthesised by coupling of living precursor blocks [see Fig. 36 (a, b)] show 1,4-PI content from 88 to 91% and 3,4-PI from 7 to 12%. In the case of the block copolymers synthesised by sequential living anionic polymerisation [see Fig. 37 (a, b)] the 1,4-PI content varies from 87 to 97% and 3,4-PI content from 3-13% calculated at different retention times. The polyisoprene block of the copolymers synthesised by the two different methods show predominantly the structure of 1,4-PI.

(a)

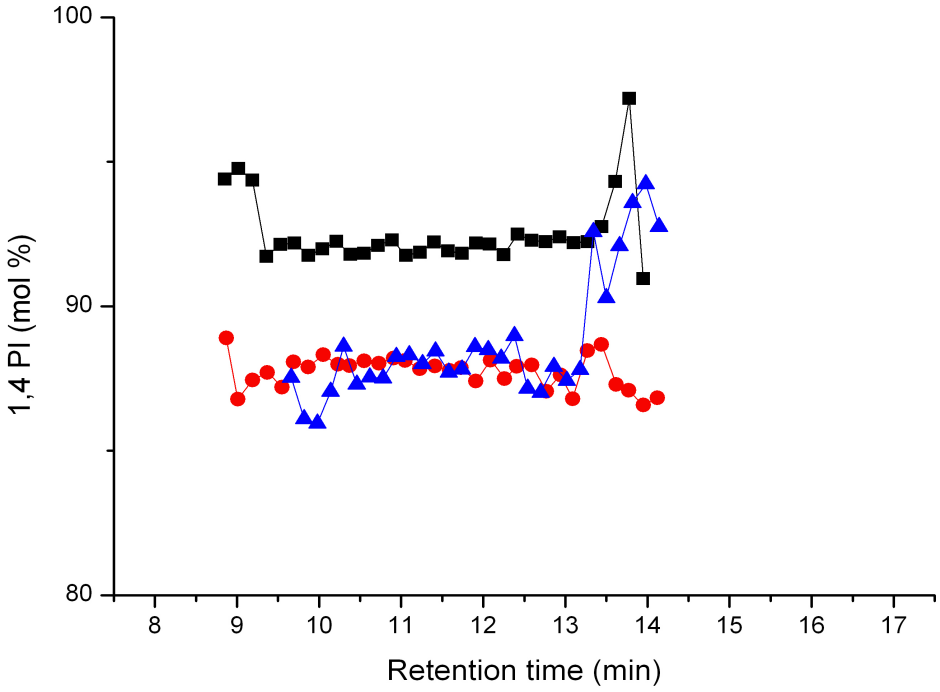

(b)

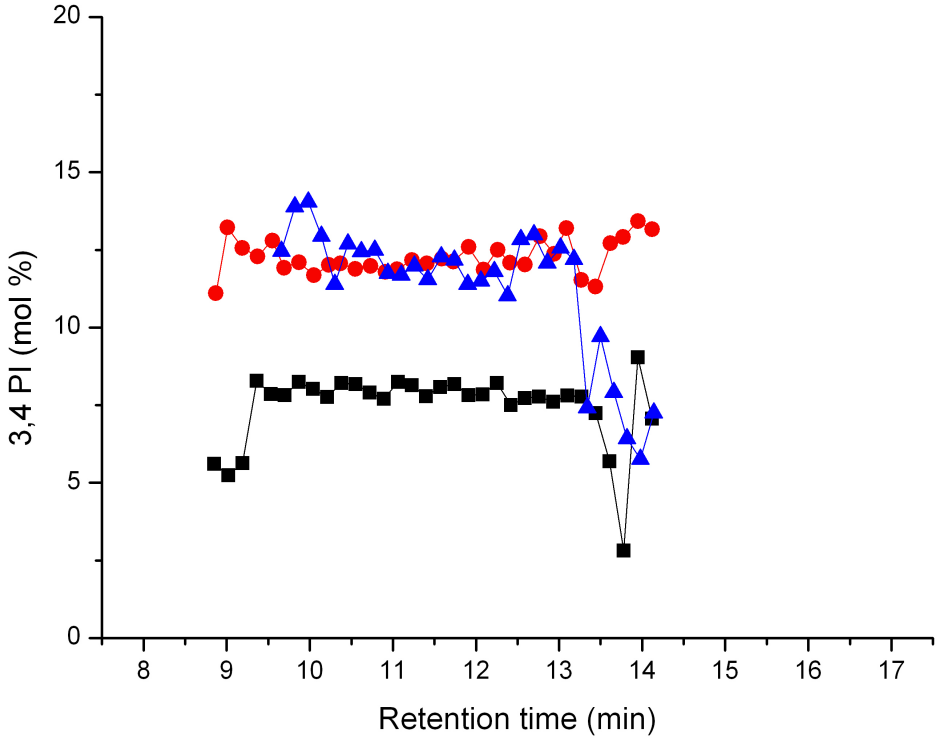

Figure 36: Stereochemistry of the PI block of PS-*b*-PI copolymers versus retention time synthesised by coupling of living precursor blocks, (a) 1,4-PI versus retention time and (b) 3,4-PI versus retention time [■ = 20, ● = 19, ▲ = 21]

(a)

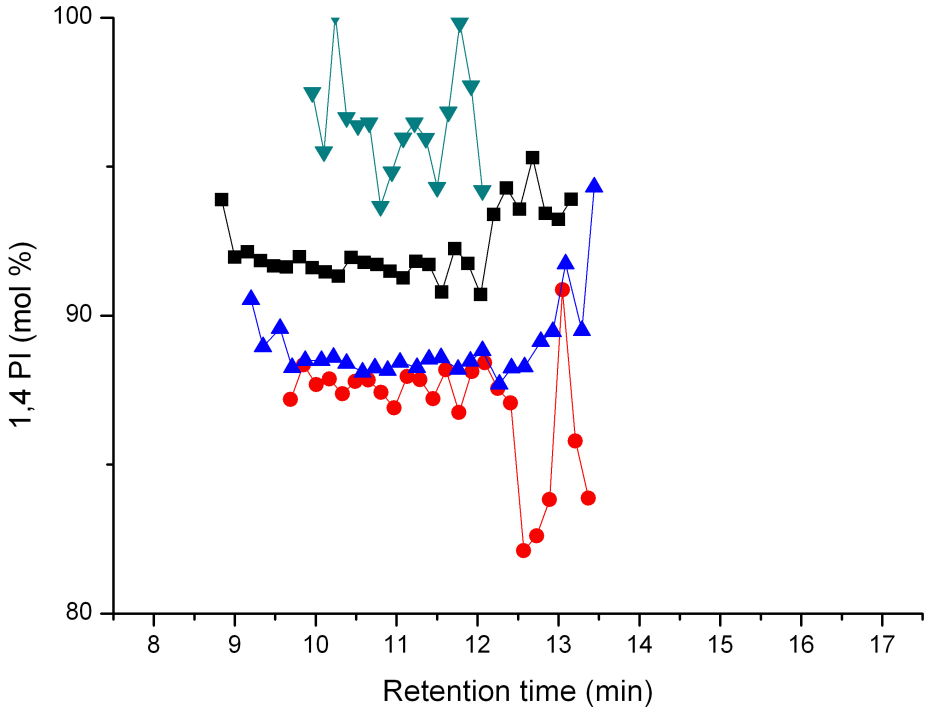
100
90
80
1,4 PI (mol %)
8
9
10
11
12
13
14
15
16
17
Retention time (min)

(b)

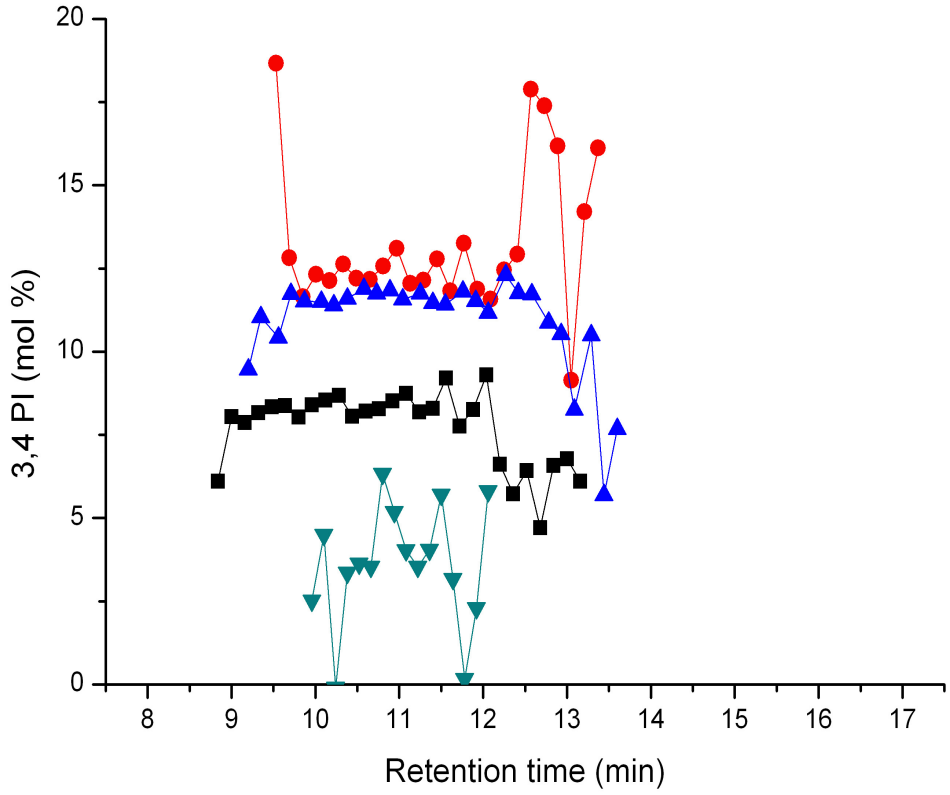
20
15
10
5
0
3,4 PI (mol %)
8
9
10
11
12
13
14
15
16
17
Retention time (min)

Figure 37: Stereochemistry of the PI block of PS-*b*-PI copolymers versus retention time synthesised by living anionic polymerisation, (a) 1,4-PI versus retention time and (b) 3,4-PI versus retention time [■ = 17, ● = 16, ▲= 15, ▼= 18]

6.4 Method development for establishing the critical conditions of 1,4-PI by using solvent mixtures

In order to separate PS-*b*-PI copolymers critical conditions were established for the 1,4-PI block. A mixture of MEK-cyclohexane as mobile phase is well suited for establishing critical conditions for 1,4-PI.

Fig. 38 shows the critical diagram obtained by using a set of reversed phase columns. 1,4-PI standards were used for establishing the critical conditions. At a mobile phase composition of MEK/cyclohexane (70:30) v/v size exclusion chromatography is seen. The critical conditions correspond to a mobile phase composition of MEK/cyclohexane (91.5:8.5) v/v. Liquid adsorption chromatography is seen at a mobile phase composition of MEK/cyclohexane (95:5) v/v. The homopolymer having molar mass 57.4 kg/mol is not seen in the Fig., as it is strongly adsorbed by the columns at a mobile phase composition MEK/cyclohexane (95:5) v/v and therefore does not elute.

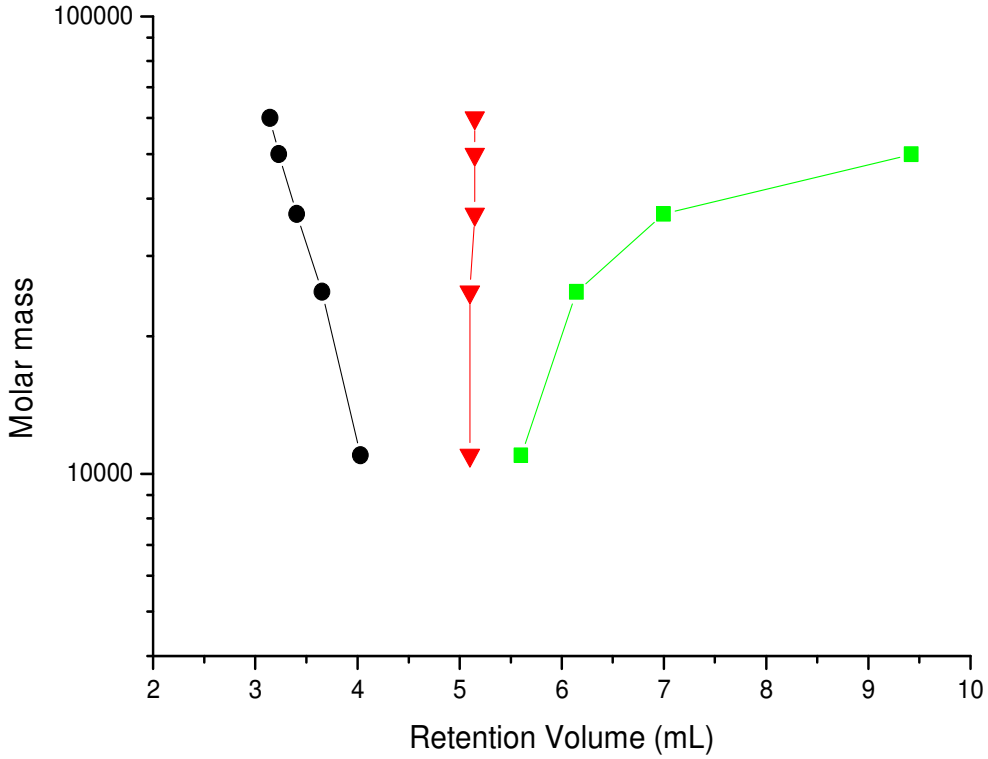

Figure 38: Critical diagram of 1,4-PI showing molar mass versus retention volume, mobile phase MEK/cyclohexane ● = 70:30, ▼= 91.5:8.5, ■ = 95:5 v/v; stationary phase: two columns of C18 300-5

The critical conditions established for 1,4-PI is then used for the analysis of PS-*b*-PI copolymers

6.5 LC-CC-^{1}H-NMR of PS-*b*-PI copolymers at critical conditions of 1,4-PI

Fig. 39 shows the ^{1}H-NMR spectra of a PS-*b*-PI copolymer dissolved in a mixture of protonated solvents MEK and cyclohexane [Fig. 39 (a)] and in deuterated THF [Fig. 39 (b)]. WET solvent suppression is applied to the signals of both MEK and cyclohexane. Four solvent signals were suppressed. It is evident from Fig. 39 that the olefinic protons of the PI block and the aromatic protons of the PS block are unaffected by suppression. These signals can then be used for determining the chemical composition distribution.

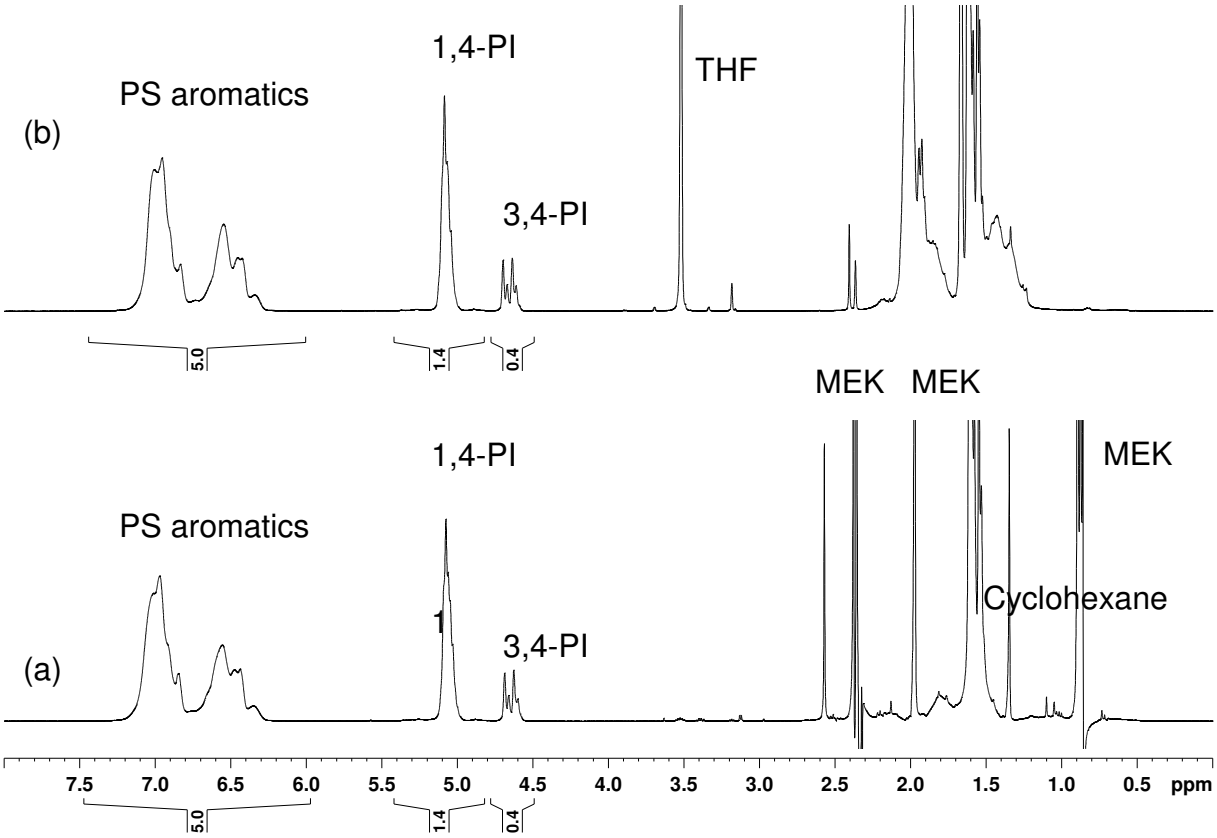

Figure 39: ^{1}H-NMR spectra of PS-*b*-PI copolymer in (a) protonated MEK/ cyclohexane with WET solvent suppression and (b) in deuterated THF respectively. The assignments are given according to Scheme 3.

6.6 Comparison of on-flow HPLC-NMR of PS-*b*-PI copolymers synthesised by sequential living anionic polymerisation and coupling of living precursor blocks at critical conditions of 1,4-PI

Fig. 40 shows the on-flow HPLC-NMR run of PS-b-PI copolymer synthesised by sequential living anionic polymerisation. The X-axis shows the proton chemical shift and the Y-axis shows the retention time in minutes. The chemical shift region from 4.4 to 7.4 ppm is shown. It is seen from this Fig. that a separation into two different components takes place. The first component elutes in SEC mode whereas the second component elutes at the critical retention time of 1,4-PI. As the first eluting peak shows coexisting signals at the olefinic and aromatic regions, this peak can be

assigned to the copolymer. The peak eluting later can be assigned to the homopolymer of PI based on the typical NMR chemical shifts of PI and also due to the critical retention time of PI. Fig. 41 represents the most intense traces of the separated components. The first trace can be assigned to the copolymer due to the typical chemical shifts as indicated by Fig. 39. The second eluting peak can be assigned to the homopolymer of PI indicated by the ^{1}H-NMR trace. Since these block copolymers are synthesised by sequential living anionic polymerisation the presence of homopolymers from the PI block was not likely. However, one of the samples synthesised by this method shows the presence of homopolymer of PI. This can only be possible if some impurities are present which cause sudden termination of the chain and the formation of the homopolymer of PI. Fig. 42 shows the HPLC-NMR on-flow run of PS-*b*-PI copolymer synthesised by coupling of living precursor blocks of PS and PI. The on-flow plot as well as the traces (see Fig. 43) shows the presence of two components. The first component can be assigned to the copolymer as it elutes in SEC mode. The second component eluting later can be assigned to the homopolymer of PI based on the typical NMR chemical shifts of PI as well as the critical retention time of PI. As these copolymers are synthesised by coupling of living precursor blocks all of them show the presence of homopolymer of PI. From the typical NMR chemical shifts, in addition to 1,4-PI these copolymers also show the presence of a minor amount of 3,4-PI.

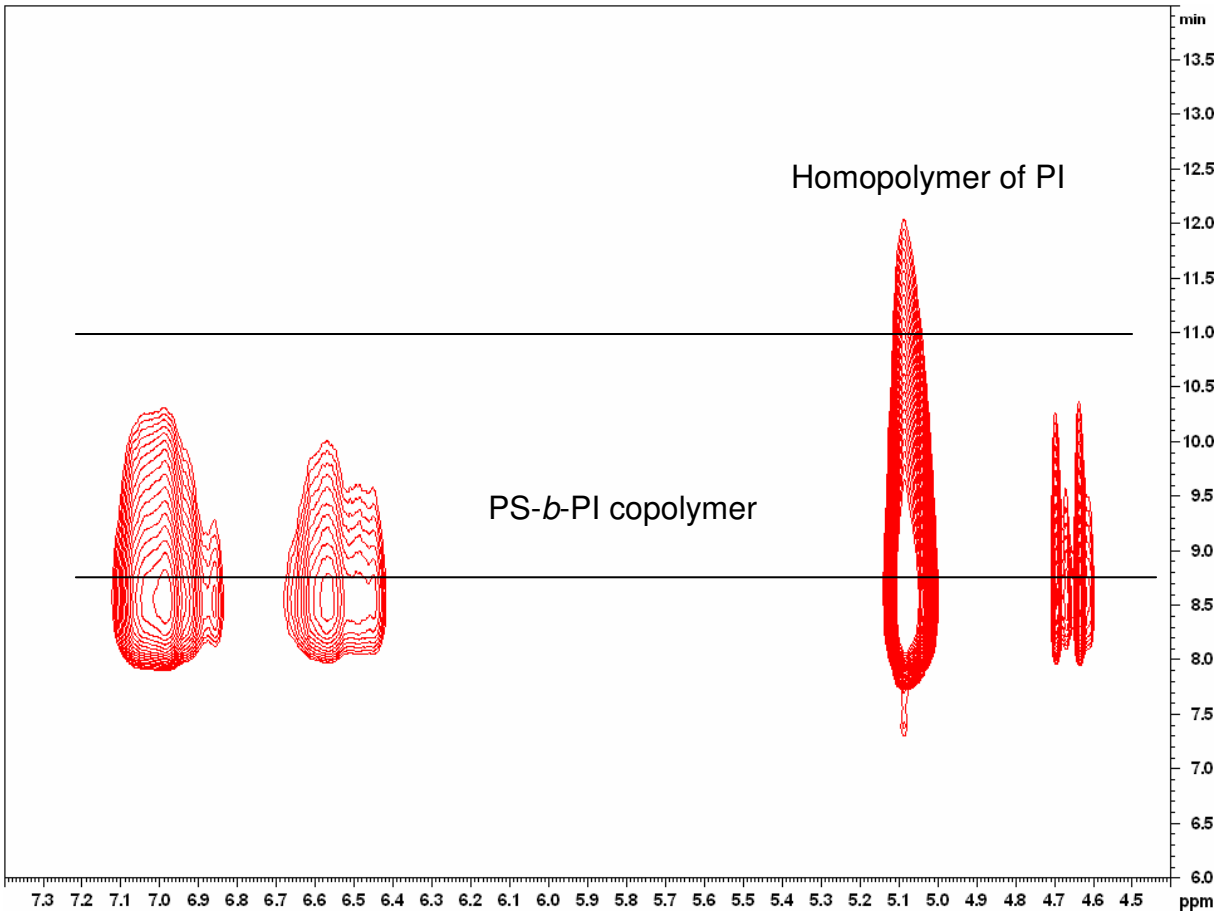

Figure 40: LC-CC-NMR on-flow run of PS-*b*-PI (sample 17) synthesised by sequential living anionic polymerisation at critical conditions of 1,4-PI

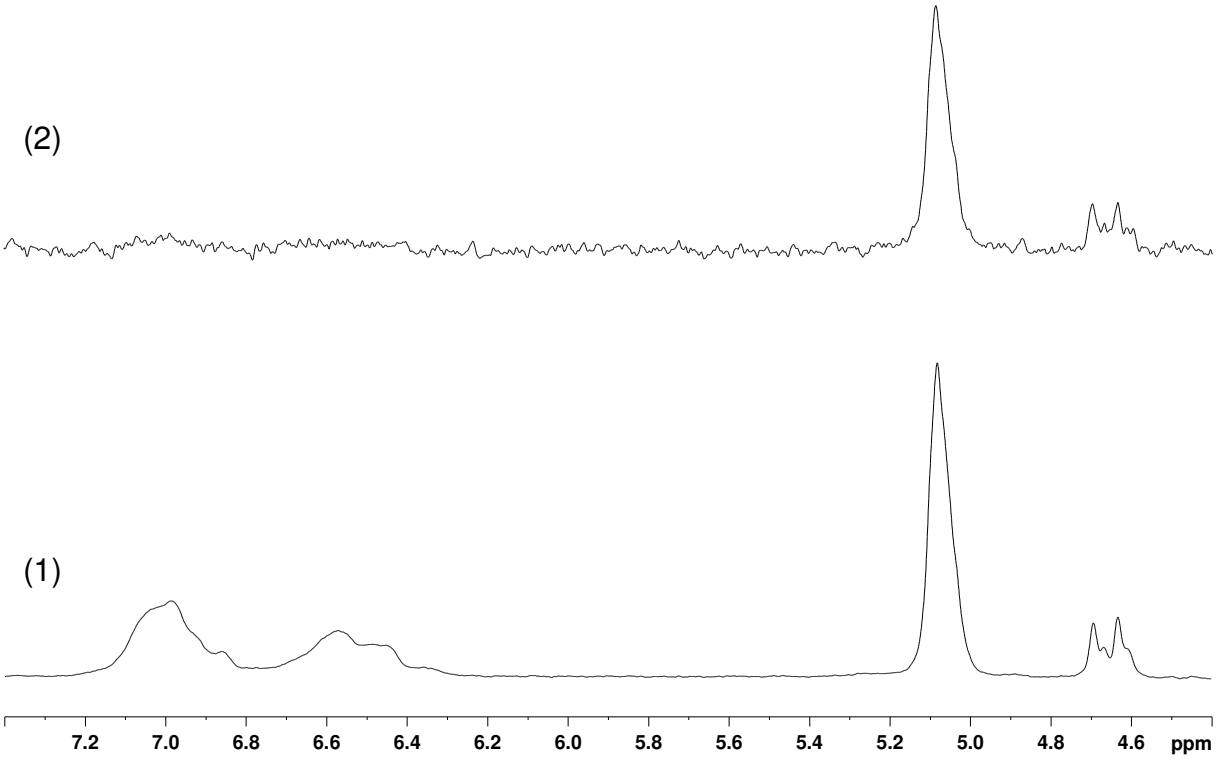

Figure 41: ^{1}H-NMR traces of the on-flow run; (1) PS-*b*-PI copolymer, (2) Homopolymer of PI

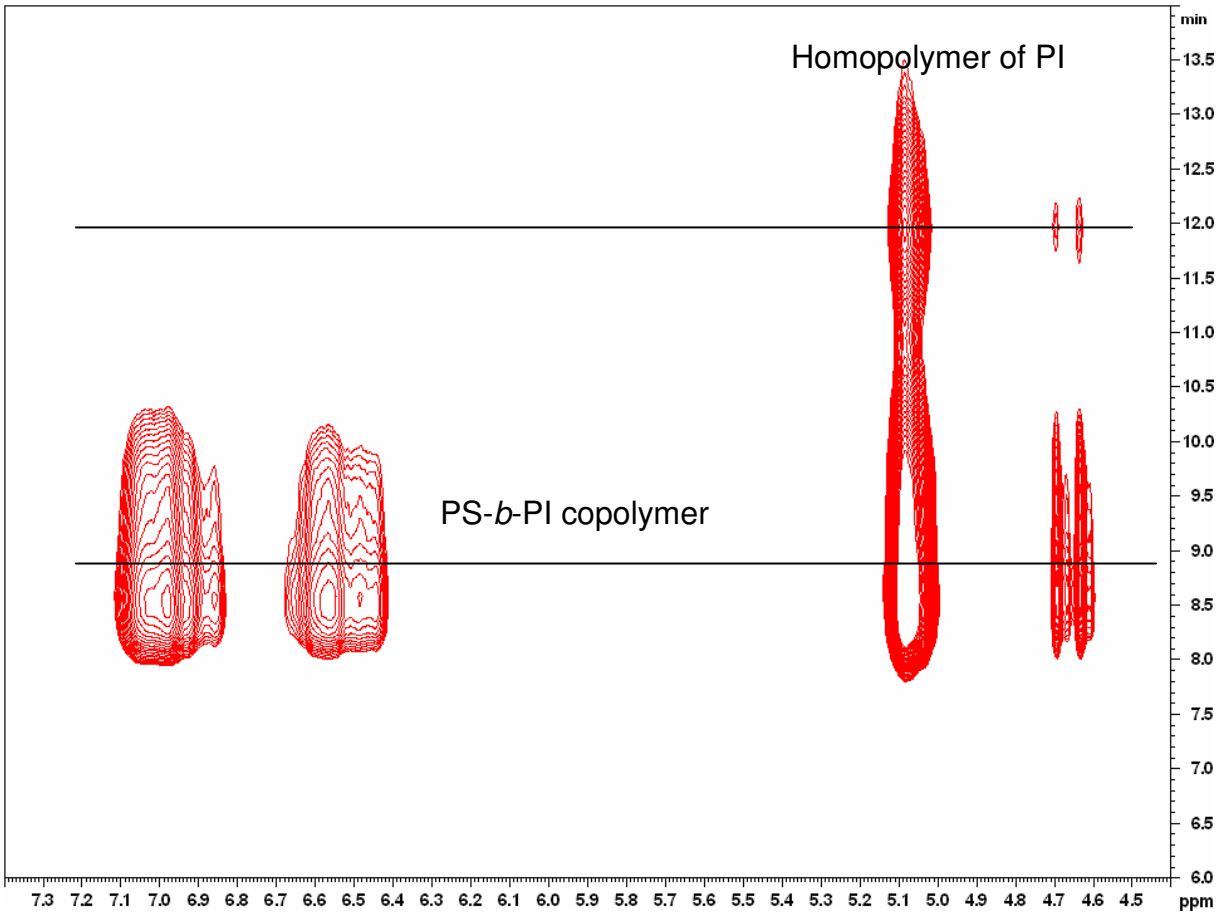

Figure 42: LC-CC-NMR on-flow run of PS-*b*-PI (sample 20) synthesised by coupling of living precursor blocks at critical conditions of 1,4-PI

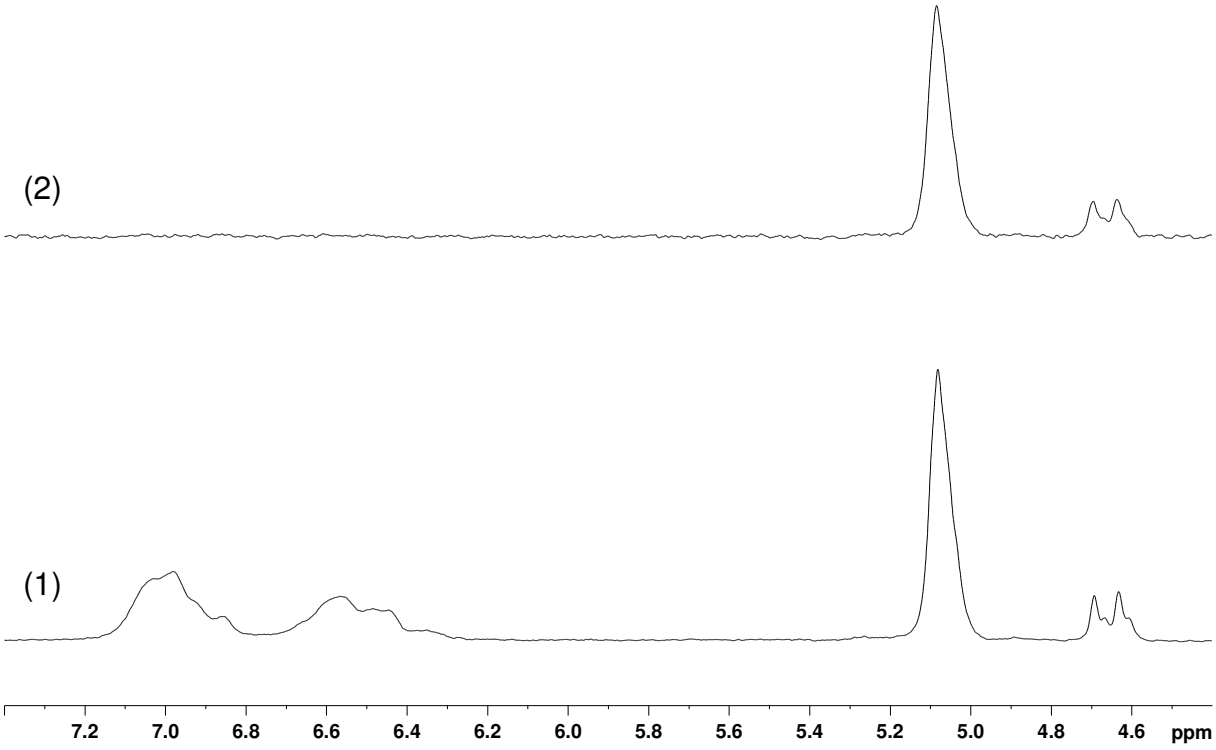

Figure 43: ^{1}H-NMR traces of the on-flow run; (1) PS-*b*-PI copolymer, (2) Homopolymer of PI

For calculating the molar masses of the PS block in PS-*b*-PI copolymers by LC-CC-NMR a calibration curve is constructed by using the PS calibration standards. Using the calibration curve given in Fig. 44 the molar masses of the PS blocks in the block copolymers were determined. In order to calculate the molar masses of the PS block present in the copolymers by LC-CC-NMR the peak maximum (M_P) of the aromatic protons is taken.

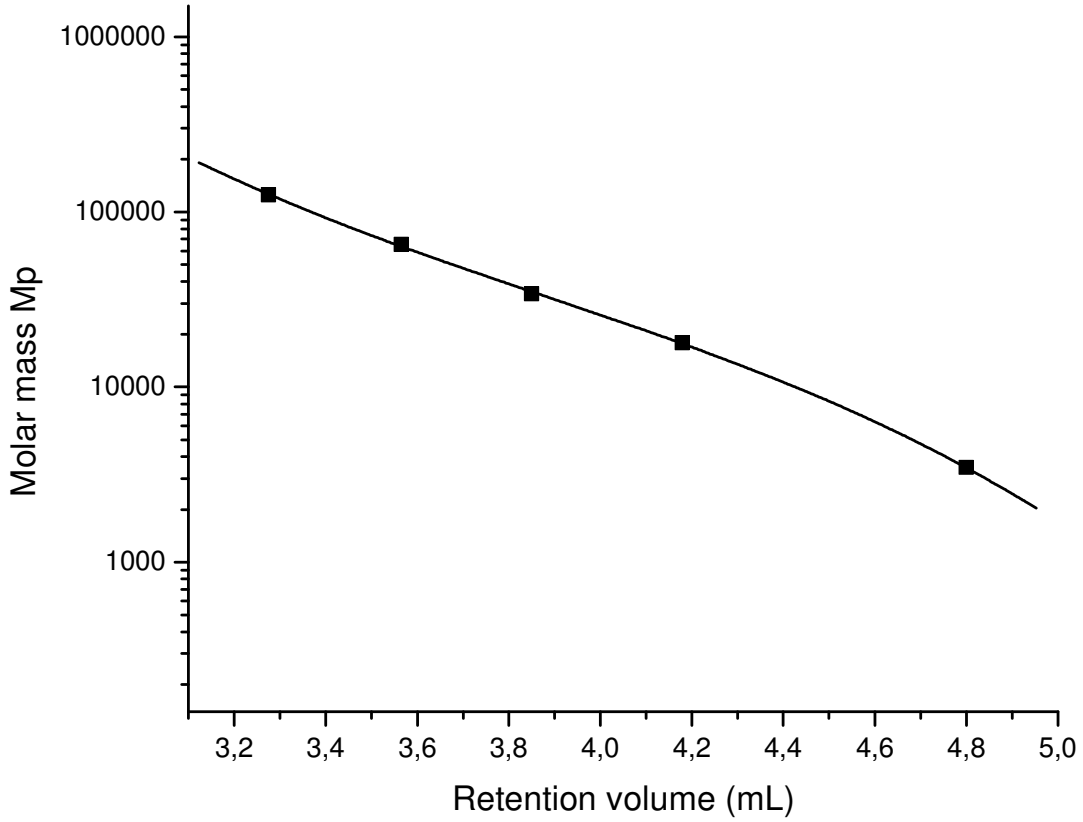

Figure 44: Calibration curve of PS showing molar mass versus retention volume, solid line = curve fitted with third order polynomial, critical point of adsorption of PI

Table 16 shows the molar masses of the PS blocks of the copolymers determined by LC-CC-NMR. These data are then compared to the molar masses of the block copolymers obtained by SEC and off-line NMR. Using the SEC data and chemical compositions of Table 12, the molar masses of the PS blocks of the copolymers can be calculated by using modified version of Equations (25-26). If we compare the values in Table 16 the molar masses of the PS blocks obtained by both the methods is nearly the same. This result gives the impression of a good consistency between the off-line measurements of the bulk samples and LC-CC-NMR.

Sample	M_p (PS block) by LCCC-NMR (kg/mol)	M_P of (PS block) by SEC and NMR (kg/mol)
15	37.4	58.1
16	45.2	67.4
17	15.1	24.5
18	96.0	96.3
19	37.8	38.3
20	15.3	21.4
21	45.2	62.9

Table 16: Molar masses of the PS block of the copolymers determined by SEC and off-line NMR with modified version of Equation (25) or LC-CC-NMR with the peak maximum of the aromatic protons

Sample	M_p (PS block) by LC-CC-NMR (kg/mol)	Styrene/Isoprene of copolymer by LC-CC-NMR (mol %)	M_P of block copolymer (kg/mol) calculated
15	37.4	38.9/61.1	75.8
16	45.2	55.9/44.1	68.5
17	15.1	16.2/83.8	66.2
18	96.0	78.2/21.8	113.5
19	37.8	32.4/67.6	89.4
20	15.3	19.0/81.0	57.9
21	45.2	68.0/32.0	59.1

Table 17: The molar masses of the PI block of the copolymers, chemical compositions and calculated total true molar masses of the block copolymers

Using the true molar mass of the PS block obtained by LC-CC-NMR and the true chemical composition obtained by adding the entire polymer traces separated from the homopolymer the total molar mass of the block copolymer is calculated.

By using LC-CC-NMR it is possible to determine the chemical composition distribution of the copolymers without using standards. Using the on-flow data presented in Figs. 40 and 42, it is possible to calculate the chemical composition at different elution volumes. Fig. 45 shows the plots of CCD versus retention time for the different block copolymers. The Fig. also shows the NMR projections of the aromatic region of PS (solid black line, normalised to one proton), olefinic protons from 1,4-PI (solid red line, normalised to one proton) and olefinic protons from 3,4-PI (solid green line, normalised to one proton). The following general conclusions can be derived from Fig. 45 [15 (a), 17 (b), 19 (c) and 20 (d)] for some of the block copolymers:

(i) Samples 15 and 17 are synthesised by sequential living anionic polymerisation. Sample 15 shows monomodal MMD (indicated by the different solid lines). This sample does not show the presence of homopolymer of PI. Only sample 17 shows tailing at higher retention time (indicated by the red solid line) which indicates the presence of homopolymer of PI. This is attributed to chain transfer side reactions; due to the presence of trace impurities (i.e. inadequately purified isoprene). This sample also shows shoulder between 7-7.5 min (indicated by the red solid line) which is attributed to coupling of two living block copolymer chains, presumably caused by the inadequately degassed methanol. The distribution at lower retention times represents PS-*b*-PI copolymer and the higher retention time distribution belongs to homopolymer of PI, as we are separating at the critical conditions of PI.

(ii) It was found that the block copolymers 15 and 17 show a moderate chemical heterogeneity. Samples 15 and 17 show a moderate dependence of the CCD versus retention time in the region of the copolymer. The higher molar mass region (low retention times) seen in sample 15 and 17 are rich in PI, the lower molar mass region (high retention times) are dominated by PS.

(iii) Samples 19 and 20 are synthesised by coupling of living precursor blocks of PS and PI. The two block copolymers show bimodal MMD (indicated by the red solid line [1,4-PI] and green solid line [3,4-PI]). The block copolymers also contain homopolymer of PI. Sample 20 also shows a

shoulder between 9-10 min that has a chemical composition different from the block copolymer. This is attributed to the PI overload (i.e. stoichiometry mismatch) during the second coupling step. As these block copolymers are synthesised by coupling reactions the shoulder indicated may be a coupling product which elutes at higher retention times. The sample 20 also shows a small shoulder between 7-7.5 min (indicated by black solid line) which is tentatively attributed to PS dimer formed during the first coupling step (i.e. PS-$SiMe_2$-PS).

(iv) Samples 19 and 20 show a moderate chemical heterogeneity distribution in the region of the copolymer.

(v) The samples 19 and 20 are rich in PI at the higher molar mass region (low retention times), the lower molar masses (high retention times) are dominated by PS.

(vi) The retention time of the PS projection profiles (aromatic region) can be used for calculating M_P of the PS block.

(a)

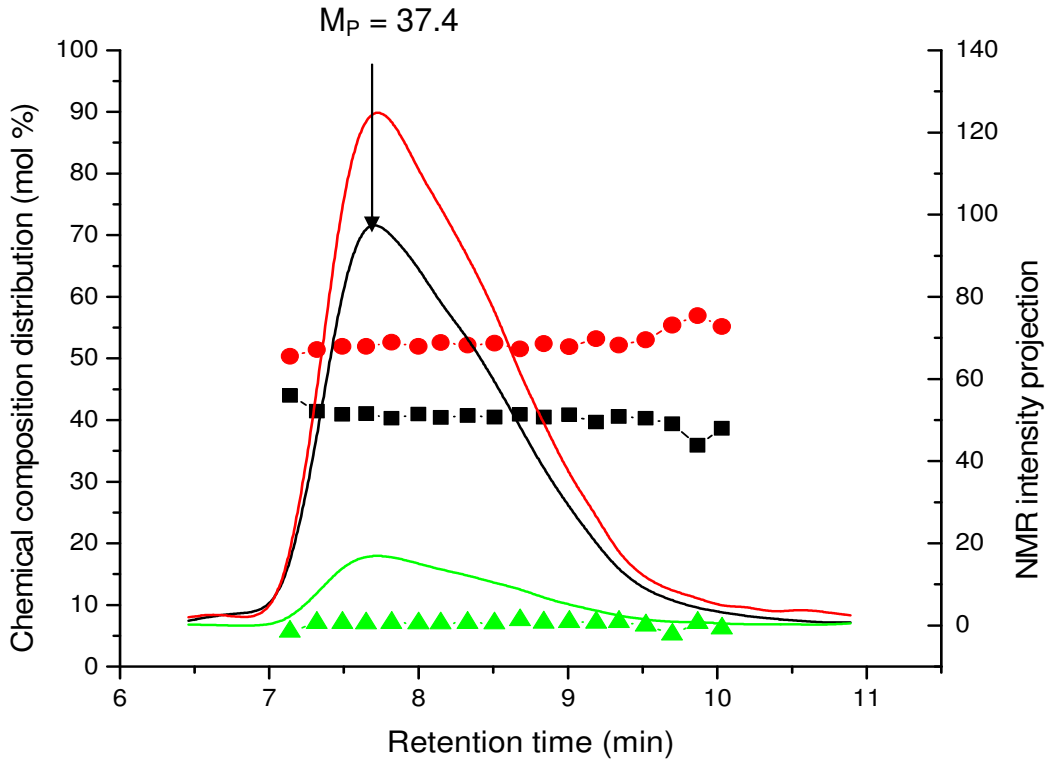

(b)

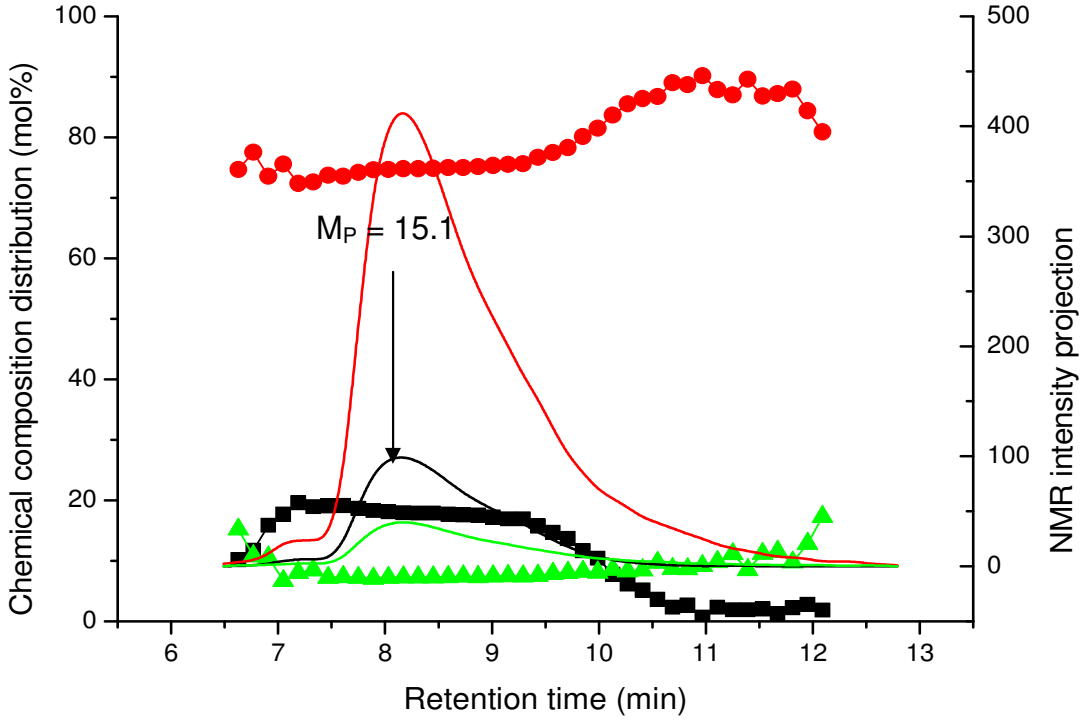
Chemical composition distribution (mol%)
NMR intensity projection
Retention time (min)
MP = 15.1

(c)

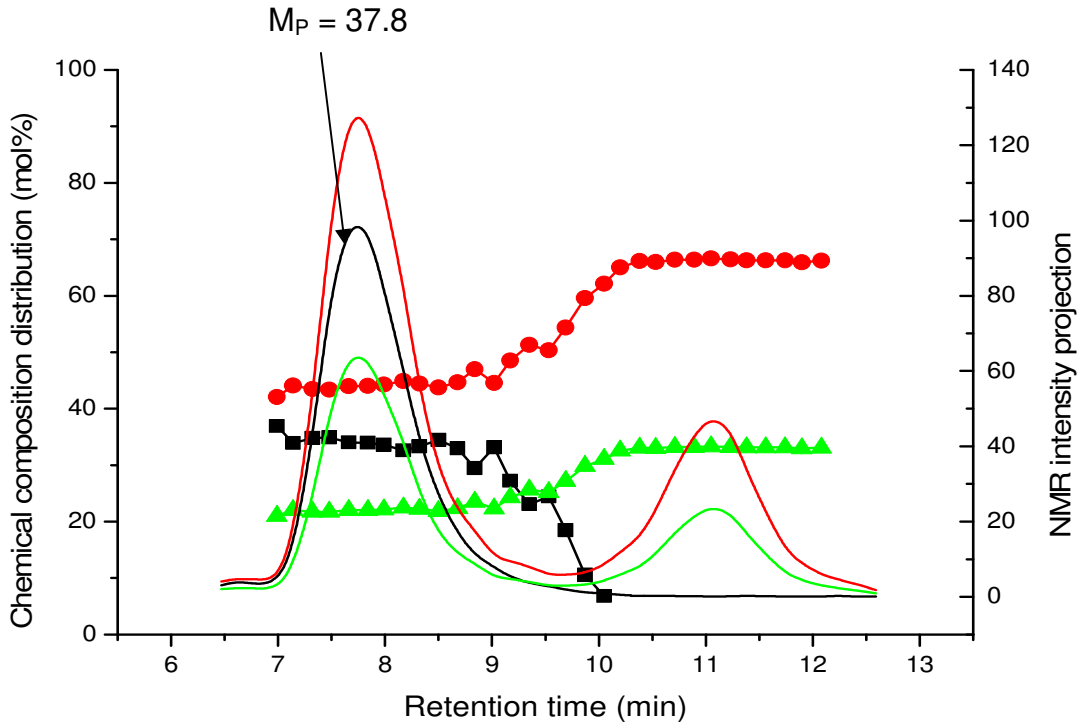
Chemical composition distribution (mol%)
NMR intensity projection
Retention time (min)
MP = 37.8

(d)

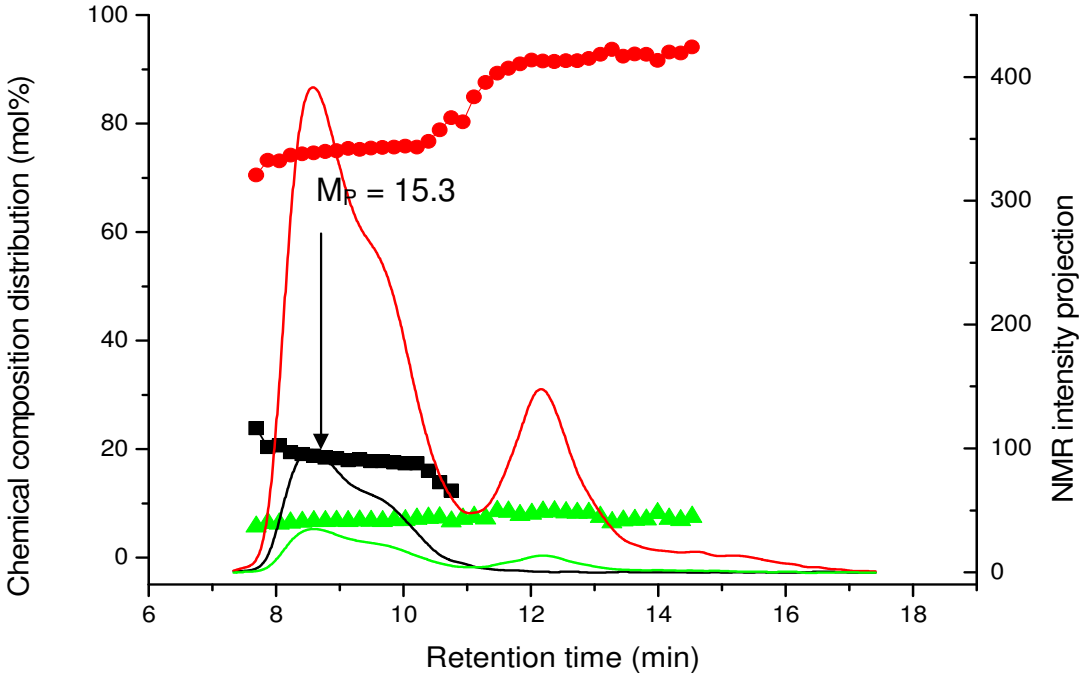

Figure 45: Chemical composition of PS-*b*-PI copolymers versus retention time (■ = mol% PS,●= mol% 1,4-PI and ▲=mol% 3,4-PI), solid black line = NMR projection of the aromatic region, solid line red = NMR projection of 1,4-PI and solid line green = NMR projection of 3,4-PI [samples 15 (a), 17 (b), 19 (c), 20 (d)]

7. Analysis of PI-*b*-PMMA copolymers

7.1 Method development for critical conditions of PI using a single solvent as mobile phase

For separating PI-*b*-PMMA copolymers critical conditions were established for the PI block. By using LC-CC it is possible to separate block copolymers regarding the different block components. Critical conditions for polymer species have been commonly established by using mixtures of solvents. However, it is not easy to reproduce the critical conditions since the retention of polymers depends sensitively on the solvent composition and purity. Furthermore, the preferential sorption of a component in a mixed solvent may cause additional problems. Therefore, the use of a single solvent is highly desirable to improve the reproducibility as well as the repeatability. Since PI is the non-polar part of the block copolymer critical conditions were established by using a single solvent and a set of reversed phase C_{18} columns. It has already been shown in Ref[110] that 1,4-dioxane as a single solvent is well suited for establishing critical conditions by varying the temperature of the columns. Using a set of non-polar stationary phases C_{18} 300-5+ C_{18} 1000-7 with column sizes of 250x4 mm inner diameter and 1,4-dioxane as mobile phase PI will elute at critical conditions whereas PMMA will elute in SEC mode. The annotations stand for C_{18}-alkyl bonded porous silica gel with average pore sizes of 300 and 1000 A.

Fig. 46 shows the critical diagram obtained by using reversed phase columns and 1,4-dioxane as a single solvent. The PI standards mentioned in the experimental section were used for establishing the critical conditions. At a column temperature of 70°C the size exclusion mode is operating. Homopolymer of PI with lowest molar mass is retained longer on the stationary phase as compared to higher molar mass PI. The critical conditions correspond exactly to a column temperature of 54°C where all the homopolymers of PI elute at the same retention volume irrespective of their molar masses. Liquid adsorption chromatography is seen at a temperature of 48°C where the lower molar mass PI elutes first followed by PI with higher molar masses.

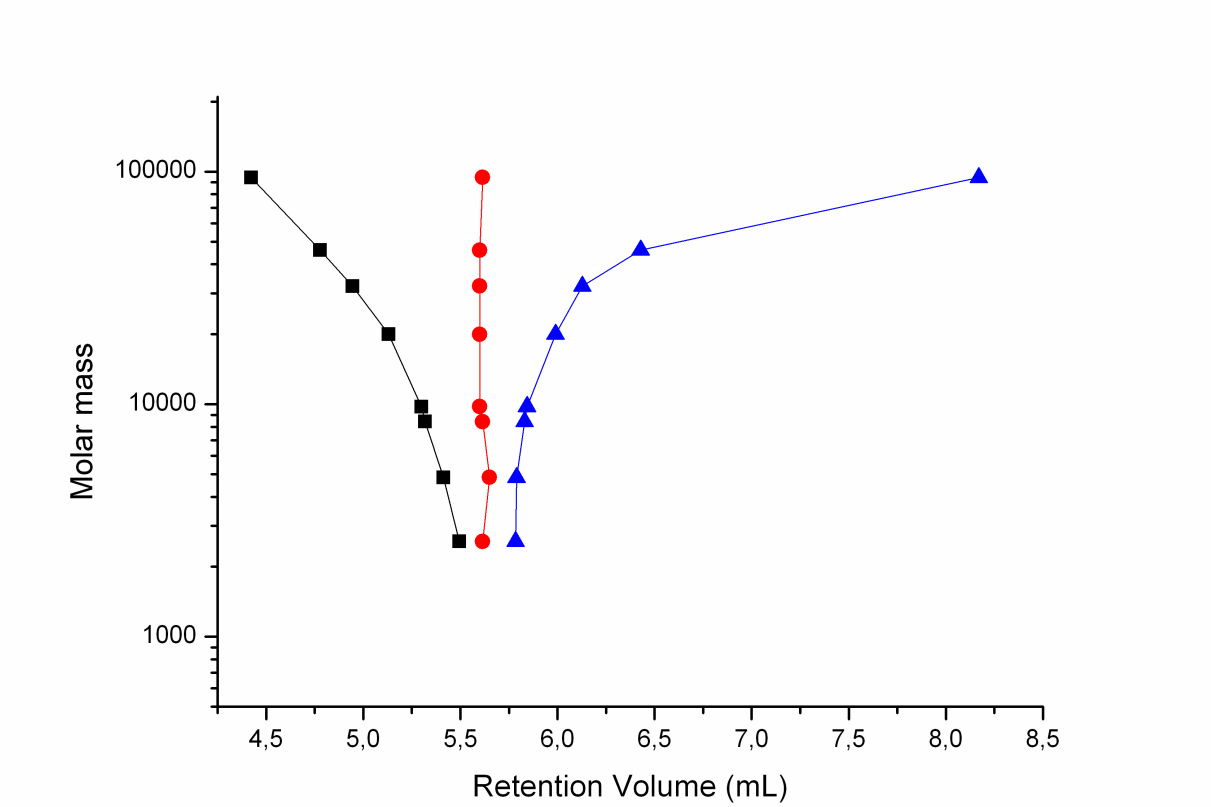

Figure 46: Critical diagram of PI showing molar mass versus retention volume, mobile phase 1,4-dioxane, temperature of column ■ = 70°C, ● = 54°C, ▲ = 48°C; stationary phase: C_{18} 300-5+C_{18} 1000-7

These critical conditions of 54°C (column temperature) are then used for the analysis of PI-*b*-PMMA copolymers.

7.2 LC-CC-^{1}H-NMR of PI-*b*-PMMA copolymers at critical conditions of PI

NMR is by far the most powerful detection method that can be used in liquid chromatography of polymers. However, when it is directly coupled to HPLC, the intrinsically low sensitivity and the effect of the mobile phase on the NMR measurement have to be addressed. Typically, LC-CC is conducted in protonated binary mobile phases. The proton signals of the mobile phase are a major concern in on-flow LC-CC-NMR since they may cover regions in the spectrum that are vital for detecting the polymer proton signals. Therefore, in the present work, critical conditions were established using a single solvent. This simplifies the spectra by

significantly reducing the number of unwanted solvent signals. The remaining solvent signals will be efficiently suppressed by suitable pulse sequences. Fig. 47 shows the ^{1}H-NMR spectra of a PI-*b*-PMMA copolymer dissolved in protonated 1,4-dioxane [Fig. 47 (a)] and in deuterated chloroform [Fig. 47 (b)]. WET solvent suppression is applied to the signal of 1,4-dioxane. One solvent signal is suppressed. It is evident from Fig. 47 that the α-CH_3 group of the PMMA block and the olefinic protons of the PI block are unaffected by solvent suppression. The signals not affected by solvent suppression can then be used for determining the chemical composition distribution. From the α-CH_3 group the tacticity of the PMMA block of the copolymer can be calculated. The different tacticities of the PMMA block are syndiotactic, atactic and isotactic which are represented by rr, mr and mm respectively. However, the OCH_3 group of PMMA overlaps with 1,4-dioxane and is suppressed.

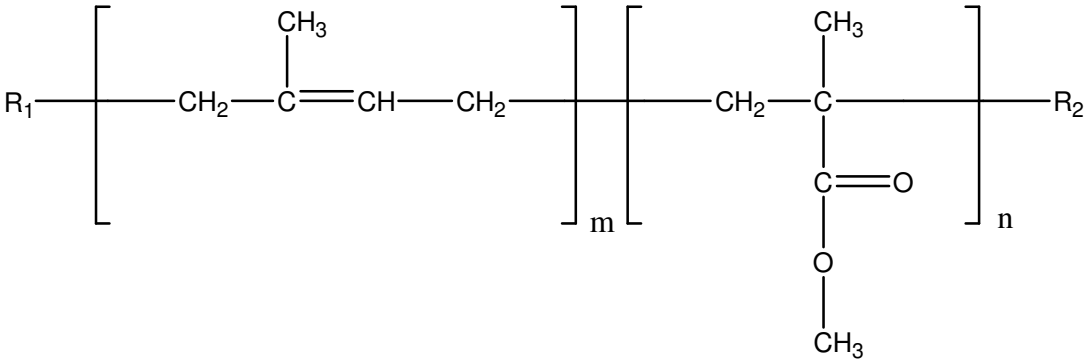

(1) 1,4-PI-*b*-PMMA

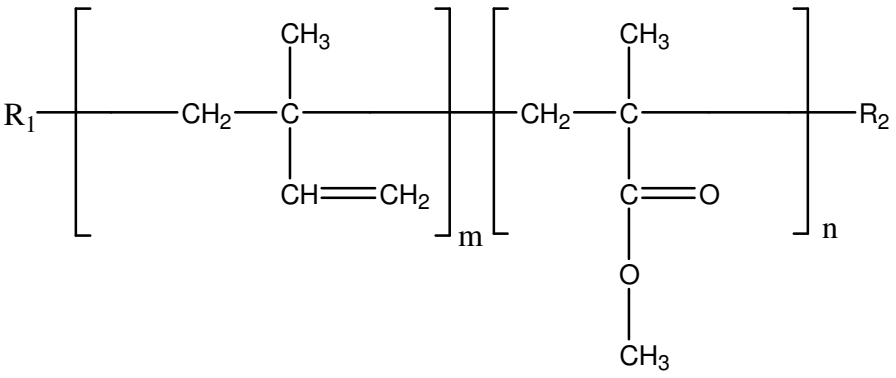

(2) 1,2-PI-*b*-PMMA

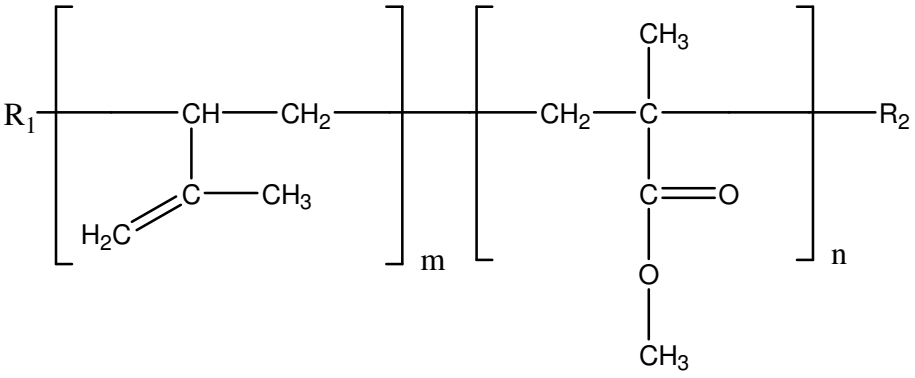

(3) 3,4-PI-*b*-PMMA

Scheme 4: Structure of PI-*b*-PMMA copolymers showing different microstructures of the PI block where (1) 1,4-PI-*b*-PMMA, (2) 1,2-PI-*b*-PMMA and (3) 3,4-PI-*b*-PMMA

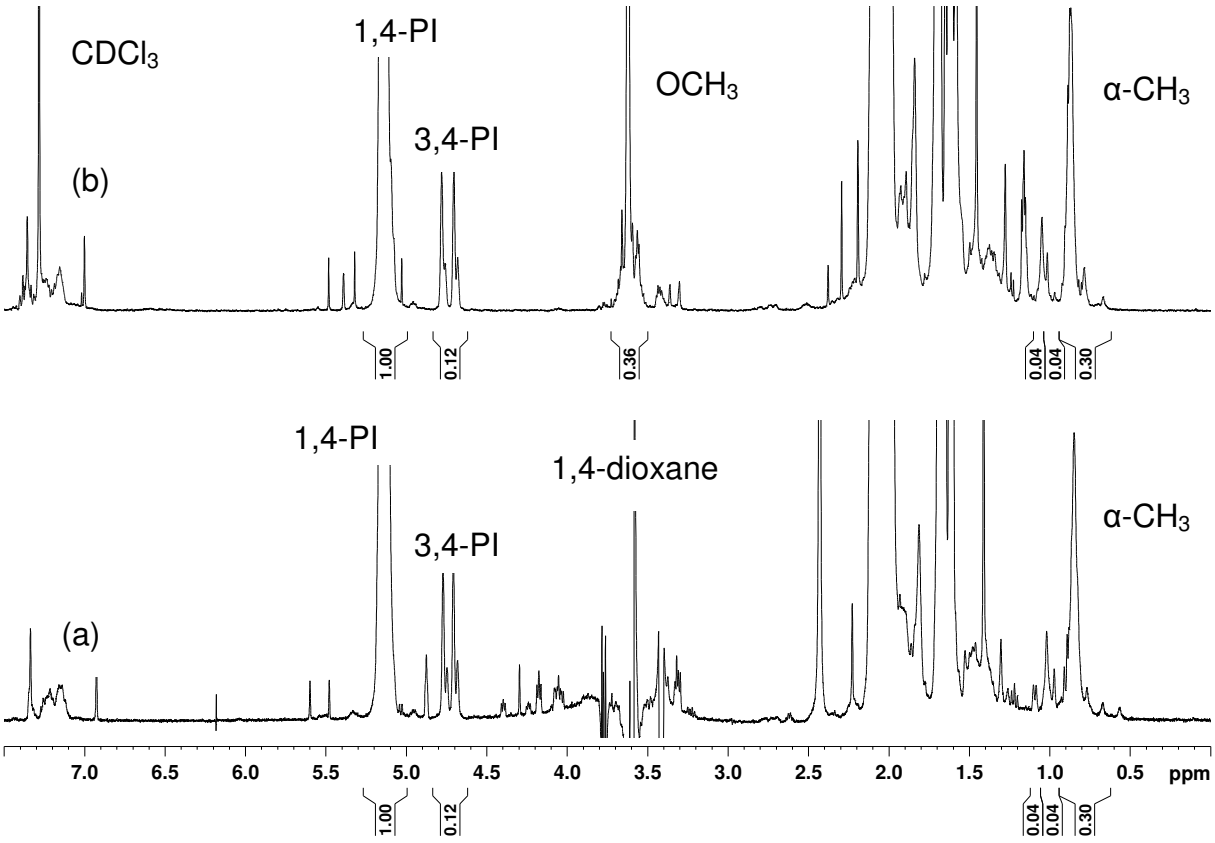

Figure 47: ^{1}H-NMR spectra of PI-*b*-PMMA copolymer in (a) non-deuterated 1,4-dioxane with WET solvent suppression and (b) in $CDCl_3$ respectively. The assignments are given according to Scheme 4.

The samples given in Table 18 are then used for the analysis.

Sample	M_P by SEC (kg/mol)	Isoprene/MMA by ^{1}H-NMR (mol %)
22	18.9	91.4/8.6
23	88.9	15.9/84.1
24	19.4	60.9/39.1
25	125.9	22.7/77.3
26	60.7	53.7/46.3

Table 18: SEC and ^{1}H-NMR analysis of the block copolymers

The block copolymers given in Table 18 are also analysed by conventional SEC and by off-line NMR. The conventional SEC data are obtained by using THF as solvent and cross-linked polystyrene as the stationary phase. The calibration is based on PS. Off-line NMR is used to determine the chemical composition of the samples. From the signal intensities of the α-CH_3 protons (methyl methacrylate) and the olefinic protons (isoprene) the average chemical composition of the block copolymers can be calculated, see Table 18. In the next step on-line coupled HPLC-NMR experiments were performed. Fig. 48 shows the HPLC-NMR on-flow run of 1,4-PI-*b*-PMMA copolymer where the X-axis indicates the proton chemical shift (ppm) and the Y-axis indicates the retention time (min).

The copolymers are synthesised by living anionic polymerisation. In the first step isoprene monomer is dissolved in a non-polar solvent cyclohexane. N-butyl lithium is used as starter. The monomer, solvent and starter are mixed in a definite proportion in a reactor. After the complete conversion of the isoprene monomer diphenylethylene is added to the reaction solution. After a couple of hours the reaction solution is transferred to a reactor containing tetrahydrofuran and cooled to -80°C. Pure and cooled methyl methacrylate is then added to the reaction mixture. The reaction is stopped after half an hour by adding methanol. The formed component is PI-*b*-PMMA copolymer. Two different types of block copolymers were synthesised containing predominantly either 1,4-PI or 3,4-PI blocks. The 1,4-PI-*b*-PMMA copolymer consists of both 1,4-PI (main component) and 3,4-PI units. However, the 3,4-PI-*b*-PMMA copolymer contains both 1,4- and 1,2-PI units.

The on-flow plot (Fig. 48) shows only one component. The eluting peak shows coexisting signals at the olefinic and aliphatic region. This peak can be assigned to the copolymer since it elutes in SEC mode due to the different molar masses of the

PMMA block. From the typical NMR chemical shift of 1,4-PI (5.1 ppm) and the critical retention time of PI the resonance peak can be assigned to 1,4-PI. The doublets at 4.65 and 4.75 ppm can be used for calculating the amount of 3,4-PI. The typical chemical shift between 0.7-1.1 ppm can be assigned to the α-CH_3 group of PMMA. This sample does not show the presence of homopolymer of PI.

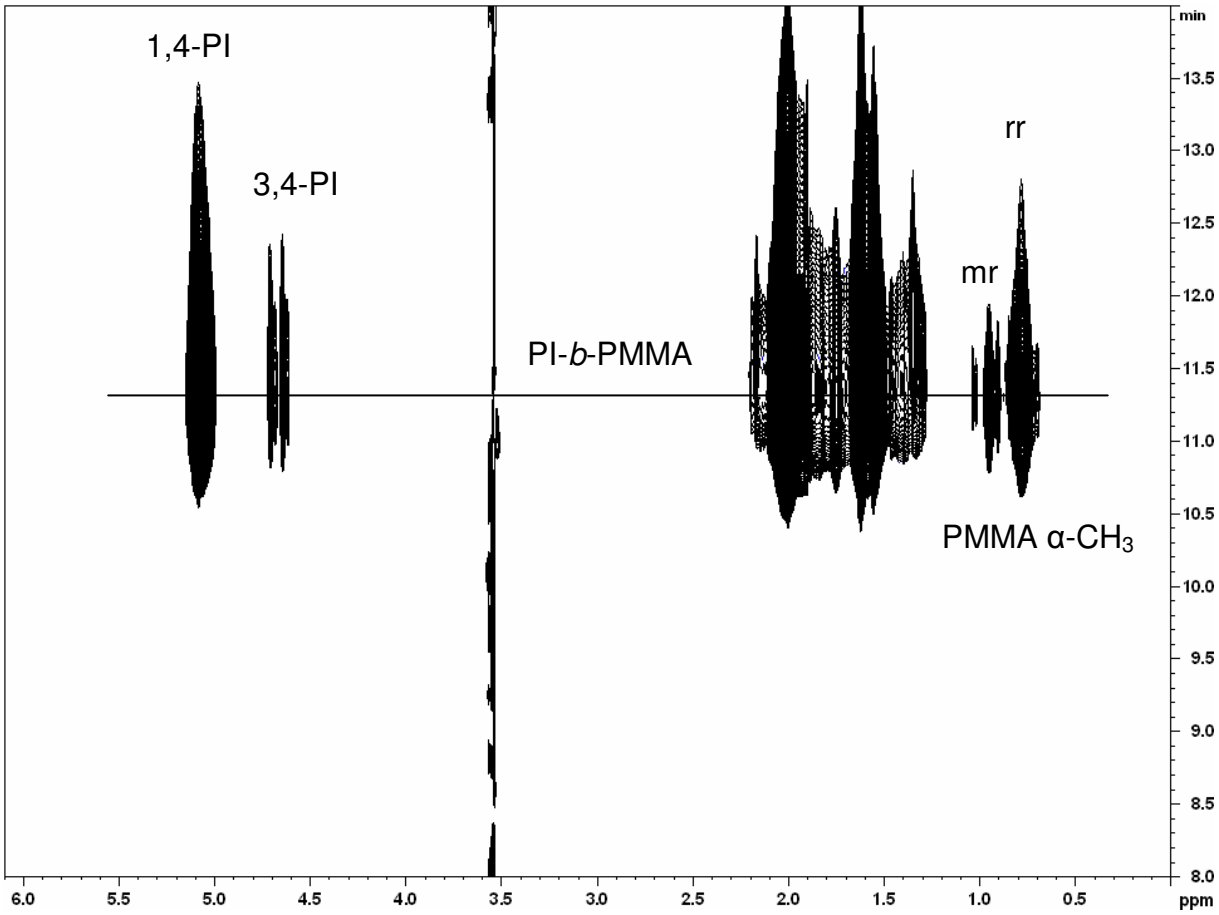

Figure 48: LC-CC-NMR on-flow run of 1,4-PI-*b*-PMMA copolymer (Sample 22: M_P = 18.9 kg/mol) measured at critical conditions of PI

Fig. 49 shows the on-flow LCCC-NMR run of 3,4-PI-*b*-PMMA. In this Fig. the block copolymer elutes first with regard to the PMMA block length which can be determined using a standard PMMA calibration curve. The olefinic regions of 1,2-, 1,4- and 3,4-PI sequences as well as the tacticity of the α-CH_3 group of PMMA are well resolved. The critical conditions of PI are also very useful for separating PI homopolymer from the block copolymer. The peak maxima of the copolymer and homopolymer regions are indicated in Fig. 49.

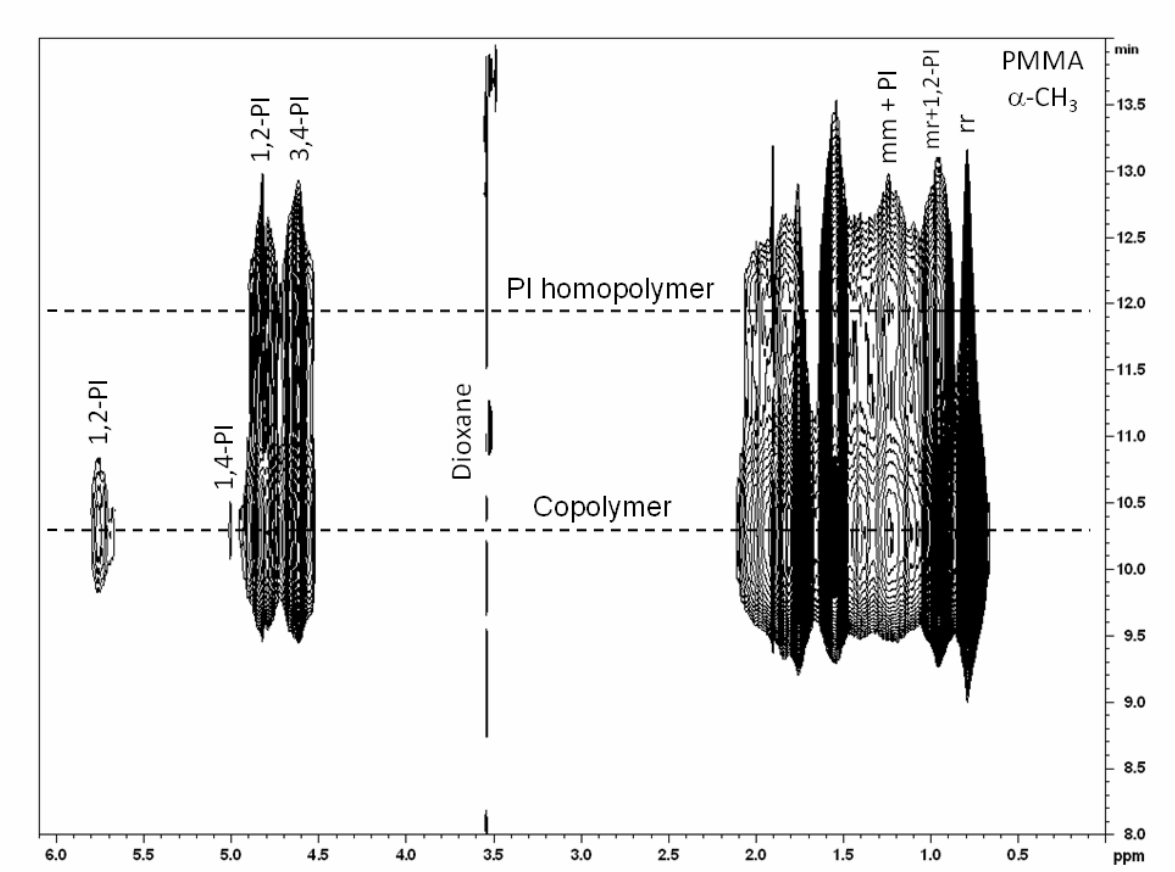

Figure 49: LC-CC-NMR on-flow run of the copolymer of 3,4-PI-*b*-PMMA copolymer (Sample 26: M_P = 60.7 kg/mol) measured at critical conditions of PI

In order to calculate the molar masses of the PMMA block in PI-*b*-PMMA copolymer by LC-CC-NMR a calibration curve is constructed by using the PMMA samples mentioned in the experimental section. By using the calibration curve shown in Fig. 50, the molar masses of the PMMA blocks in PI-*b*-PMMA copolymers were determined.

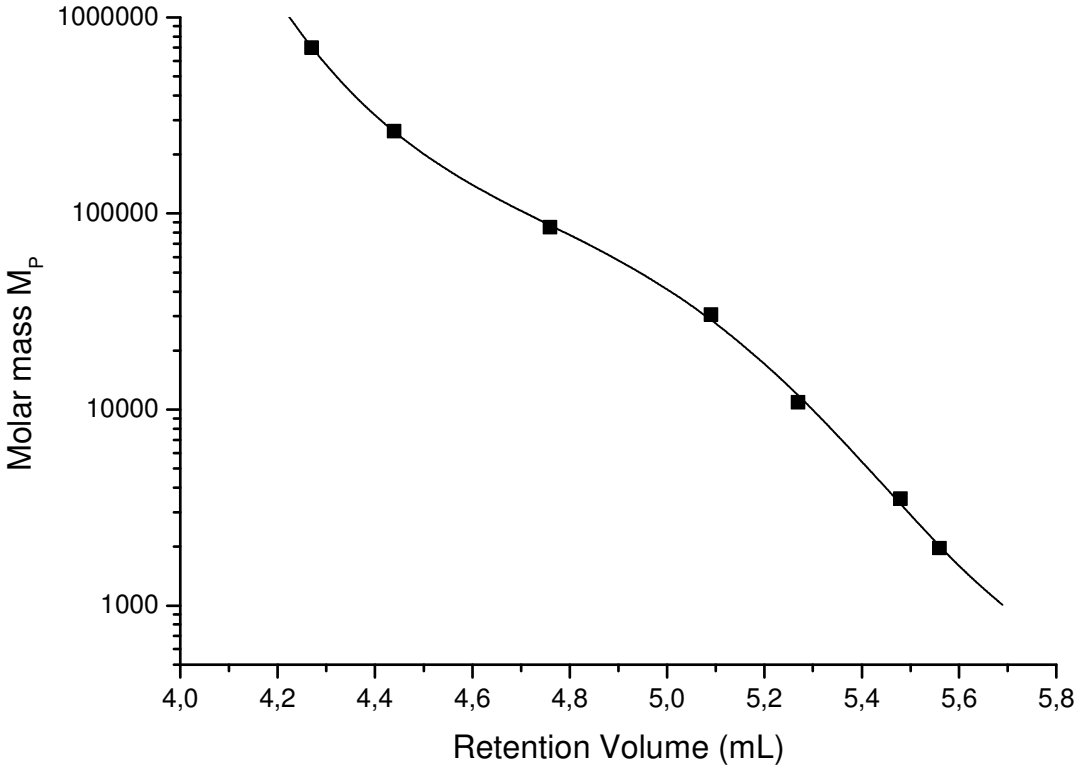

Figure 50: Calibration curve of PMMA showing molar mass versus retention volume at the critical point of adsorption of PI, solid line = curve fitted with fifth order polynomial

Table 19 shows the molar masses of the PMMA blocks of PI-*b*-PMMA copolymer measured by LC-CC-NMR by taking the peak maximum (M_P) of the α-CH_3 group of PMMA. The molar masses obtained by LC-CC-NMR were then compared to the molar masses obtained by SEC and off-line NMR. Using the chemical composition and the SEC data of Table 18 and modified version of Equation (25-26) the molar masses of the blocks of the copolymers can be calculated. The calculated molar masses of the PMMA blocks of the bulk samples are summarised in Table 19 and compared to the molar masses that were obtained by LC-CC-NMR. The molar masses obtained by SEC and off-line NMR are different than that obtained by LC-CC-NMR, this is so because the calibration is based on PS and the PS calibration curve overestimates or underestimates the PMMA molar masses.

Sample	M_p (PMMA block) by LC-CC-NMR (kg/mol)	M_p (PMMA block) by SEC and NMR (kg/mol)
22	1.1	2.3
23	83.9	78.8
24	7.9	9,4
25	90.1	104.9
26	29.5	33.9

Table 19: Molar masses of the PMMA block of the copolymers determined by SEC and off-line NMR with modified version of Equation (26) or LC-CC-NMR with the peak maximum (M_P) of the α-CH_3 group

Sample	M_p (PMMA block) by LC-CC-NMR (kg/mol)	Isoprene/MMA of copolymer by LC-CC-NMR (mol %)	M_p of block copolymer (kg/mol) calculated
22	1.1	88.9/11.1	7.1
23	83.9	38.3/61.7	109.9
24	7.9	50.1/49.9	13.3
25	90.1	8.1/91.9	95.5
26	29.5	33.9/66.1	39.8

Table 20: The molar masses of the PMMA block of the copolymers, chemical compositions and calculated total molar masses of the block copolymers at critical conditions of PI

Table 20 shows the molar mass, chemical composition and molar mass of the block copolymers calculated by LC-CC-NMR. The chemical composition calculated by LC-CC-NMR is different from that determined by ^{1}H-NMR of the bulk sample which indicates that by using this method the homopolymer can be separated.

Fig. 51 shows the chemical composition as a function of retention time for the block copolymers determined from the on-flow experiments of Figs. 48 and 49. It also shows the individual NMR chromatograms of the different microstructure moieties.

Sample 22 (a) shows monomodal distributions for all monomer units at critical conditions of PI. This indicates the absence of homopolymer of PI. This sample was synthesised by using a non-polar solvent cyclohexane. By using this solvent the block copolymer formed has 1,4-PI as the major component with minor amounts of 3,4-PI units. The block copolymer is homogenously distributed with regard to the chemical composition distribution. The chemical composition measured by off-line

NMR is compared to that measured by LC-CC-NMR. It is seen from Tables 18 and 20 that the values are nearly the same which indicates the absence of homopolymer of PI.

In Sample 26 (b) monomodal distributions for the syndiotactic (rr) and atactic (mr) α-CH_3 groups of PMMA are observed. On the other hand, bimodal distributions for the olefinic 1,2-, 1,4- and 3,4-PI components are found. This is a clear indication for the existence for the existence of a block copolymer fraction (retention time 9-11 min) and PI homopolymer fraction (retention time 11-13 min). Based on these curves the correct molar mass of the PMMA block can be determined from the peak maximum (M_P) of the rr and mr triads of the α-CH_3 groups of PMMA. The first eluting part (retention time 9-11 min) provides the true CCD of the separated block copolymer. This sample contains all the three microstructures of PI since it was synthesised by using a polar solvent tetrahydrofuran. The block copolymer is moderately distributed with regard to the CCD. If we compare Tables 18 and 20 the chemical composition analysis provides significantly lower content of PI (33.9 mol %) in the copolymer compared to the bulk measurements (53.7 mol %). Using additionally the chemical composition the molar mass of the entire copolymer (39.8 kg/mol) is calculated. This molar mass is also lower compared to the results of the bulk sample. This is due to the separation of the block copolymer from homopolymer of PI.

(a)

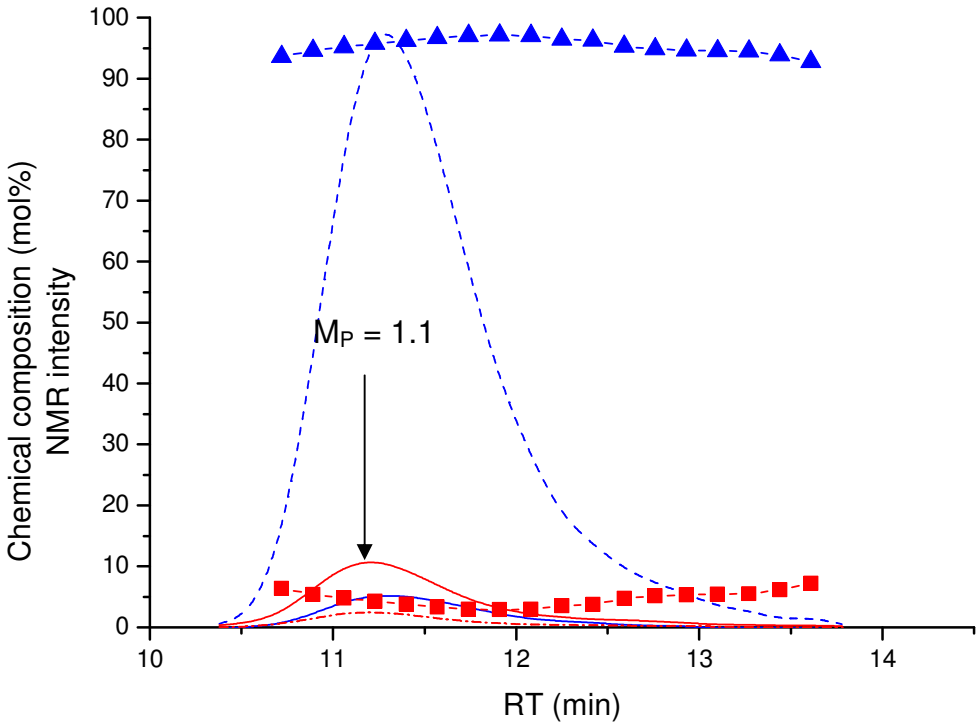
Chemical composition (mol%)
NMR intensity
MP = 1.1
RT (min)

(b)

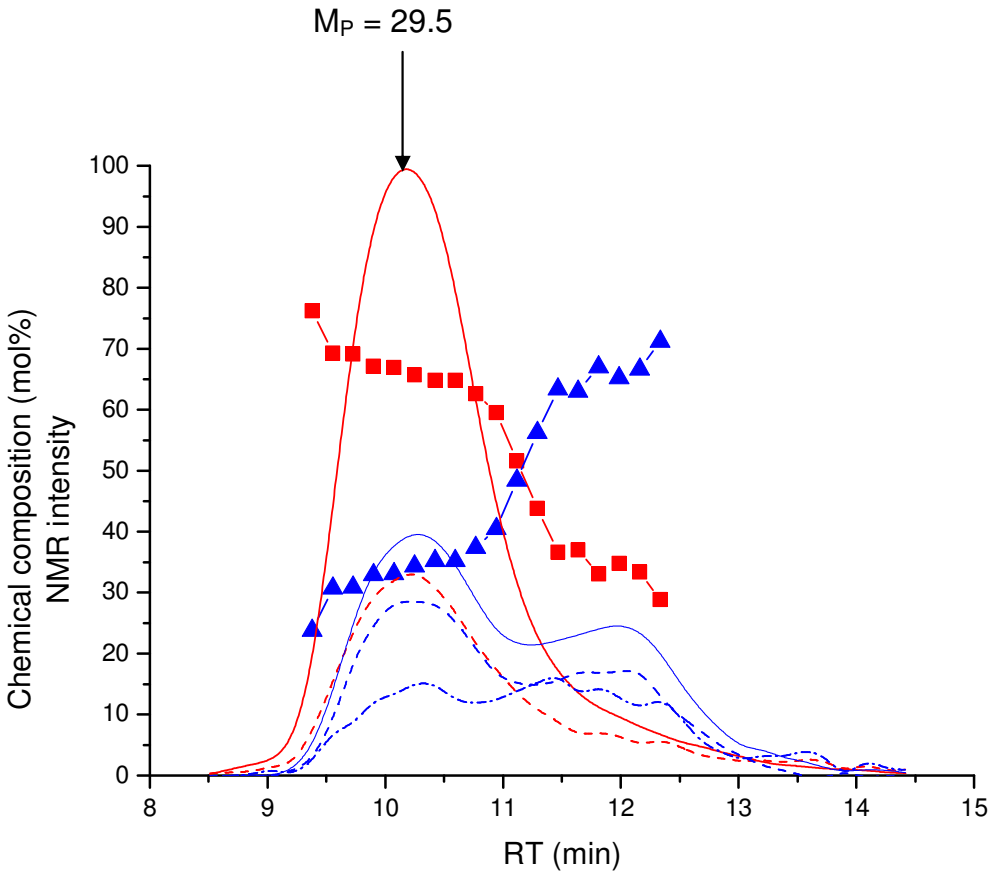
MP = 29.5
Chemical composition (mol%)
NMR intensity
RT (min)

Figure 51: Chemical composition of PI-*b*-PMMA copolymers versus retention time (■ = mol % PMMA and ▲= mol % PI). Lines are the NMR projections (NMR chromatograms): solid red line = syndiotactic (rr) α-CH_3 of PMMA, dashed red line = atactic (mr) α-CH_3 of PMMA, solid blue line = olefinic 3,4-PI, dashed blue line = olefinic 1,2-PI, dotted blue line = olefinic 1,4-PI [Samples 22 (a) and 26 (b)]

Fig. 52 shows the contents of the PMMA triads and the PI microstructures which can be directly calculated from the individual NMR chromatograms.
In case of Sample 22 (a) the syndiotactic (rr) and atactic (mr) triads as well as 1,4-PI are constant with increasing retention time. This sample has a very high amount of 1,4-PI with very minor amounts of syndiotactic and atactic triads. Since the amount of 3,4-PI is negligible it is not shown in the Fig. This behaviour indicates the chemical homogeneity of the copolymer.
In the case of Sample 26 (b) the copolymer region between 9-11 min indicates a slight decrease of the rr and mr triads with increasing retention times which finally results into the decrease of the total PMMA content with decreasing molar masses. The opposite tendency is seen for the polyisoprene block, 1,2-, 1,4- and 3,4-PI are equally increasing with decreasing molar masses. This behaviour is an indication for a chemical heterogeneity of the copolymer.

(a)

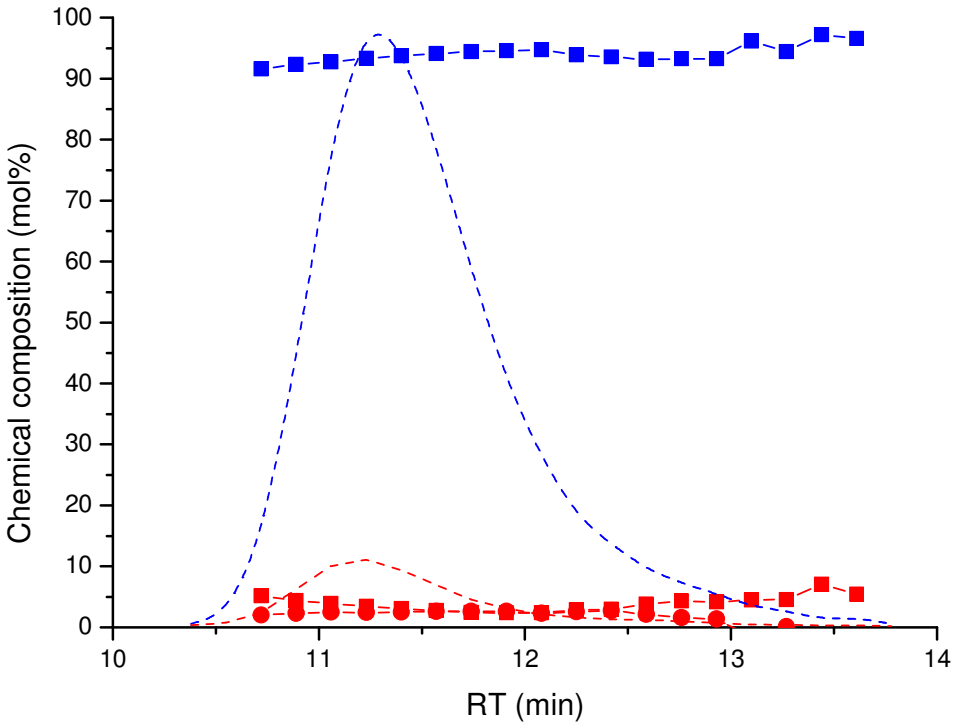
Chemical composition (mol%)
100
90
80
70
60
50
40
30
20
10
0
10
11
12
13
14
RT (min)

(b)

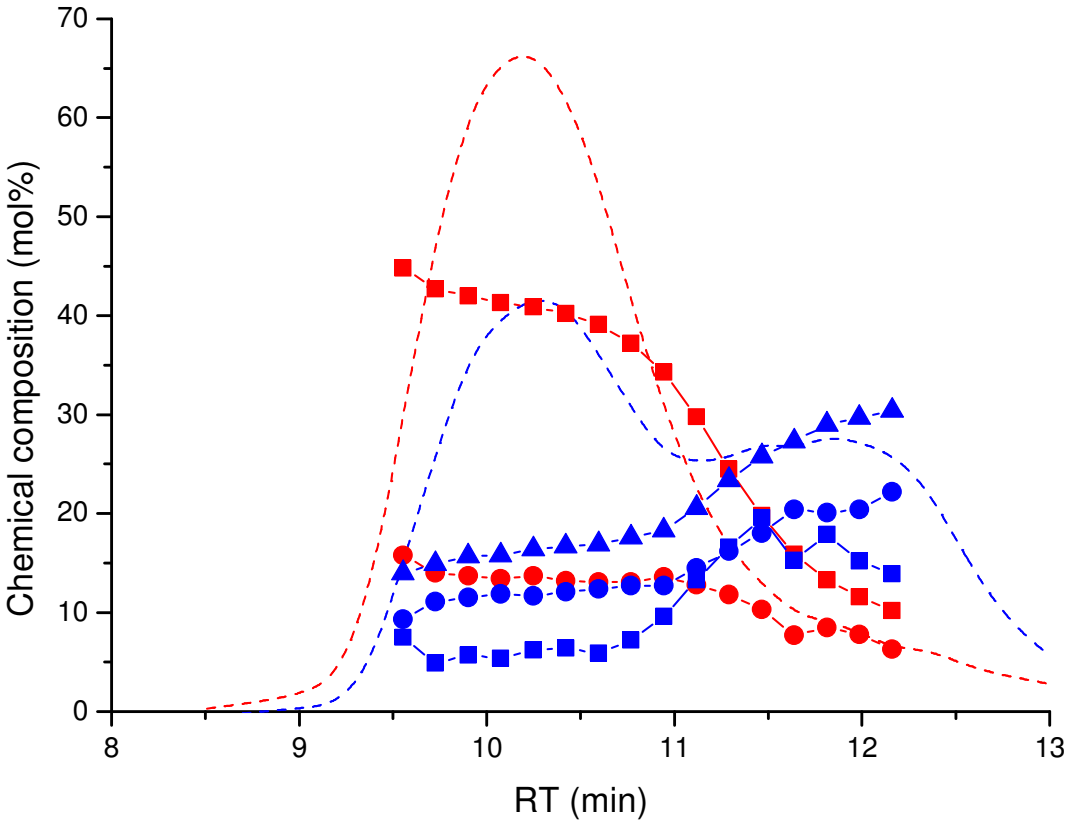

Figure 52: Chemical composition of the microstructures of PI-*b*-PMMA copolymers versus retention time measured at critical conditions of PI:
(■ = mol % of syndiotactic (rr) α-CH_3 of PMMA, ● = mol % of atactic (mr) α-CH_3 of PMMA, ▲ = mol % of olefinic 3,4-PI, ● = mol % of olefinic 1,2-PI, ■ = mol % of olefinic 1,4-PI, dotted red line = NMR chromatogram of total PMMA, dotted blue line = NMR chromatogram of total PI) [Samples 22 (a) and 26 (b)]

7.3 Method development for critical conditions of PMMA using a single solvent as mobile phase

To separate PI-*b*-PMMA copolymers critical conditions were established for the PMMA block. Since PMMA is the polar part of the block copolymer critical conditions were established by using a single solvent and a set of normal phase Si columns. Critical conditions were established by using ethyl acetate as the eluent and by varying the temperature of the columns. A set of polar stationary phases Si 300-5 + 1000-7 with column sizes of 200x4.6 mm inner diameter were used for establishing the critical conditions. Si indicates unmodified polar silica gel. Using this set of columns and ethyl acetate as the mobile phase, PMMA will elute at critical conditions whereas PI will elute in SEC mode. For establishing the critical conditions of PMMA same experimental conditions were used as that for the critical conditions of PI. PMMA and PI standards mentioned in the experimental section were used for establishing the critical conditions.

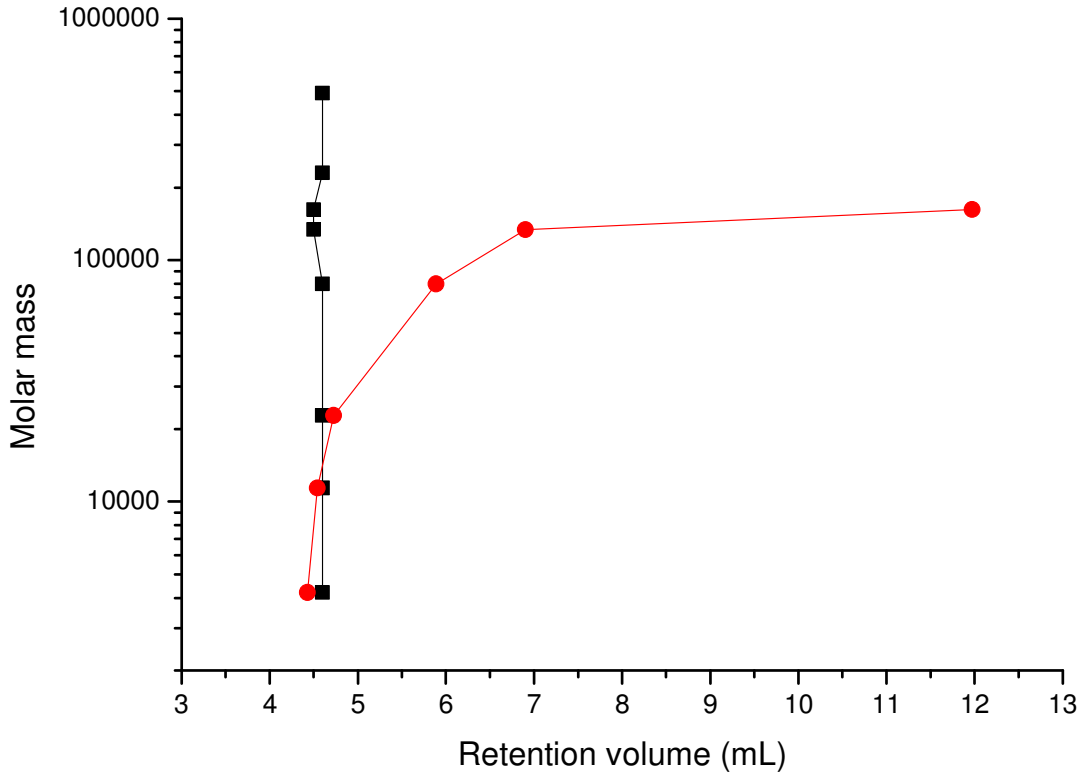

Figure 53: Critical diagram of PMMA showing molar mass M versus retention volume, mobile phase is ethyl acetate, column temperature ■ = 10 °C and ● = 60 °C, stationary phase: Si 300-5 + Si 1000-7

Fig. 53 shows the critical diagram for PMMA obtained by using normal phase Si columns and ethyl acetate as a single solvent. The critical conditions were established by varying the column temperature. In general, the solute retention in adsorption chromatography decreases with temperature increase, indicating that the solute sorption process to the stationary phase is enthalpy-wise favourable *($\Delta H^\circ < 0$)*. Also, in many cases, the sorption process appears entropically unfavourable *($\Delta S^\circ < 0$)*. This behaviour is easy to comprehend because the adsorbed polymer chains will lose some conformational degree of freedom while the sorption process should be energetically favourable to retain the solute in the column *($\Delta G^\circ < 0$)*. This is the enthalpy driven retention process often found in adsorption chromatography. Less frequently, however, the contrary temperature dependence is found whereby the retention increases with temperature increase, indicating ($\Delta H^\circ > 0$). In this case, the entropy change has to be positive to retain the solute in the column ($\Delta G^\circ < 0$). To put it in another way, the sorption of polymer solutes to the stationary phase is driven by entropy increase.[111-113] At a column temperature of 60 °C adsorption chromatography is observed. As the column temperature increases the retention volume also increases. Critical conditions are observed exactly at a temperature of 10 °C where all the PMMA homopolymers elute at the same retention volume irrespective of the molar mass.

The established critical conditions are used for the analysis of PI-*b*-PMMA copolymers.

7.4 LCCC-^{1}H-NMR of PI-*b*-PMMA copolymers at critical conditions of PMMA

These experiments were carried out in order to verify whether the proton signals of interest of the copolymer are affected by solvent suppression. Fig. 54 shows the ^{1}H-NMR spectra of a PI-*b*-PMMA copolymer dissolved in protonated ethyl acetate [Fig. 54 (a)] and in deuterated chloroform [Fig. 54 (b)]. WET solvent suppression is applied

to the signals of ethyl acetate. Three solvent signals are suppressed. It is evident from Fig. 54 that the α-CH_3 and OCH_3 group of the PMMA block and the olefinic protons of the PI block are unaffected by solvent suppression. These signals can be used for determining the chemical composition distribution. This Fig. also indicates that the stereochemistry of the PI block can be calculated by using the olefinic protons. Different microstructures of PI such as 1,4-PI, 3,4-PI and 1,2-PI can be identified and calculated.

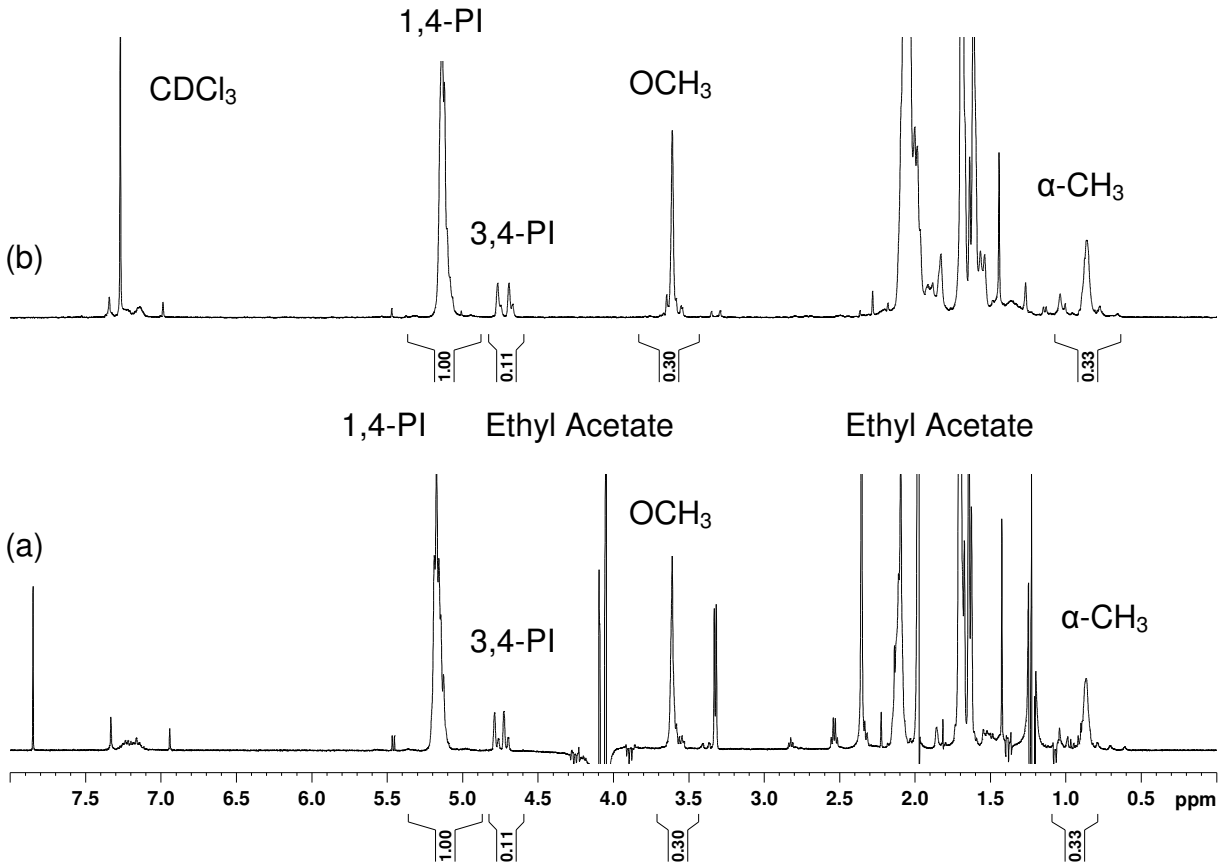

Figure 54: ^{1}H-NMR spectra of PI-*b*-PMMA copolymer in (a) non-deuterated ethyl acetate with WET solvent suppression and (b) in $CDCl_3$ respectively. The assignments are given according to Scheme 4.

The samples given in Table 18 are used for the analysis of PI-*b*-PMMA copolymers at critical conditions of the PMMA block. For performing the HPLC-NMR measurements, same experimental conditions were used as in the case for establishing the critical conditions of PI. Fig. 55 shows the HPLC-NMR on-flow run of 1,4-PI-*b*-PMMA copolymer. The on-flow plot shows only one component. The eluting

peak shows coexisting signals at the olefinic and aliphatic region. This peak can be assigned to the copolymer. The different copolymer samples elute in SEC mode due to the different molar masses of the PI block. From the typical NMR chemical shift of PI (5.1 ppm) the resonance peak can be assigned to 1,4 PI. The doublets at 4.65 and 4.75 ppm can be used for calculating the amount of 3,4 PI. The typical chemical shift between 0.7-1.1 ppm can be assigned to the α-CH_3 group of PMMA. The resonance peak at 3.6 ppm can be assigned to OCH_3 group of PMMA. This sample does not show the presence of any homopolymer.

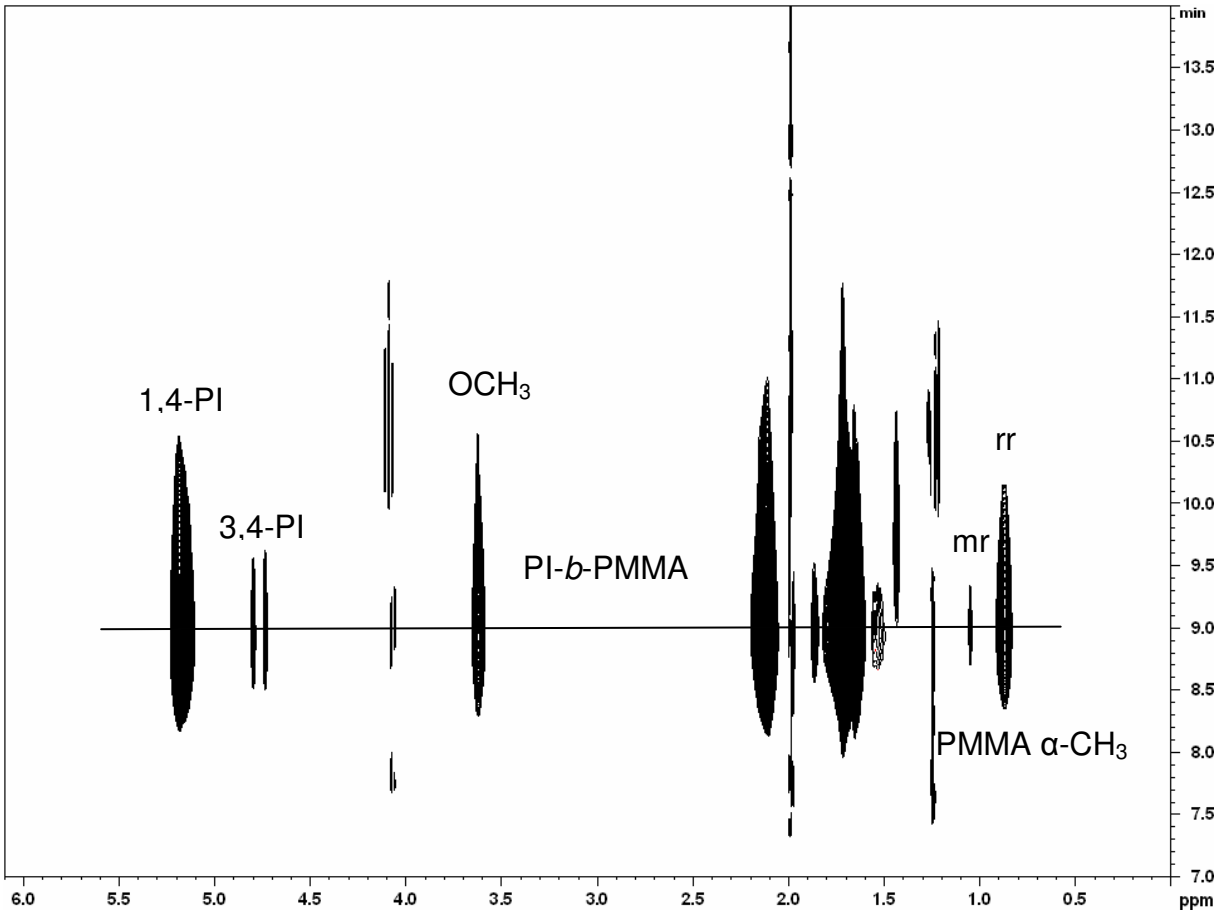

Figure 55: LCCC-NMR on-flow run of the copolymer of 1,4-PI-*b*-PMMA copolymer (Sample 22: M_P = 18.9 kg/mol) measured at the critical conditions of PMMA

Fig. 56 shows the LCCC-NMR on-flow run of 3,4-PI-*b*-PMMA copolymer. This Fig shows the block copolymer due to the co-existing signals of α-CH_3 group in the aliphatic region as well as the olefinic protons of PI. Full information of the methoxy group of PMMA and the olefinic region is obtained, but partial overlapping of a 1,2-isoprene signal with the α-CH_3 of PMMA is observed. In any case, it is possible to calculate the chemical composition of the copolymer at any given retention time. This copolymer does not show the presence of PMMA homopolymer.

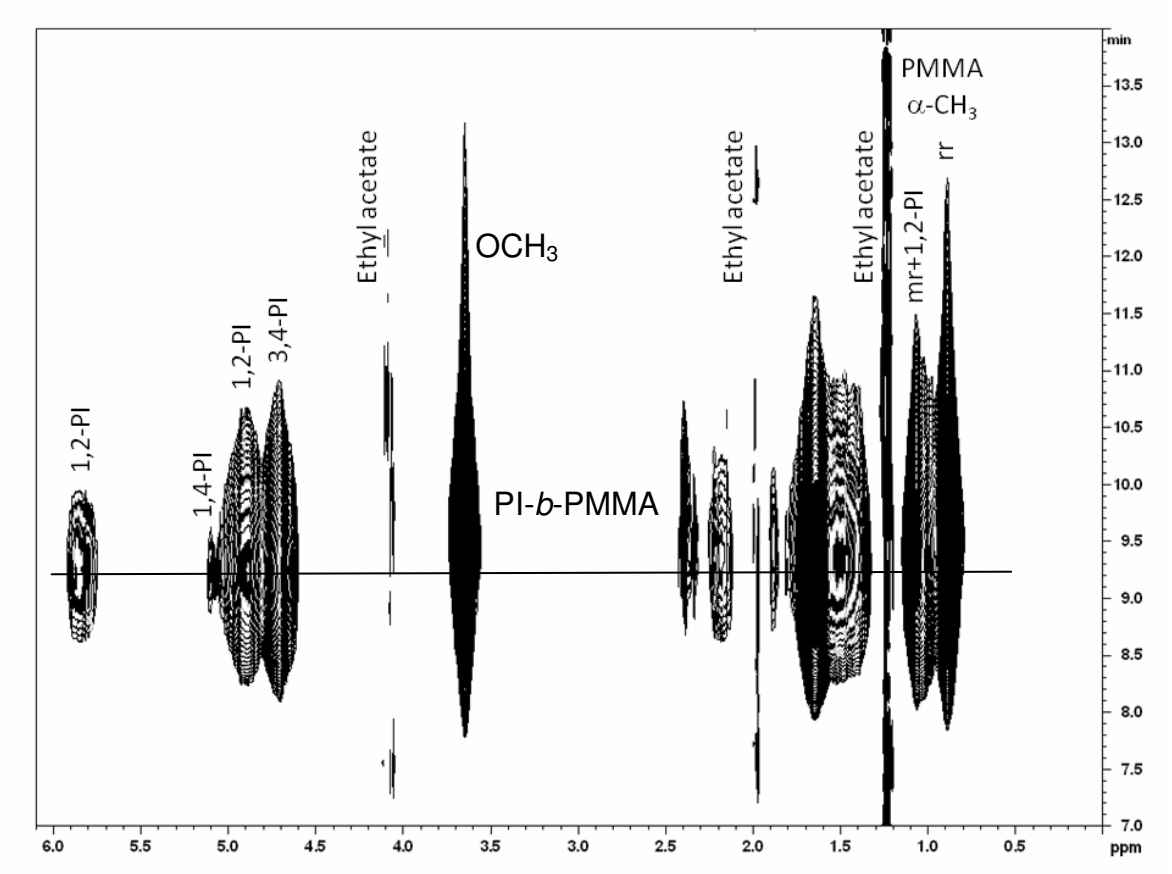

Figure 56: LCCC-NMR on-flow run of the copolymer of 3,4-PI-*b*-PMMA copolymer (Sample 26: M_P = 60.7 kg/mol) measured at the critical conditions of PMMA

In order to calculate the molar masses of the PI block in PI-*b*-PMMA copolymer by LCCC-NMR a calibration curve is constructed by using the PI standards mentioned in the experimental section. Using the calibration curve given in Fig. 57, the molar masses of the PI blocks in PI-*b*-PMMA copolymers were determined. The molar mass was calculated by taking the peak maximum (M_P) of the olefinic protons of PI.

Higher molar mass PI was not used for constructing the calibration curve because they were not soluble in ethyl acetate.

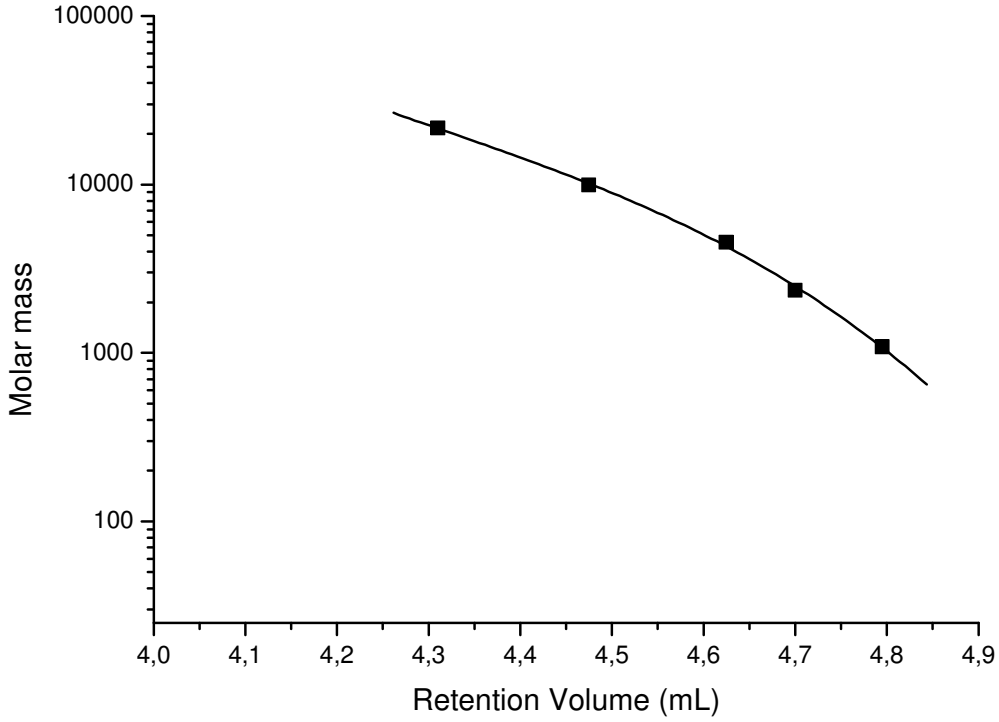

Figure 57: Calibration curve of PI showing molar mass versus retention volume at critical conditions of PMMA, solid line = curve fitted with third order polynomial

Table 21 shows the molar masses of the PI block calculated by LC-CC-NMR. These data are then compared to the molar masses of the block copolymers obtained by SEC and off-line NMR. Using the SEC data and chemical compositions of Table 18, the molar masses of the PI blocks of the copolymers can be calculated by using modified version of Equations (25-26). If we compare the values given in Table 21 the molar masses of the PI block obtained by SEC and off-line NMR is more than that obtained by LC-CC-NMR. This is because the bulk sample contains PI homopolymer. Another reason could be that the PI homopolymer present in the copolymer is not separated at the critical conditions of PMMA which can cause strong deviations from the correct molar mass and the chemical composition of the copolymer.

Sample	M_p (PI block) by LCCC-NMR (kg/mol)	M_p (PI block) by SEC and NMR (kg/mol)
22	8.7	16.6
23	8.1	10.1
24	1.9	10.0
25	12.8	21.0
26	3.6	26.8

Table 21: Molar masses of the PI block of the copolymers determined by SEC and off-line NMR with modified version of Equation (25) or LC-CC-NMR with the peak maximum (M_P) of the olefinic protons

Sample	M_p (PI block) by LC-CC-NMR (kg/mol)	Isoprene/MMA of copolymer by LC-CC-NMR (mol %)	M_p of block copolymer (kg/mol) calculated
22	8.7	90.1/9.9	10.1
23	8.1	53.5/46.5	18.5
24	1.9	55.3/44.7	4.2
25	12.8	9.1/90.9	103.7
26	3.6	54.3/45.7	8.1

Table 22: The molar masses of the PI block of the copolymers, chemical compositions and calculated total molar masses of the block copolymers at critical conditions of PMMA

Using the true molar mass of the PI block obtained by LC-CC-NMR and the true chemical composition obtained by adding all the polymer traces separated from the homopolymer the total molar mass of the block copolymer can be calculated.

There is hardly any agreement between the data obtained by LC-CC-NMR compared to that obtained by SEC and off-line NMR. Higher molar mass PI standards were not soluble in ethyl acetate. The PI block of the copolymer having molar masses higher than the calibration standards will deliver incorrect molar masses.

Since the critical conditions were established by varying the temperature of the column maybe some error may have occurred while establishing these conditions.

In case of the SEC measurements since the calibration is based on PS, the PS calibration may overestimate the molar mass of the block copolymers.

One major benefit of HPLC-NMR is the ability to determine the chemical composition distribution of the block copolymers. By using the on-flow data presented in Figs. 55

and 56, it is possible to calculate the chemical composition at different retention times.

Sample 22 (a) shows monomodal distributions for all monomer units at critical conditions of PMMA. This indicates the absence of PMMA homopolymer. The main component of the block copolymer is 1,4-PI with minor amounts of 3,4-PI and PMMA. The block copolymer is homogenously distributed with regard to the chemical composition distribution. The chemical composition measured by off-line NMR is compared to that measured by LCCC-NMR. It is seen from Tables 18 and 22 that the values are nearly the same which indicates the absence of PMMA homopolymer.

Sample 26 (b) also shows monomodal distributions for all monomer units. In this case no differentiations between different species are possible. All curves show almost the same maximum. However, this separation clearly indicates that the sample does not contain PMMA homopolymer. Ethyl acetate suppression partially affects the mr triad intensity which is slightly diminished and shifted. The block copolymer is moderately distributed with regard to the CCD. As the retention time increases the amount of PI decreases with an increase in the amount of PMMA.

(a)

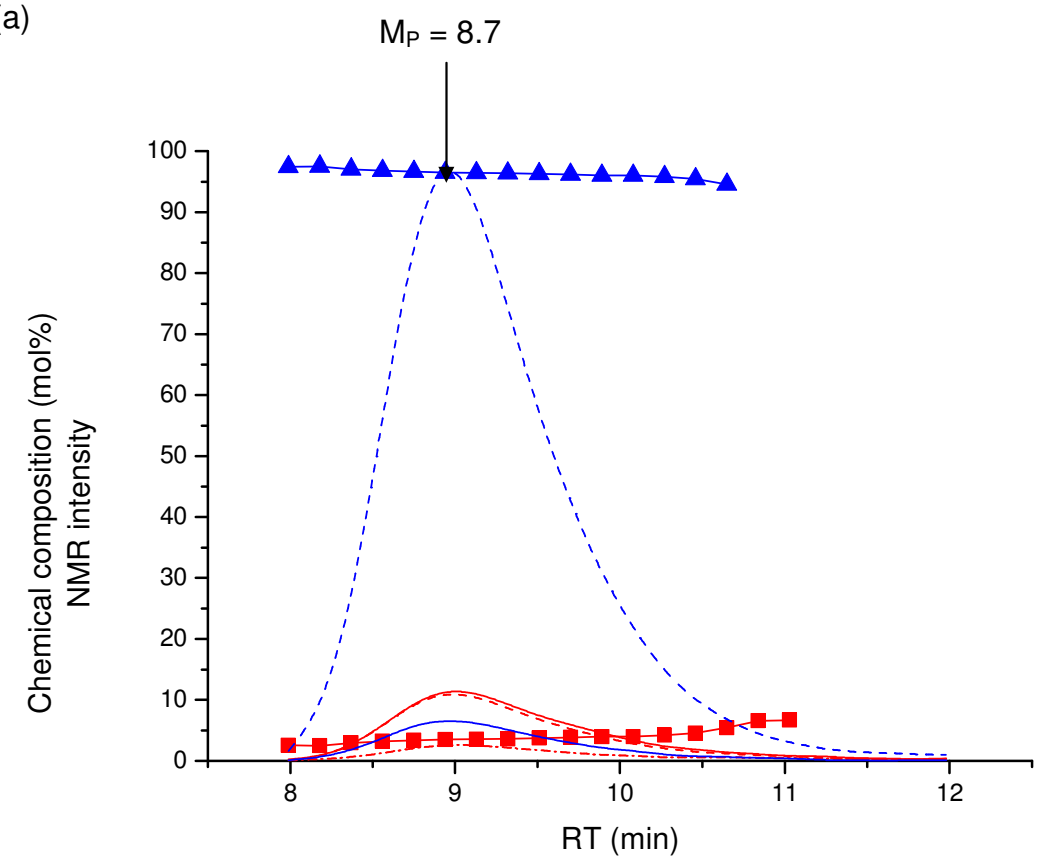

(b)

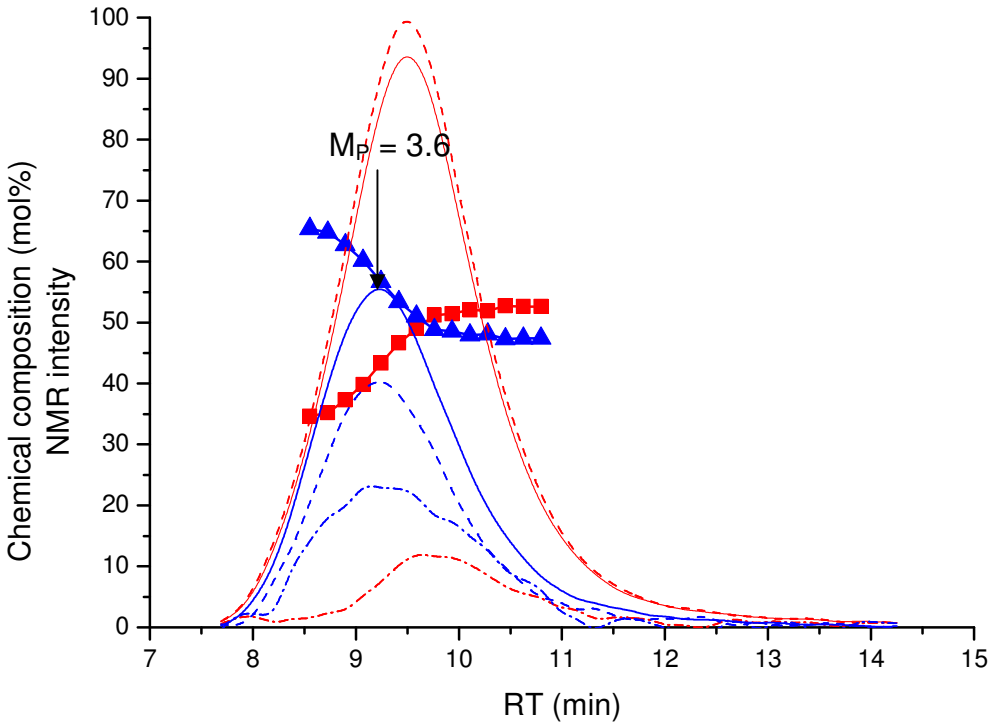

Figure 58: Chemical composition of PI-*b*-PMMA copolymers versus retention time (■ = mol % PMMA and ▲= mol % PI). Lines are the NMR projections (NMR chromatograms): solid red line = syndiotactic (rr) α-CH_3 of PMMA, dashed red line = atactic (mr) α-CH_3 of PMMA, dotted red line = OCH_3 of PMMA, solid blue line = olefinic 3,4-PI, dashed blue line = olefinic 1,2-PI, dotted blue line = olefinic 1,4-PI [Samples 22 (a) and 26 (b)]

Fig. 59 shows the different PI microstructures and the PMMA triads which can be directly calculated from the individual NMR chromatograms.

In sample 22 (a) the amount of 1,4-PI as well as the syndiotactic (rr) and atactic (mr) triads remains constant with increase in retention time. This sample has major component of 1,4-PI with minor amounts of PMMA triads. Since the amount 3,4-PI is negligible it is not shown in the Fig.

In sample 26 (b) the amount of syndiotactic (rr) and atactic (mr) triads increase with increase in retention time and then becomes constant. The amount of 1,2-, 3,4- and 1,4-PI decreases with increase in retention time. This sample predominantly shows the microstructure of 3,4-PI.

(a)

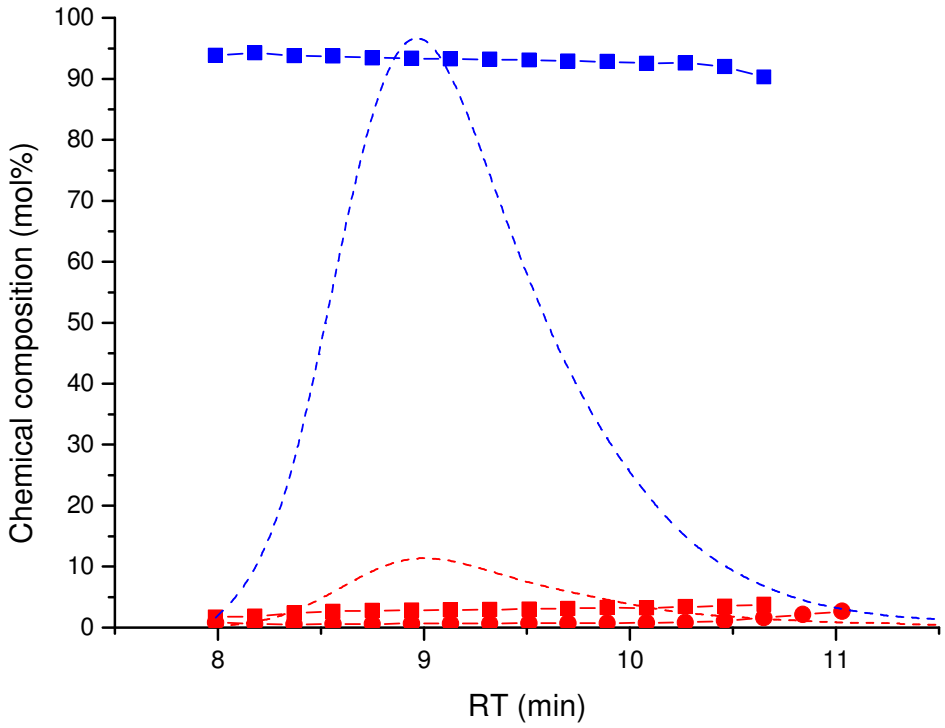

(b)

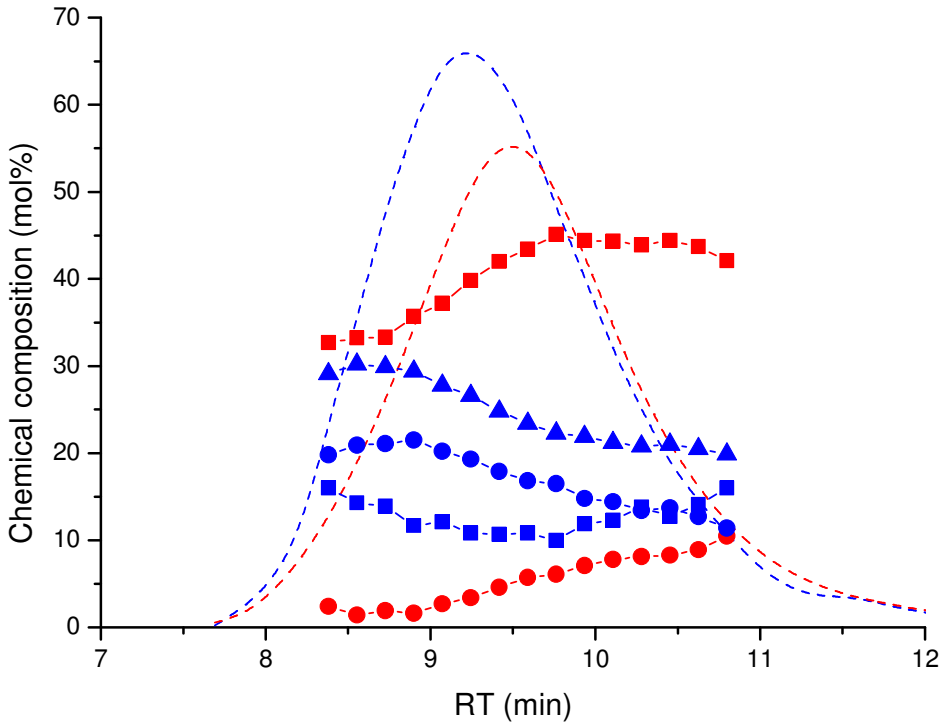

Figure 59: Chemical composition of the microstructures of PI-*b*-PMMA copolymers versus retention time measured at critical conditions of PMMA:
(■ = mol % of syndiotactic (rr) α-CH_3 of PMMA, ● = mol % of atactic (mr) α-CH_3 of PMMA, ▲ = mol % of olefinic 3,4-PI, ● = mol % of olefinic 1,2-PI, ■ = mol % of olefinic 1,4-PI, dotted red line = NMR chromatogram of total PMMA, dotted blue line = NMR chromatogram of total PI) [Samples 22 (a) and 26 (b)]

8. Experimental Part

8.1 Chemicals

8.1.1 Solvents used for chromatography

- Acetonitrile (ACN), HPLC grade (Acros Organics, Geel, Belgium)
- Ethyl acetate for HPLC (Acros Organics, Geel, Belgium)
- Technical grade tetrahydrofuran (THF) was refluxed and distilled from CaH_2
- Cyclohexane (c-hexane), methyl ethyl ketone (MEK) and 1,4-dioxane were used for HPLC VWR CHROMANORM (VWR, Darmstadt, Germany)

8.1.2 Polymer standards

For determining the critical conditions polymer standards of polystyrene (PS), polymethyl methacrylate (PMMA), 1,4-polyisoprene (PI) and 3,4-polyisoprene (PI) produced by Polymer Standards Service GmbH (PSS, Mainz, Germany) having different molar masses and narrow polydispersities were used. Some homopolymers of PMMA and 1,4-PI synthesised by T. Wagner and J. Thiel at the Max-Planck-Institute for Polymer Research (MPI, Mainz, Germany) were also used.

8.1.3 Copolymers

PS-*b*-PMMA copolymers were synthesised by Polymer Standards Service GmbH (PSS, Mainz, Germany). PI-*b*-PMMA copolymers were synthesised at the Max-Planck-Institute for Polymer Research (MPI, Mainz, Germany) by T. Wagner and J. Thiel. PS-*b*-PI copolymers were synthesised at the Institute of Technical and Macromolecular Chemistry of Darmstadt University of Technology (TUD, Darmstadt, Germany) by Dr. V. Bellas. All the block copolymers mentioned above were used for the analysis.

8.1.4 Chromatographic columns

The following columns were used:

A. Nucleosil C_{18}: particle size 5 µm, pore diameter 300 Å, column dimensions 250x4 mm i.d. (Macherey-Nagel, Düren, Germany)

B. Nucleosil C_{18}: particle size 7 µm, pore diameter 1000 Å, column dimensions 250x4 mm i.d. (Macherey-Nagel, Düren, Germany)

C. Nucleosil Si: particle size 5 µm, pore diameter 300 Å, column dimensions 200x4.6 mm i.d. (Macherey-Nagel, Düren, Germany)

D. Nucleosil Si: particle size 7 µm, pore diameter 1000 Å, column dimensions 200x4.6 mm i.d. (Macherey-Nagel, Düren, Germany)

E. Nucleosil Si: particle size 5 µm, pore diameter 300 Å, column dimensions 250x4.6 mm i.d. (Macherey-Nagel, Düren, Germany)

8.2 Equipment used for chromatography

8.2.1 Liquid chromatography at critical conditions (LC-CC)

All measurements were performed using an Agilent 1100 series HPLC system (Agilent Technologies GmbH, Böblingen, Germany) consisting of a vacuum degasser (G1322A), a quaternary pump (G1311A), an auto-sampler (G1313A), a column oven (G1316A) and a variable wavelength UV-detector (G1314A). In addition an evaporative light scattering detector (ELS 1000, Polymer Laboratories Inc. Church Stretton, England) was used.
In order to establish the critical conditions of both the monomer units of PS-*b*-PMMA copolymers, PS and PMMA calibration standards were used. The calibration standards had the following weight average molar masses (M_w): PS: 4.05, 5.7, 8.1, 15, 35, 49, 65, 145, 470 kg/mol; PMMA: 1.9, 10.9, 29, 84.9, 253, 640 kg/mol. The

concentration of the injected sample in all the cases was 0.5 mg/mL. 10 µL of the polymer solutions were injected. The column temperature was maintained at 22°C.
For the separation of blends of 1,4-PI and 3,4-PI critical conditions were established by using 1,4-PI and 3,4-PI calibration standards. The standards had the following weight average molar masses (M_W): 1,4-PI: 1.04, 4.46, 9.91, 21.2, 57.4 kg/mol; 3,4-PI: 1.09, 9.39, 33.3, 53.3, 76.7 kg/mol. The column temperature was maintained at 30°C.
For PS-*b*-PI copolymers critical conditions were established for both the monomer units. PS and PI calibration standards were used. They had the following weight average molar masses (M_W): PS: 18.3, 38, 53.2, 78.2 kg/mol; 1,4-PI: 1.04, 4.46, 9.91, 21.2, 57.4 kg/mol. In this case the column temperature was also maintained at 30°C.
For separating PI-*b*-PMMA copolymers critical conditions were established for both PI as well as PMMA. PI and PMMA calibration standards had the following weight average molar masses (M_W): PI: 1.09, 2.35, 2.57, 4.54, 4.84, 8.43, 9.76, 9.93, 19.97, 21.60, 32.21, 45.91, 94.43 kg/mol; PMMA: 1.90, 3.60, 4.21, 10.90, 11.4, 22.7, 29.00, 79.68, 84.90, 133.60, 162.10, 230, 253, 491.50, 640 kg/mol.
Normal HPLC grade solvents of acetonitrile, tetrahydrofuran, methyl ethyl ketone, cyclohexane, 1,4-dioxane and ethyl acetate were used as mobile phases. A flow rate of 0.5 mL/min was maintained for all the measurements. The chromatographic system was controlled by the Hystar software version 1.3 (Bruker Biospin GmbH, Rheinstetten, Germany).

8.2.2 Size Exclusion Chromatography (SEC)

All SEC measurements were performed using a Waters system (Waters Corporation, USA) consisting of a 515 HPLC pump, an auto-sampler AS 100 from Thermo Separation Products, a column oven, a Waters 410 differential refractometer and a Waters 486 tunable absorbance detector. Data collection and processing was performed using PSS WinGPC software version 6 from Polymer Standards Service GmbH (PSS, Mainz, Germany). For all samples THF was used as eluent. Sample concentrations were 1.5 mg/mL. The injected sample volume was 100 µL. The column temperature for all the experiments was 35°C and the flow rate was 1

mL/min. The columns used were SDV 10^3, 10^5 and 10^6 from Polymer Standards Service GmbH (PSS, Mainz, Germany).

8.3 Equipment used for nuclear magnetic resonance spectroscopy (NMR)

8.3.1 Proton nuclear magnetic resonance spectroscopy (^{1}H-NMR)

The NMR experiments were conducted on a Bruker Avance 400 MHz spectrometer (Bruker Biospin GmbH, Rheinstetten, Germany). The measurements were performed with a BBI 400 MHz SI 5mm probe. The probe was an inverse detection broad band probe equipped with a shielded pulsed field-gradient coil. Thirty-two scans using 30 degree pulses were acquired with an acquisition time of 3.5 s and a relaxation delay of 5 s. For the ^{1}H-NMR measurements 20 mg/mL of PS-*b*-PMMA were dissolved in 0.7 mL of deuterated dichloromethane (CD_2Cl_2), PI-*b*-PMMA was dissolved in deuterated chloroform ($CDCl_3$) and PS-*b*-PI was dissolved in deuterated tetrahydrofuran (C_4D_8O). Data were processed using Topspin software version 1.3 (Bruker Biospin GmbH, Rheinstetten, Germany).

8.3.2 Hyphenation of LC-CC and ^{1}H-NMR

The outlet of the UV detector of the Agilent HPLC unit was connected to the peak sampling unit (BPSU-12) from Bruker Biospin GmbH, Rheinstetten, Germany. The peak sampling unit was then connected with capillaries to the continuous flow probe in the cryomagnet. The measurements were conducted with a continuous flow probe containing a 60 µL flow cell. The probe was a ^{1}H {^{13}C} inverse detection probe equipped with a shielded pulsed field-gradient coil. The gradient strength was 53 G/cm. The 90° ^{1}H pulse was 4.6 µs. WET solvent suppression was applied to the HPLC grade solvents used for chromatography. On-flow experiments were performed for studying the critical conditions. Eight scans per free induction decay (FID) were acquired with an acquisition time of 1.1 s (16 Kb data points) and a relaxation delay of 0.1 s. For the on-line coupled HPLC-^{1}NMR measurements 20 mg/mL was the concentration of the block copolymers. In case of the blends of PS and PMMA concentration was 3 mg/mL for each blend component. Blends of 1,4-PI

and 3,4-PI was prepared by dissolving 10 mg/mL of each component in the solvent mixture. For all the experiments the volume injected was 50 µL.

Normal HPLC grade solvents of acetonitrile, tetrahydrofuran, methyl ethyl ketone, cyclohexane, 1,4-dioxane, and ethyl acetate were used as the mobile phases. The flow rate for all the measurements was 0.5 mL/min. The HPLC-^{1}NMR system was controlled by the Hystar Software version 1.3 (Bruker Biospin GmbH, Rheinstetten, Germany).

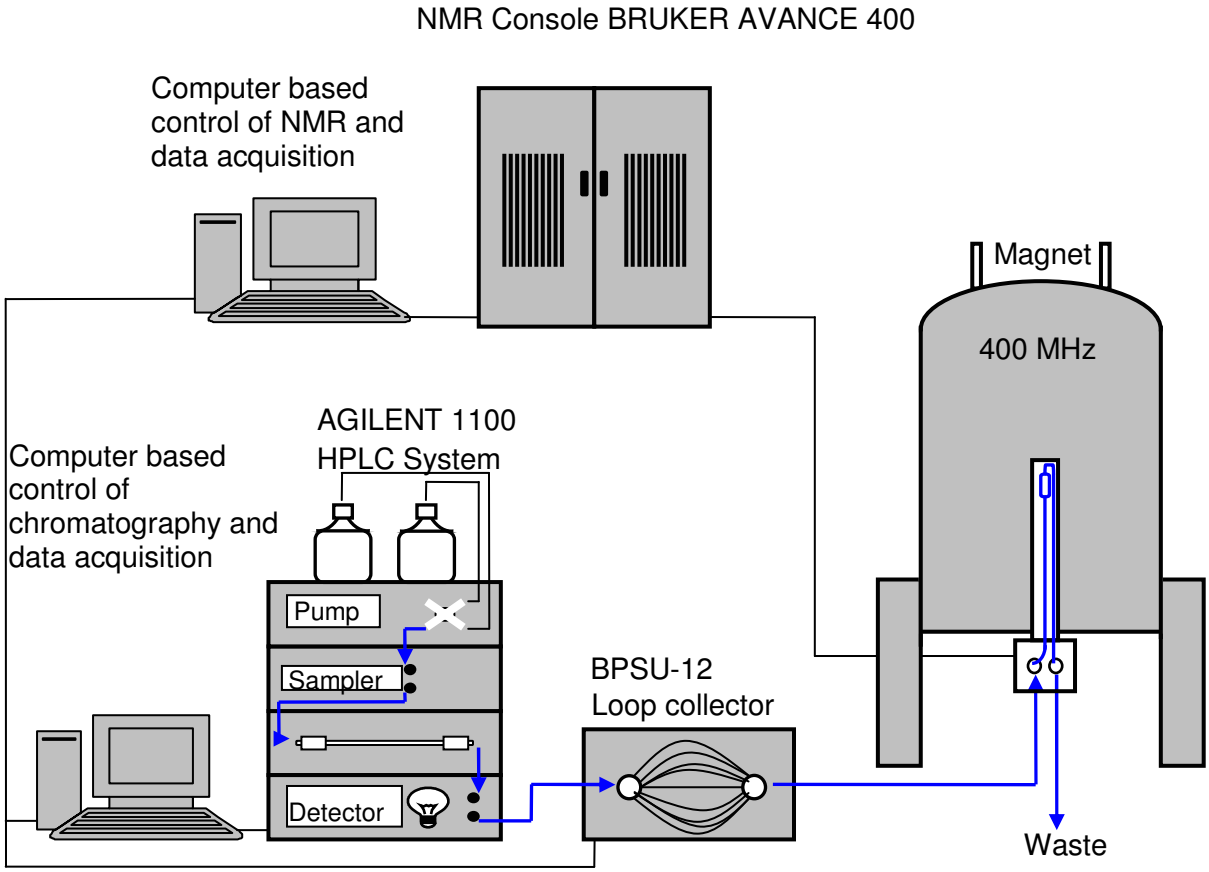

Figure 60: Scheme of the experimental set-up used for HPLC-NMR coupling

9 Conclusions

Block copolymers are extremely complex macromolecular systems that exhibit chemical composition distributions in addition to the typical molar mass distributions. In specific cases blocks are composed of tactic monomers and, therefore, the block copolymers exhibit a tacticity type distribution. In the present work selective chromatographic methods for separations with regard to molar mass, chemical composition, and tacticity were developed that were on-line coupled with ^{1}H-NMR as a highly selective detector. The results of the work can be summarized as follows:

(A) Fractionation and analysis of PS-*b*-PMMA copolymers using mixed mobile phases at critical conditions of both PMMA and PS

The investigations have shown that HPLC-^{1}H-NMR is a versatile tool for the analysis of PS-*b*-PMMA block copolymers. In particular, it is possible to determine the chemical composition distributions of the block copolymers at chromatographic conditions that correspond to the critical point of the PMMA block by using MEK/cyclohexane as the mobile phase. For selective adsorptive interactions of the PMMA block a polar stationary phase of silica gel was used. The average chemical compositions of the bulk samples were analysed by LCCC-NMR and off-line ^{1}H-NMR and very good agreement has been found. The molar masses of the PS blocks in the block copolymers were determined at critical conditions of PMMA by using a calibration procedure based on on-flow NMR experiments. It was shown that the molar masses of the PS blocks were only correct when the samples were pure block copolymers. When they contain PS homopolymer fractions then a higher content of styrene is obtained and, accordingly, a too high molar mass of the PS block is calculated. Thus, the amount of PS homopolymer in the samples must be determined.

At the critical point of PS it is also possible to determine the chemical heterogeneity of the copolymers. In this case a mobile phase of THF/ACN is used and the stationary phase is a C_{18}-bonded silica gel. It was confirmed that the PS-*b*-PMMA copolymers are chemically heterogeneous and contain fractions of PS homopolymer. In addition, block copolymer fractions of different chemical compositions were identified. The molar masses of the PMMA blocks in the block copolymers were

determined using a standard SEC calibration procedure. Moreover, it was found that the true chemical compositions as well as the true molar masses of the block copolymers are determined best by on-line coupled LCCC-^{1}H-NMR. These can significantly differ from the average chemical compositions of the bulk samples. Finally, the tacticity of the PMMA blocks was determined. The on-flow LCCC-^{1}H-NMR experiments were used for analysing the syndiotactic and heterotactic triads as a function of molar mass. The tacticity of the PMMA blocks is constant and does not depend on molar mass. The experiments clearly showed that a correct molar mass determination of the blocks can only be guaranteed when the samples are analysed at both critical conditions.

(B) Fractionation and analysis of blends of 1,4- and 3,4-PI using mixed mobile phases at critical conditions of 1,4-PI

Polyisoprene shows different types of isomeric structures of the monomer units such as 1,4-PI, 3,4-PI and 1,2-PI. By operating at the critical conditions of 1,4-PI using MEK/cyclohexane as the mobile phase and a reversed stationary phase RP-C_{18} it is possible to separate blends of 1,4- and 3,4-PI. From ^{1}H-NMR it is seen that the 1,4- and 3,4-PI samples are not pure with regard to the tactic units but contain some amount of the other species. 1,4-PI contains minor amounts of 3,4-PI whereas 3,4-PI contains some amounts of 1,4- and 1,2-PI. By coupling HPLC and ^{1}H-NMR it is possible to identify and quantify the different microstructures in the polyisoprene samples.

(C) Fractionation and analysis of PS-*b*-PI copolymers by using mixed mobile phases at critical conditions of both PS and PI

Block copolymers of PS and PI were synthesised by two different methods: sequential living anionic polymerisation and coupling of living precursor blocks. In both cases there is possibility for the formation of PS homopolymer. By using ^{1}H-NMR the average chemical compositions of the copolymers were calculated. Using liquid chromatography at critical conditions a separation with regard to chemical composition was achieved. By operating at the critical conditions of PS the block copolymer fractions were separated from PS homopolymer. At these

chromatographic conditions the molar mass of the PI block was calculated using standard SEC calibration procedure. The stereochemistry of the PI block was determined from the on-flow experiments where the LC-CC separation was coupled to ^{1}H-NMR.

When the block copolymers are synthesised by coupling of living precursor blocks there is also a possibility for the formation of homopolymer of PI. The block copolymers synthesised by this method have been found to be chemically heterogeneous. Small amounts of PI homopolymer were separated from the copolymer fractions by operating at critical conditions of PI. At the same time the chemical composition distribution of the copolymers and the molar masses of the PS blocks were determined. It has been shown that for the complete characterisation of the block copolymers it is necessary to establish critical conditions for both blocks of the copolymer.

(D) Fractionation and analysis of PI-*b*-PMMA copolymers by using single solvents and different column temperatures at critical conditions of both PI and PMMA

Solvent suppression is a significant issue in HPLC-NMR coupling. It is a major advantage to use single solvents instead of solvent mixtures as mobile phases in HPLC. In the present case, the critical conditions of PI with 1,4-dioxane and PMMA with ethyl acetate as single solvents were established by varying the column temperature. The application of single solvent mobile phases accelerates the search for critical conditions, minimizes the consumption of HPLC solvents and improves the quality of the NMR spectra significantly.

To summarize, NMR spectroscopy is unsurpassed as an analytical tool to determine structures of small molecules but requires relatively pure samples. HPLC is a powerful tool to separate complex mixtures into their individual components. The on-line combination of HPLC separations with NMR detection represents a convenient and practical union that can harness the individual strengths of both techniques. LCCC-NMR is the only method known so far which can provide both the CCD and MMD of the block copolymers. The NMR detector acts as an absolute concentration detector and at the same time as a selective detector for the different polymer

structures. Therefore, the combination of HPLC and NMR provides quantitative information on the distributions of molar mass, chemical composition and tacticity in one experiment.

10 List of Abbreviations and Symbols

PS	Polystyrene
PMMA	Poly(methyl methacrylate)
PI	Polyisoprene
CCD	Chemical composition distribution
MMD	Molar mass distribution
MI	Macroinitiator
NMR	Nuclear magnetic resonance
FTIR	Fourier transform infrared
HPLC	High performance liquid chromatography
SEC	Size exclusion chromatography
LAC	Liquid adsorption chromatography
LC-CC	Liquid chromatography at critical conditions
ΔG	Free Gibbs energy difference
ΔH	Change in interaction enthalpy
ΔS	Change in conformational entropy
R	Universal gas constant
T	Absolute temperature
K_d	Distribution coefficient
V_R	Retention volume of the analyte
V_p	Pore volume of the stationary phase
V_i	Interstitial volume of the column
K_{SEC}	Contribution of size exclusion to distribution coefficient
K_{LAC}	Contribution of adsorption to distribution coefficient
V_O	Void volume of the column
V_{stat}	Volume of the stationary phase
B_0	Magnetic field strength
ω_0	Larmour frequency
γ	Gyromagnetic ratio
CW	Continuous wave spectroscopy
FID	Free induction decay
B_{eff}	Effective magnetic field strength
σ	Magnetic shielding constant

$\nu_{Substance}$	Resonance frequency of the substance
$\nu_{Reference}$	Resonance frequency of the reference
TMS	Tetramethylsilane
S/N	Signal to noise ratio
NS	Number of transients
T_1	Spin lattice relaxation time
T_2	Transverse relaxation time
NOE	Nuclear overhauser effect
^{1}H-NMR	Proton nuclear magnetic resonance
^{13}C-NMR	Carbon nuclear magnetic resonance
τ	Residence time
W	Signal half width
PRT	Pulse repetition time
AQ	Acquisition time
D1	Relaxation delay
NOESY	Nuclear Overhauser Enhancement Spectroscopy
WATERGATE	WATER by GrAdient Tailored Excitation
PFGs	Pulsed field gradients
BPPSTE	BiPolar gradient Pulsed Stimulated Echo
RF	Radio frequency pulse
WET	Water suppression enhanced through T1 effects
2D-NMR	Two-dimensional nuclear magnetic resonance
UV	Ultraviolet detector
D_2O	Deuterium oxide
rr	Syndiotactic
mr	Heterotactic
mm	Isotactic
ACN	Acetonitrile
THF	Tetrahydrofuran
c-hexane	Cyclohexane
MEK	Methyl ethyl ketone
$CDCl_3$	Deuterated chloroform
CD_2Cl_2	Deuterated dichloromethane
C_4D_8O	Deuterated tetrahydrofuran

11 Bibliographic References

[1] N. Hadjichristidis, M. Pitsikalis, S. Pispas, H. Iatrou, *Chem. Rev.*, **2001**, 101, 3747

[2] S.O. Kim, H.H. Solak, M.P. Stoykovich, N.J. Ferrier, J.J. de Pablo, P.F. Nealey, *Nature*, **2003**, 424, 411

[3] K. Müller, M. Klapper, K. Müllen, *J. Polym. Science A, Polym. Chem.*, **2007**, 45, 1101

[4] C. Batis, G. Karanikolopoulos, M. Pitsikalis, N. Hajichristidis, *Macromolecules*, **2000**, 33, 8541

[5] S.N. Nazhat, S. Parker, P.D. Riggs, M. Branden, *Biomaterials*, **2001**, 22, 2087

[6] R.R. Li, P.D. Dapkus, M.E. Thompson, W.G. Jeong, C. Harrison, P.M. Chaikin, R.A. Register, D.H. Adamson, *Appl. Phys. Lett.*, **2000**, 76, 1689

[7] T. Chang, *Adv. Polym. Sci.*, **2003**, 163, 1

[8] S. Mori, H.G. Barth, *Size Exclusion Chromatography*, Eds., Springer, Berlin, New York, **1999**

[9] H.C. Lee, T. Chang, *Macromolecules*, **1996**, 29, 7294

[10] H.J.A. Philipsen, B. Klumpermann, A.L. German, *J. Chromatogr., A*, **1996**, 746, 211

[11] H. Pasch, *Adv. Polym. Sci.*, **1997**, 128, 1

[12] L.R. Synder, J.J. Kirkland, *Introduction to Modern Liquid Chromatography*, 2nd Edition, John Wiley & Sons Inc., New York, USA, **1979**

[13] Y. Brun, Y. Alden, *J. Chromatogr. A*, **2002**, 699, 25

[14] G. Glöckner, *Gradient HPLC of Copolymers and Chromatographic Cross-fractionation*, Chapter 3, Springer, Berlin Heidelberg New York, **1991**

[15] H. Pasch, B. Trathnigg, *HPLC of Polymers*, Springer-Verlag, Berlin Heidelberg, Germany, **1998**

[16] *Macromolecular Engineering Precise Synthesis, Material Properties, Applications, Volume 3: Structure-Property Correlation and Characterization Techniques*, Edited by K. Matyjaszewski, Y. Gnanou, L. Leibler, WILEY-VCH Verlag GmbH & Co. KgaA, Weinheim, **2007**

[17] W. Radke, *Macromol. Theory Simul.*, **2001**, 10, 668

[18] B. Trathnigg, *Size-exclusion Chromatography of Polymers*, In: Meyers RA, Editor. *Encyclopedia of Analytical Chemistry*. John Wiley & Sons Ltd., **2000**,

8008

[19] A. A. Gorbunov, A. M. Skvortsov, *Adv. Colloid Interface Sci.*, **1995**, 62, 31

[20] G. Glöckner, *Adv. Polym. Sci.*, **1986**, 79, 159

[21] G. Glöckner, *Polymercharakterisierung durch Flüssigchromatographie,* VEB Deutscher Verlag für Wissenschaften, Berlin, **1980**

[22] S.G. Entelis, V.V. Evreinov, A.V. Gorshkov, *Adv. Polym. Sci.*, **1986**, 76, 129

[23] S.G. Entelis, V.V. Evreinov, A.I. Kuzaev, *Reactive Oligomers*, Khimiya Moscow, **1985**

[24] B.G. Belenkii, E.S. Gankina, M.B. Tennikov, L.Z. Vilenchik, *Dokl. Akad. Nauk SSR*, **1976**, 231, 1147

[25] B.G. Belenkii, M.D. Valchikhina, I.A. Vakhtina, E.S. Gankina, O.G. Tarakanov, *J. Chromatogr.,* **1976**, 129, 115

[26] B.G. Belenkii, E.S. Gankina, M.B. Tennikov, L.Z. Vilenchik, *J.Chromatogr.*, **1978,** 147, 99

[27] A.M. Skvortsov, B.G. Belenkii, E.S. Gankina, M.B. Tennikov, *Vysokomol. Soed. A.,* **1978**, 20, 678

[28] A.M. Skvortsov, A.A. Gorbunov, *J. Chromatogr.*, **1986**, 358, 77

[29] A. Gorbunov, B. Trathnigg, *J. Chromatogr. A*, **2002**, 955, 9

[30] T. Macko, D. Hunkeler, D. Berek, *Macromolecules*, **2002**, 35, 1797

[31] A.V. Gorshkov, H. Much, H. Becker, H. Pasch, V.V. Evreinov, S.G. Entelis, *J. Chromatogr.*, **1990**, 523, 91

[32] Y. Mengerink, R. Peters, Sj. van der Wal, H.A. Claessens, C.A. Cramers, *J. Chromatogr. A*, **2002**, 949, 337

[33] W. Lee, H. Lee, H.C. Lee, D. Cho, T. Chang, A.A. Gorbunov, J. Roovers, *Macromolecules*, **2002**, 35, 529

[34] H. Pasch, A. Deffieux, I. Henze, M. Schappacher, L. Rique-Lurbet, *Macromolecules*, **1996**, 29, 8776

[35] T. Biela, A. Duda, K. Rode, H. Pasch, *Polymer*, **2003**, 44, 1851

[36] W. Radke, K. Rode, A.V. Gorshkov, T. Biela, *Polymer*, **2005**, 46, 5456

[37] H. Kukula, H. Schlaad, J. Falkenhagen, R.P. Krüger, *Macromolecules*, **2002**, 35, 7157

[38] X. Jiang, V. Lima, P.J. Schoenmakers, *J. Chromatogr. A*, **2003**, 1018, 19

[39] J. Adrian, D. Braun, H. Pasch, *Angew. Makromol. Chem.*, **1999**, 267, 82

[40] J. Adrian, D. Braun, K. Rode, H. Pasch, *Angew. Makromol. Chem.*, **1999**, 267,

73
[41] H. Pasch, I. Zammert, *J. Liq. Chromatogr.*, **1994**, 17, 3091
[42] H. Pasch, C. Brinkmann, Y. Gallot, *Polymer*, **1993**, 34, 4100
[43] H. Pasch, M. Augenstein, *Makromol. Chem.*, **1993**, 194, 2533
[44] H. Pasch, Y. Gallot, B. Trathnigg, *Polymer*, **1993**, 34, 4986
[45] H. Pasch, C. Brinkmann, H. Much, U. Just, *J. Chromatogr.*, **1992**, 623, 315
[46] H. Pasch, M. Augenstein, B. Trathnigg, *Macromol. Chem. Phys.*, **1994**, 195, 743
[47] J. Falkenhagen, H. Much, W. Stauf, A.H.E. Müller, *Macromolecules*, **2000**, 33, 3687
[48] H. Lee, T. Chang, D. Lee, M.S. Shim, H. Ji, W.K. Nonidez, J.W. Mays, *Anal. Chem.*, **2001**, 73, 1726
[49] J. Adrian, E. Esser, G. Hellmann, H. Pasch, *Polymer*, **2000**, 41, 2439
[50] H. Pasch, M. Adler, F. Rittig, S. Becker, *Macromol. Rapid Commun.*, **2005**, 26, 438
[51] H. Pasch, *Polymer*, **1993**, 34, 4095
[52] E. Esser, D. Braun, H. Pasch, *Angew. Makromol. Chem.*, **1999**, 271, 61
[53] H. Pasch, K. Rode, *Polymer*, **1998**, 39, 6377
[54] H. Pasch, K. Rode, N. Chaumien, *Polymer*, **1996**, 37, 4079
[55] D. Berek, M. Janco, K. Hatada, T. Kitayama, N. Fujimoto, *Polym. J.*, **1997**, 29, 1029
[56] T. Macko, D. Hunkeler, *Adv. Polym. Sci.*, **2003**, 163, 61
[57] W. Lee, D. Cho, T. Chang, *Macromolecules*, **2001**, 34, 2353
[58] H. Pasch, A. Brüll, K. Cabrera, *e-Polymers*, **2005**, 20
[59] J. Adrian, D. Braun, H. Pasch, *LC&GC Int.*, **1998**, January, 32
[60] P. A. Mirau, *A Practical Guide to Understanding the NMR of Polymers*, John Wiley & Sons, Inc., Hoboken, New Jersey, **2005**
[61] B. Blümich, *Essential NMR for Scientists and Engineers*, Springer-Verlag Berlin Heidelberg, **2005**
[62] J.L. Koenig, *Spectroscopy of Polymers 2nd Edition*, Elsevier Science Inc., New York, **1999**
[63] H. Friebolin, *Ein und zweidimensionale NMR-Spektroskopie Eine Einführung Dritte Auflage*, Wiley-VCH, Weinheim, **1999**
[64] A.E. Derome, *Modern NMR Techniques for Chemistry Research Volume 6*,

Pergamon Press GmbH, **1987**

[65] J.B. Stothers, *Carbon-13 NMR Spectroscopy*, Academic Press, New York, **1972**

[66] J.C. Randall, *Polymer Sequence Determination Carbon-13 NMR Method*, Academic Press, New York, **1977**

[67] F.A. Bovey, *Chain Structure and Conformation of Macromolecules*, Academic Press, New York, **1989**

[68] K. Albert, E. Dreher, H. Straub, A. Rieker, *Magn. Reson. Chem.*, **1987**, 25, 919

[69] K. Albert, G. Kruppa, K.P. Zeller, E. Bayer, F.Z. Hartmann, *Naturforsch., C,* **1984**, 89, 859

[70] P. Hütter, K. Albert, E. Bayer, K.P. Zeller, F. Hartmann, *Biochem. Pharmacol.*, **1987**, 36, 2729

[71] K. Albert, J.L. Sudmeier, M. Anwer, W.W. Bachovchin, *Magn. Reson. Med.*, **1989**, 11, 309

[72] K. Albert, E. Bayer, G. Patonay, *HPLC Detection Newer Methods*, VCH Publishers, New York, **1992**

[73] K. Albert, *On-Line LC-NMR and Related Techniques*, John Wiley & Sons Ltd, England, **2002**

[74] K. Albert, Habilitationsscript, Tübingen University, **1988**

[75] J. Sudmeier, U. Günther, K. Albert, W. Bachovchin, *J. Magn. Reson. A*, **1996**, 118, 145

[76] N. Watanbe, E. Niki, *Proc. Jpn. Acad., Ser. B*, **1978**, 54, 194

[77] E. Bayer, K. Albert, M. Nieder, E. Grom, T. Keller, *J. Chromatogr.*, **1979**, 186, 197

[78] J.F. Haw, T.E. Glass, D.W. Hausler, E. Motell, H.C. Dorn, *Anal. Chem.*, **1980**, 52, 1135

[79] E. Bayer, K. Albert, M. Nieder, E. Grom, Z. An, *Fresenius Z. Anal. Chem.*, **1980**, 404, 111

[80] J. Buddruss, H. Herzog, *Org. Magn. Reson.*, **1980**, 13, 153

[81] J. Buddruss, H. Herzog, J.W. Cooper, *J. Magn. Reson.*, **1981**, 42, 453

[82] J.F. Haw, T.E. Glass, H.C. Dorn, *Anal. Chem.*, **1981**, 53, 2327

[83] J.F. Haw, T.E. Glass, H.C. Dorn, Anal. Chem., **1981**, 53, 2332

[84] E. Bayer, K. Albert, M. Nieder, E. Grom, G. Wolff, M. Rindlisbacher, *Anal. Chem.*, **1982**, 54, 1747

[85] J.F. Haw, T.E. Glass, H.C. Dorn, *J. Magn. Reson.*, **1982**, 49, 22

[86] J.F. Haw, T.E. Glass, H.C. Dorn, *Anal. Chem.*, **1983**, 55, 22

[87] J. Buddruss, H. Herzog, *Anal. Chem.*, **1983**, 55, 1611

[88] D.A. Jr. Laude, C.L. Wilkins, *Anal. Chem.*, **1984**, 56, 2471

[89] H.C. Dorn, *Anal. Chem.*, **1984**, 56, 747A

[90] K. Albert, M. Nieder, M. Bayer, M. Spraul, *J. Chromatogr.*, **1985**, 346, 17

[91] K. Albert, *J. Chromatogr. A*, **1995**, 703, 123

[92] S.A. Korhammer, A. Bernreuther, *Fresenius J. Anal. Chem.*, **1996**, 354, 131

[93] J.C. Lindon, J.K. Nicholson, I.D. Wilson, *Prog. NMR Spectroc.*, **1996**, 29, 1

[94] U.G. Sidelmann, E.M. Lenz, M. Spraul, M. Hofmann, J. Troke, P.N. Sanderson, J.C. Lindon, I.D. Wilson, J.K. Nicholson, *Anal. Chem.*, **1996**, 68, 106

[95] A. Höltzel, G. Schlotterbeck, K. Albert, E. Bayer, *Chromatographia*, **1996**, 42, 499

[96] G. Schlotterbeck, H. Pasch, K. Albert, *Polymer Bull.*, **1997**, 38, 873

[97] M. Gueron, P. Plateau, M. Decorps, *Prog. NMR Spectrosc.*, **1991**, 23, 135

[98] P.J. Hore, *Methods Enzymol.*, **1989**, 176, 64

[99] S.L. Patt, *J. Magn. Res.*, **1991**, 95, 94

[100] T.L. Hwang, A.J. Shaka, *J. Magn. Res. Ser. A*, **1995**, 112, 275

[101] M. Piotto, V. Saudek, V. Sklenar, *J. Biomol. NMR*, **1992**, 2, 661

[102] V. Sklenar, A. Bax, *J. Magn. Reson*, **1987**, 74, 469

[103] D. Wu, A. Chen, C.J. Johnson, *J. Magn. Res. Ser. A*, **1995**, 115, 260

[104] J. Wu, K. Beshah, *NMR Spectroscopy of Polymers in Solution and in the Solid State, ACS Symposium Series 834, Americal Chemical Society, Washington, DC*, **2002**, 345

[105] M.A. McCoy, L. Mueller, *J. Am. Chem. Soc.*, **1992**, 114, 2108

[106] S.H. Smallcombe, S.L. Patt, P.A. Keifer, *J. Magn. Res. Ser. A*, **1995**, 117, 295

[107] E. Kupce, R. Freemann, *J. Magn. Res. Ser. A*, **1995**, 115, 273

[108] R.J. Ogg, P.B. Kingsley, J.S. Taylor, *J. Magn. Res. Ser. B*, **1994**, 104, 1

[109] M.V.S. Elipe, *Analytica Chimica Acta*, **2003**, 497, 1

[110] W. Lee, S. Park, T. Chang, *Anal. Chem.*, **2001**, 73, 3884

[111] C.H. Lochmüller, M.A. Moebus, Q.C. Liu, C. Jiang, M. Elomaa, *J. Chromatogr. Sci.*, **1996**, 34, 69

[112] D. Cho, J. Hong, S. Park, T. Chang, *J. Chromatogr. A*, **2003**, 986, 199

[113] D. Cho, S. Park, J. Hong, T. Chang, *J. Chromatogr. A*, **2003**, 986, 191

[114] W.Hiller, P.Sinha, H.Pasch, *Macromol. Chem. Phys.*, **2009**, 210, 605

[115] W.Hiller, P.Sinha, H.Pasch, *Macromol. Chem. Phys.*, **2007**, 208, 1965

Curriculum Vitae

Name:	Pritish Sinha
Date of Birth:	16.November.1979
Place of Birth:	Calcutta, India
Nationality:	Indian
Marital status:	Single

Education

1985 - 1997	Loyola High School, Pune, India
June 1997	Secondary School Certificate Exam

Academic career

August 1997- July 2002	Bachelor of Polymer Engineering (B.E.), Maharashtra Institute of Technology, University of Pune, India Bachelor Thesis: Study of effect of Fillers on Rotomoulded Products
April 2003- June 2005	Masters in Applied Polymer Science, Martin Luther University, Halle-Wittenberg, Germany Master Thesis: Influence of selected reaction parameters on the graft copolymerisation reaction of irradiated PTFE micro powders with styrene-a systematic study
Since February 2006	Doctoral thesis under the supervision of Prof. Dr. H. Pasch at Technical University Darmstadt, Germany Topic: Characterisation of Block Copolymers by On-line HPLC-NMR

Pritish Sinha
Bleichstr 6
64283 Darmstadt

14.Mai.2009

Eidesstattliche Erklärung

Ich erkläre hiermit an Eides Statt, dass ich meine Dissertation selbstständig und nur mit den angegebenen Hilfsmitteln angefertigt habe.

Darmstadt, den 14. Mai.2009

Pritish Sinha
Bleichstr. 6
64283 Darmstadt

14.Mai.2009

Erklärung

Ich erkläre hiermit, noch keinen Promotionsversuch unternommen zu haben.

Darmstadt, den 14. Mai.2009